EMITTER International Journal of Engineering Technology
Vol.2, No.1, June 2014
ISSN:2355-391X

A Combination of PD Controller and PIAFC for Stabilization of "x" Configuration Quadcopter

Ni'am Tamami , Endra Pitowarno , I Gede Puja Astawa

Electronics Engineering Polytechnic Institute of Surabaya
Kampus PENS, Jalan Raya ITS, Sukolilo, Surabaya 60111, INDONESIA
E-mail: {niam,epit,puja}@pens.ac.id

Abstract

This paper presents a stabilization control method for "x" configuration quadcopter. The control method used the combination of PD (Proportional Derivative) controller and PIAFC (Proportional Integral Active Force Control). PD is used to stabilize quadcopter, and PIAFC is used to reject uncertainty disturbance (e.g. wind) by estimating disturbance torque value of quadcopter. The PD with PIAFC provided better result where PIAFC could minimize uncertain disturbance effect. The simulation has succesfull give comparation about controller performance (PD, PD-AFC, PD-PIAFC) by calculate RMS (Root Mean Square) value. PD with AFC gives better result than PD. AFC optimization using PI (PD-PIAFC) give best result if compared with PD or PD-AFC. PD-PIAFC has lowest RMS value of result control signal, 0.0389 for constant disturbance and 0.1008 for fluctuated disturbance.

Keywords: "x" configuration quadcopter, stability, PD, PIAFC.

1. INTRODUCTION

Multicopter, a type of UAV is popular among hobbyist and researchers. It has advantages in thrust, fast maneuver and VTOL ability (Vertical Take Off Landing). Multicopter has motors located at each end of the frame to produce greater thrust than other UAV in same size. Muticopter has a good handling even in a narrow space due to its fast response maneuverability. During development, multicopter able to turn into high speed UAV by altering the orientation and control techniques on quadcopter (quadshoot) that developed by Massachusetts Institute of Technology. VTOL capability facilitates multicopter for take off and landing on a narrow area. In addition, the quadcopter is an interesting research material among researchers for many novelties that can be applied, for example in the control system, navigation techniques, real-time systems and robotics.

Copyright © 2014 EMITTER International Journal of Engineering Technology - Published by EEPIS

This paper focuses on quadcopter. Quadcopter has a simple structure. It utilises rotors which are directed upwards and placed at the end of a crossed frame. The quadcopter is controlled by adjusting the rotation speed of each rotors. This research use "x" configuration quadcopter because this configuration is considered more stable than "+" quadcopter configuration [1]. The "x" configuration quadcopter has a better distribution of rotor forces during flying. The "x" quadcopter configuration structure can be found in section 2.

Quadcopter is excellent object for investigating issues in control science. There are many research about quadcopter control algorithm and uncertainty disturbance rejection. Bouabdallah et al. designed an LQ controller and PID controller then compare it [2]. The result PID controller better than LQ controller. Jun Li and Yuntang Li designed PID controller to control angular and linear position, and succes to stabilize quadcopter [3]. Mokhtari and Benallegue applied state parameter control to quadcopter rotation angle [4]. By using state observer, quadcopter can measure external disturbance. Bora and Erdinc have been controlling position of quadcopter using PD controller and combined by using vision system [5]. Pounds et al. developed independent linear SISO controllers to regulate quadcopter using PID controller [6]. Inkyu Sa and Peter Corke develop Verticle infrastructure inspection using a quadcopter and shared autonomy control using PID method and successful stabilize quadcopter [7]. Sumantri et al. designed a sliding mode control using a nonlinear sliding surface (NSS) to design a robust tracking controller for a quad-rotor helicopter [8]. Chen and Huzmezan used linear H∞ controller to achieve stabilization in angular rates, vertical velocity, longitudinal velocity, lateral velocity, yaw angle and height of a quadcopter [9]. A linear H∞ controller can be designed to obtain stabilization and tracking performance using a systematical approach [10]. Pitowarno have designed Active Force Control and Knowledge-Based System for planar two-joint robot arm to improve performance of Active Force Control [11]. Katsura et al. have been modeled force sensing using disturbance observer without force sensor [12]. Chen et al. designed disturbance observer control for non linear system to control robotic manipulator [13]. Achtelik et al. has develop quadcopter using Model Reference Adaptive Control to reject uncertainty disturbance. Controller has been successful stabilize quadcopter [14].

It is very important to make a simple control algorithm to control the quadcopter stability although get uncertainty disturbance from environment, because in real system control algorithm will be embed in low speed data processing unit. PD can stabilize quadcopter but not good enough to maintain the quadcopter against uncertainty disturbance such as wind. PIAFC has the ability to estimate the force on the system without using complicated mathematical computation.

The purpose of this work is modelling and combining PD and PIAFC to control "x" configuration quadcopter when hover even if get uncertainty

disturbance. This paper is structured as follows. Section 2, presents a quadcopter dinamic modelling. Section 3, deals quadcopter controller design. Section 4, presents the performance of the controller is shown in numerical simulations. Finally, in Section 5 conclusions of this work.

2. QUADCOPTER MODELLING

In this section the mathematical model of the quadcopter will be presented. This dynamic model contain the model of the rotor force and torque, gyroscopic effect, and the derrived force model of "x" configuration quadcopter.

Figure 1 is the design of "x" configuration quadcopter. The rotors (M1, M2, M3, M4) are placed in sequence π/4, 3π/4, 5π/4, 7π/4. Two diagonal rotors (M1 and M3) are rotating in the same direction (counter clockwise) whereas the others (M2 and M4) in the clockwise direction to eliminate the anti-torque that caused by rotor rotation.

Absolute position of the quadcopter can be described by a coordinate position of the body frame {B} with reference earth frame {E}. Absolute attitude of the quadcopter can be described by three Euler's angles, (ϕ,θ,ψ),which are roll, pitch and yaw with reference body frame {B} when XB, YB and ZB axis in parallel with X, Y and rotating 180 degree of Z axis.

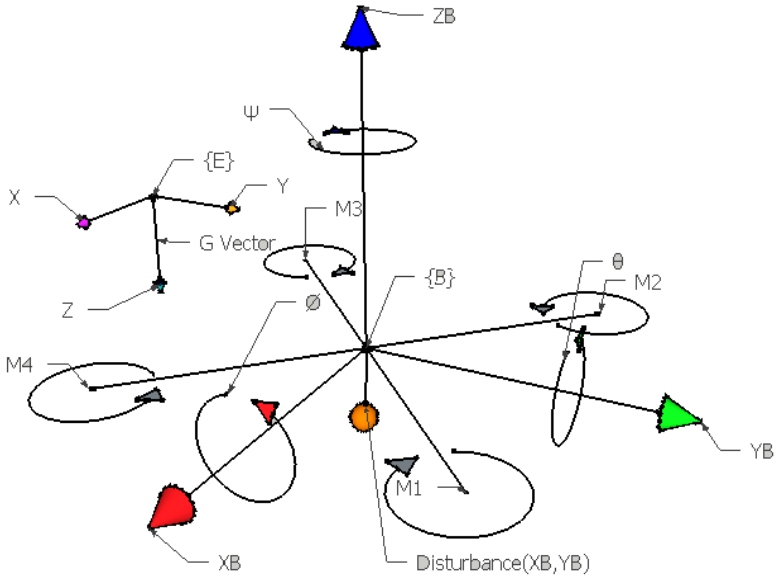

Figure 1. An "x" configuration quadcopter

To make a movement along XB axis, quadcopter must produce pitch torque (τ_y). It means, quadcopter decreases rotor speed at M1 and M4, and increase rotor speed at M2 and M3. Likewise to make movement along YB axis, quadcopter must produce roll torque (τ_x). Quadcopter decreases rotor speed at M1 and M2, and increase rotor speed at M3 and M4. Then, to change

quadcopter heading, quadcopter must produces yaw torque (τ_z) by increasing M1 and M3 rotor speed, and decreasing M2 and M4 rotor speed.

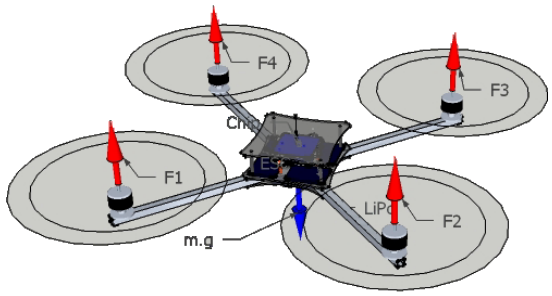

Figure 2. Force distribution in quadcopter

Figure 2 shows the force distribution in quadcopter. "F1, F2, F3, F4" arrows are thrust force each motor, and "m.g" arrow is weight force of quadrotor. From Li et al., the thrust and hub force for each rotor (F_i, H_i) can be represented in (1), and (2) [3]. Thrust force is the resultant of the vertical forces acting on all the blade elements. Hub force is the resultant of the horizontal forces acting on all the blade elements. Where ρ is air density. C_T is thrust constant that depend on polar lift slope, geometric blade, velocity trough motor, the ratio the surface area and rotor disk area [6]. C_d is drag constant, and Ω_i is propeller rotation speed.

$$F_i = 0.5\rho C_T \Omega_i^2 = k_t \Omega_i^2 \quad (1)$$

$$H_i = \rho C_d \Omega_i^2 = k_d \Omega_i^2 \quad (2)$$

Quadcopter can change its position by combining translation and rotation angle. Linear movement on the quadcopter can be produced by total thrust force of the four rotor (3), whereas changes in the angle of rotation (roll, pitch, yaw) will cause a change in the direction of translational movement quadcopter. Total force of the quadcopter can be decomposed into force element in each axis (F_x, F_y, F_z). Figure 3 shows the illustration of force decomposition to each axis in body frame {B}.

$$F_{total} = \sum_{i=1}^{4} F_i \quad (3)$$

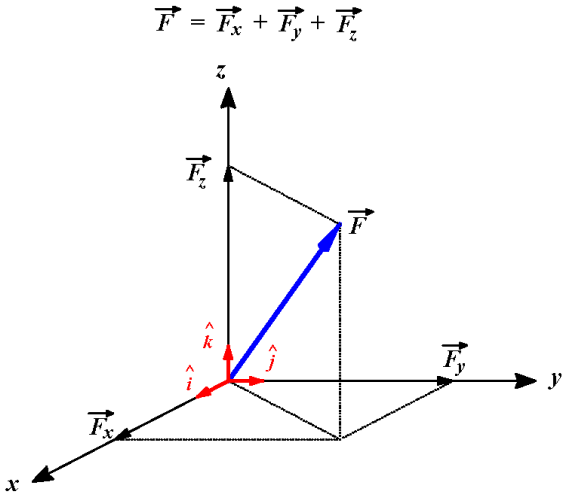

Figure 3. Total forces illustration that decomposed into each axis

Equation (4) is rotation matrix of quadcopter. C, S are cosine function and sine function respectively.

$$R = \begin{bmatrix} C\phi C\theta & C\phi S\theta s\psi - C\psi S\phi & S\phi S\psi + C\phi C\psi S\phi \\ C\theta S\phi & C\phi C\psi + S\phi S\theta S\psi & C\psi S\phi C\theta - C\phi S\psi \\ -S\theta & C\theta S\psi & C\theta C\psi \end{bmatrix} \quad (4)$$

The derrived model of quadcopter translational movement can be represented as (5). Where $\ddot{x}, \ddot{y}, \ddot{z}$ are linear acceleration in of quadcopter in each axis.

$$m\begin{bmatrix} \ddot{x} \\ \ddot{y} \\ \ddot{z} \end{bmatrix} = R\begin{bmatrix} 0 \\ 0 \\ F\,total \end{bmatrix} - \begin{bmatrix} 0 \\ 0 \\ mg \end{bmatrix} \quad (5)$$

The model also contain gyroscopic effect. Derrived torque model of quadcopter are presented at (6), (7), (8).

$$\tau x = \begin{bmatrix} F1 \\ F2 \\ F3 \\ F4 \end{bmatrix}^T l \begin{bmatrix} C(\frac{\pi}{4}) \\ C(\frac{3\pi}{4}) \\ C(\frac{5\pi}{4}) \\ C(\frac{7\pi}{4}) \end{bmatrix} + \dot{\theta}\dot{\psi}(I_{yy} - I_{zz}) \quad (6)$$

$$\tau_y = \begin{bmatrix} F1 \\ F2 \\ F3 \\ F4 \end{bmatrix}^T l \begin{bmatrix} S(\frac{\pi}{4}) \\ S(\frac{3\pi}{4}) \\ S(\frac{5\pi}{4}) \\ S(\frac{7\pi)}{4} \end{bmatrix} + \dot{\phi}\dot{\psi}(I_{zz} - I_{xx}) \tag{7}$$

$$\tau_z = K_d l(-F1 + F2 - F3 + F4) + \dot{\theta}\dot{\phi}(I_{xx} - I_{yy}) \tag{8}$$

τ_x, τ_y, τ_z are roll, pitch, yaw torque respectively. l is distance of rotor between center of mass. $\dot{\phi}, \dot{\theta}, \dot{\psi}$ are roll, pitch, yaw angular body speed respectively. I_{xx}, I_{yy}, I_{zz} are roll, pitch, yaw body inertia respectively. K_d is force resistance constant in (2).

Let us define the control inputs of quadcopter are u_1, u_2, u_3, u_4. Where u_1 is total force control input. Total force control input can derrived by subtitute (1) to (3). u_2 is roll torque control input, u_3 is pitch torque control input, and u_4 is yaw torque control input can derrived by subtitute (1) to (6), (7) and (2) to (8). Where, k_t and k_d are constant value from (1), (2).

$$\begin{aligned} u1 &= F_{total} \\ &= k_t \sum_{i=1}^{4} \Omega_i^2 \\ u2 &= \tau_x \\ &= k_t l \sum_{i=1}^{4} \Omega_i^2 \cos(\frac{\pi}{2}(i-1) + \frac{\pi}{4}) \\ u3 &= \tau_y \\ &= k_t l \sum_{i=1}^{4} \Omega_i^2 \sin(\frac{\pi}{2}(i-1) + \frac{\pi}{4}) \\ u4 &= \tau_z \\ &= k_d l \sum_{i=1}^{4} (-1)^i \Omega_i^2 \end{aligned} \tag{9}$$

By subtitute (9) into (5), (6), (7), (8), the derrived model of quadcopter in (10). Where $\ddot{\phi}, \ddot{\theta}, \ddot{\psi}$ are roll, pitch, yaw, angular acceleration at quadcopter body.

$$\ddot{x} = \frac{(s\phi s\psi + c\phi c\psi s\theta)u1}{m}$$
$$\ddot{y} = \frac{(c\psi s\phi c\theta - c\phi s\psi)u1}{m}$$
$$\ddot{z} = \frac{(c\theta s\psi)u1}{m} - g$$
$$\dot{\phi} = \frac{u2 + \dot{\theta}\dot{\psi}(I_{yy} - I_{zz})}{I_{xx}}$$
$$\ddot{\theta} = \frac{u3 + \dot{\phi}\dot{\psi}(I_{zz} - I_{xx})}{I_{yy}}$$
$$\dot{\psi} = \frac{u4 + \dot{\theta}\dot{\phi}(I_{xx} - I_{yy})}{I_{zz}} \quad (10)$$

Mechanical energy there are kinetic energy (E_K) and potential energy (E_P) in quadcopter can define as

$$E_K = 0.5I_{xx}(\dot{\phi} - \dot{\psi}s\theta) + 0.5I_{yy}(\dot{\theta}c\phi + c\theta s\phi)^2 + 0.5I_{zz}(\dot{\theta}s\phi - \dot{\psi}c\theta c\phi)^2$$
$$= 0.5I_{xx}\dot{\phi}^2 + 0.5I_{yy}\dot{\theta}^2 + 0.5I_{zz}\dot{\psi}^2 \quad (11)$$

$$E_P = \int xdm(x).(-gs\theta) + \int ydm(y).(c\theta s\phi) + \int zdm(z).(c\phi c\theta) \quad (12)$$

3. QUADCOPTER CONTROLLER DESIGN

In this section, the control algorithm of quadcopter is presented. The purpose is to combine PD and PIAFC as rotational controller to stabilize quadcopter. Figure 4 shows the proposed rotational controller to stabilize quadcopter.

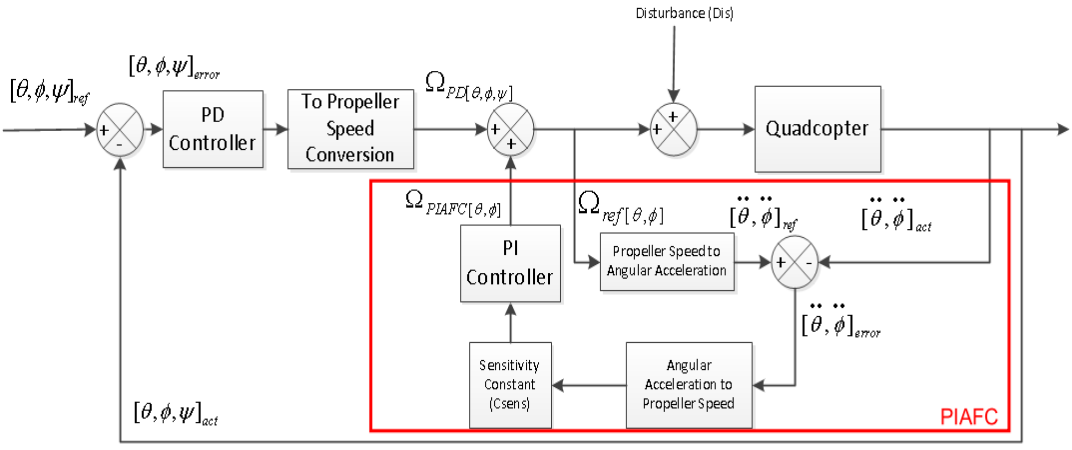

Figure 4. The proposed rotational controller

Figure 5 shows quadcopter control structure. In this simulation, translational movement are neglected. The controller design is focused to stabilize the quadcopter toward disturbance. PD controller is used to stabilize quadcopter and PIAFC to reject uncertainty disturbance from environment. In this simulation, quadcopter get constant and fluctuated disturbance.

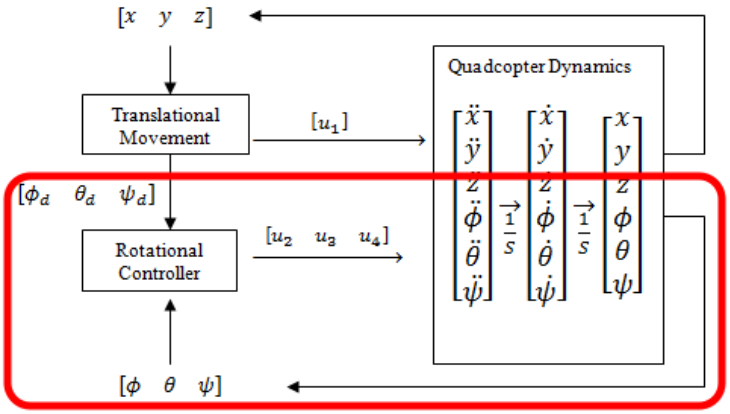

Figure 5. Quadcopter control structure

From Figure 5, the relationship of each input and each state can be represented as (13).

$$\begin{aligned} \dot{X} &= AX + BU \\ X &= \begin{bmatrix} \phi & \theta & \psi & \dot{\phi} & \dot{\theta} & \dot{\psi} \end{bmatrix}^T \\ U &= \begin{bmatrix} u_1 & u_2 & u_3 & u_4 \end{bmatrix} \\ X &= \begin{bmatrix} \dot{\phi} & \dot{\theta} & \dot{\psi} & \ddot{\phi} & \ddot{\theta} & \ddot{\psi} \end{bmatrix}^T \end{aligned} \tag{13}$$

The system matrix (A) can be represented as (14).

$$A = \begin{bmatrix} 0 & 0 & 0 & 1 & 0 & 0 \\ 0 & 0 & 0 & 0 & 1 & 0 \\ 0 & 0 & 0 & 0 & 0 & 1 \\ 0 & 0 & 0 & 0 & \dfrac{\dot{\psi}(I_{yy} - I_{xx})}{2I_{xx}} & \dfrac{\dot{\theta}(I_{yy} - I_{xx})}{2I_{xx}} \\ 0 & 0 & 0 & \dfrac{\dot{\psi}(I_{zz} - I_{xx})}{2I_{yy}} & 0 & \dfrac{\dot{\phi}(I_{zz} - I_{xx})}{2I_{yy}} \\ 0 & 0 & 0 & \dfrac{\dot{\theta}(I_{xx} - I_{yy})}{2I_{zz}} & \dfrac{\dot{\phi}(I_{xx} - I_{yy})}{2I_{zz}} & 0 \end{bmatrix} \tag{14}$$

The control matrix (B) can be represented as (15).

$$B = \begin{bmatrix} 0 & 0 & 0 & 0 \\ 0 & 0 & 0 & 0 \\ 0 & 0 & 0 & 0 \\ 0 & \frac{1}{I_{xx}} & 0 & 0 \\ 0 & 0 & \frac{1}{I_{yy}} & 0 \\ 0 & 0 & 0 & \frac{1}{I_{zz}} \end{bmatrix} \quad (15)$$

3.1 Disturbance Model

In this subsection, the model of disturbance will be presented. The disturbance vector (Dis) that used in this paper consists of two types. First simulation use constant disturbance (Dis_{CX}), and second simulation fluctuated/uncertainty disturbance (Dis_{FX}). Figure 1 shows disturbance position of quadcopter, disturbance mass located at (L_{DXB}, L_{DYB}) from the center of quadcopter in (XB, YB) axis. By including disturbance vector, state equation (13) can be written as follows:

$$\dot{X} = AX + BU + Dis \quad (16)$$

First simulation with constant disturbance:

$$Dis = \begin{bmatrix} 0 & 0 & 0 & Dis_{CX} & L_{DYB} & Dis_{CX} & L_{DXB} & 0 \end{bmatrix}^T \quad (17)$$

Second simulation with fluctuated disturbance:

$$Dis = \begin{bmatrix} 0 & 0 & 0 & Dis_{FX} & L_{DYB} & Dis_{FX} & L_{DXB} & 0 \end{bmatrix}^T \quad (18)$$

3.2 PD Controller Design

PD control algorithm is designed without disturbance parameter. The controller design is focused to stabilize quadcopter when hover without get uncertainty disturbance. The model that presented at section 2 is completed by gyroscopic effect. If we design quadcopter stabilize at hover, it can be ignored because it dont have significant effect at quadcopter system [15]. The model can be simplified:

$$\ddot{\phi} = \frac{k_t l \sum_{i=1}^{4} \Omega_i^{\,2} \cos(\frac{\pi}{2}(i-1) + \frac{\pi}{4})}{I_{xx}}$$

$$\ddot{\theta} = \frac{k_t l \sum_{i=1}^{4} \Omega_i^{\,2} \sin(\frac{\pi}{2}(i-1) + \frac{\pi}{4})}{I_{yy}} \quad (19)$$

$$\ddot{\psi} = \frac{k_d \sum_{i=1}^{4} (-1)^i \Omega_i}{I_{zz}}$$

The simulation purposes is to stabilize roll, pitch and yaw angle. By using twice integral operation at (19), the model can be rewritten as :

$$\ddot{\phi} = \frac{k_t l \sum_{i=1}^{4} \Omega_i{}^2 \cos(\frac{\pi}{2}(i-1)+\frac{\pi}{4})}{I_{xx} s^2}$$
$$\ddot{\theta} = \frac{k_t l \sum_{i=1}^{4} \Omega_i{}^2 \sin(\frac{\pi}{2}(i-1)+\frac{\pi}{4})}{I_{yy} s^2} \quad (20)$$
$$\ddot{\psi} = \frac{k_d \sum_{i=1}^{4} (-1)^i \Omega_i}{I_{zz} s^2}$$

From (20), the model is second order form, therefore it can use classical controller to stabilize quadcopter. PD controller will be presented to stabilize quadcopter. The reason is this controller very simple and easy implemented. This is PD controller each orientation angle.

$$u_2, u_3, u_4 = P_{\phi,\theta,\psi}(\phi,\theta,\psi) + D_{\phi,\theta,\psi}(\phi,\theta,\psi) \quad (21)$$

Where u_2, u_3, u_4 are control input for roll, pitch, yaw torque respectively. $P_{\phi,\theta,\psi}(\phi,\theta,\psi)$ are proporsional control for roll, pitch, and yaw respectively. $D_{\phi,\theta,\psi}(\phi,\theta,\psi)$ are derrivative control for roll, pitch, and yaw respectively.

3.3 PIAFC Controller Design

PIAFC controller is designed to reject uncertainty disturbance from environment. It is combined PI controller and AFC Controller. Figure 6 shows the PIAFC block diagram that used in simulation. This block has two inputs, first is measured angular velocity that differentiated into actual angular acceleration (22). Second input is applied propeller speed that converted into angular acceleration reference (24). To get estimated disturbance, actual angular acceleration is compared by angular acceleration reference (25). Last, convert the disturbance acceleration into propeller speed (26) then add the result with PD controller result.

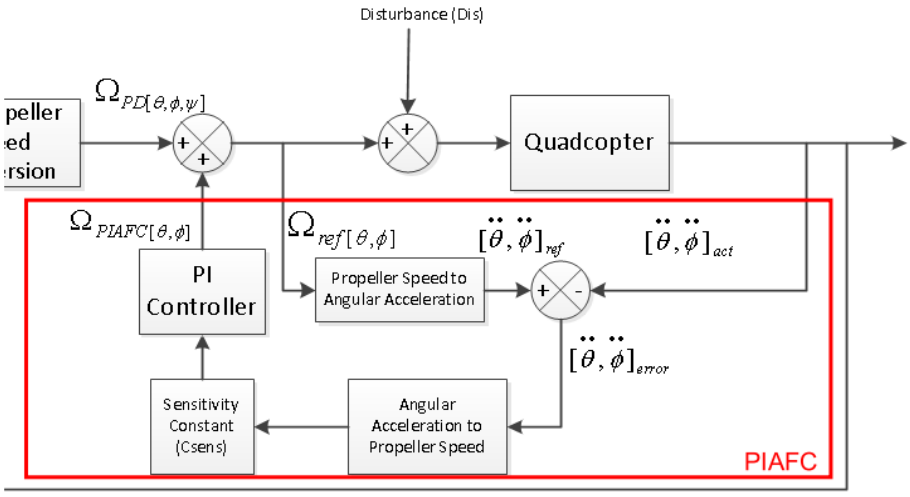

Figure 6. AFC block diagram

Let us difine γ is rotation angle roll and pitch axis (ϕ,θ),

$$\ddot{\gamma} = \frac{d\dot{\gamma}}{dt} \tag{22}$$

$$\Omega_{\phi} = \Omega_1 + \Omega_2 - \Omega_3 - \Omega_4$$
$$\Omega_{\theta} = \Omega_1 - \Omega_2 - \Omega_3 + \Omega_4 \tag{23}$$

$$\ddot{\gamma}_{ref} = \frac{0.5\rho C_t l \Omega_{\gamma} |\Omega_{\gamma}|}{I_{xx,yy}} \tag{24}$$

$$\ddot{\gamma}_{AFC} = \ddot{\gamma}_{ref} - \ddot{\gamma} \tag{25}$$

$$\Omega_{PIAFC} = P(\ddot{\gamma}_{AFC}) + I(\ddot{\gamma}_{AFC}) \tag{26}$$

$\ddot{\gamma}_{AFC}$ is disturbance angular acceleration estimation. Ω_{PIAFC} is propeller speed calculation form PIAFC controller output.

3.4 Stability Analysis

From (10), let us define angular equation motion within controller as,

$$I_{xx}\ddot{\phi} = u_2 + \dot{\theta}\dot{\psi}(I_{xx} - I_{zz})$$
$$I_{yy}\ddot{\theta} = u_3 + \dot{\phi}\dot{\psi}(I_{zz} - I_{yy}) \tag{27}$$

Because u_2, u_3 is input control, and the value of gyroscopic torque is very small, then the equation can be rewritten as,

$$I_{xx}\ddot{\gamma} = P(\gamma) + D(\gamma) + P(\ddot{\gamma}_{AFC}) + I(\ddot{\gamma}_{AFC}) \tag{28}$$

From (11), kinetic energy (E_K) in XB axis as Lyapunov function (V),

$$V = 0.5 I_{xx,yy} \dot{\gamma}^2 \tag{29}$$

Then,

$$\dot{V} = I_{xx,yy} \dot{\gamma} \ddot{\gamma}$$
$$\dot{V} = (K_P(\gamma_{ref} - \gamma) + K_D(\gamma_{ref} - \gamma) + K_{PIAFC}(\gamma_{AFC} - \gamma))\dot{\gamma} \tag{30}$$

Where $\lfloor \gamma_{ref}, \dot{\gamma}_{ref,}, \ddot{\gamma}_{ref} \rfloor = [0,0,0]$, the equation can be rewritten as,

$$\dot{V} = (-K_P(\gamma) - K_D(\dot{\gamma}) + K_{PIAFC}(\ddot{\gamma}))\dot{\gamma} \tag{31}$$

$\dot{V}$ is negative definite, and thus the stability of the closed loop dynamics in is guaranteed.

4. SIMULATION AND ANALYSIS

In this section, comparison result of PD, PD-AFC, and PD-PIAFC (AFC that optimized by PI controller) presented. Table 1 presents the quadcopter parameters that used in this simulation as follows are those for the experimental system in our laboratory.

Table 1 Quadcopter simulation parameter

Parameter	Unit	Value
m	Kg	1.025
L	Meter	0.270
k_t	Ns^2	3.122e-06
k_d	Nms^2	1.759e-08
Ixx	kgm^2	0.012
Iyy	kgm^2	0.012
Izz	kgm^2	0.048
Dis_{CX}	Newton	0.2
Dis_{FX}	Newton	$0.2S(2\pi 0.4t)$
L_{DXB}	mm	0
L_{DYB}	mm	190

Table 2 PD coefficients simulation parameter

Parameter	Value
KP*	0.097
KD*	0.036
KP**	1.000
KI **	0.100

Note : * for PD, ** for PIAFC.

PD coefficients that used for simulation are derrived by trial and error to get best performance, the controller constant parameter are listed in Table 2. First simulation compares PD, PD-AFC, and PD-PIAFC performance if get constant disturbance. Second simulation compares PD, PD-AFC, and PD-PIAFC performance if get fluctuated disturbance. Root Mean Square (RMS) method is used to determine the controller performance analisys. Lower RMS value means better performance of controller.

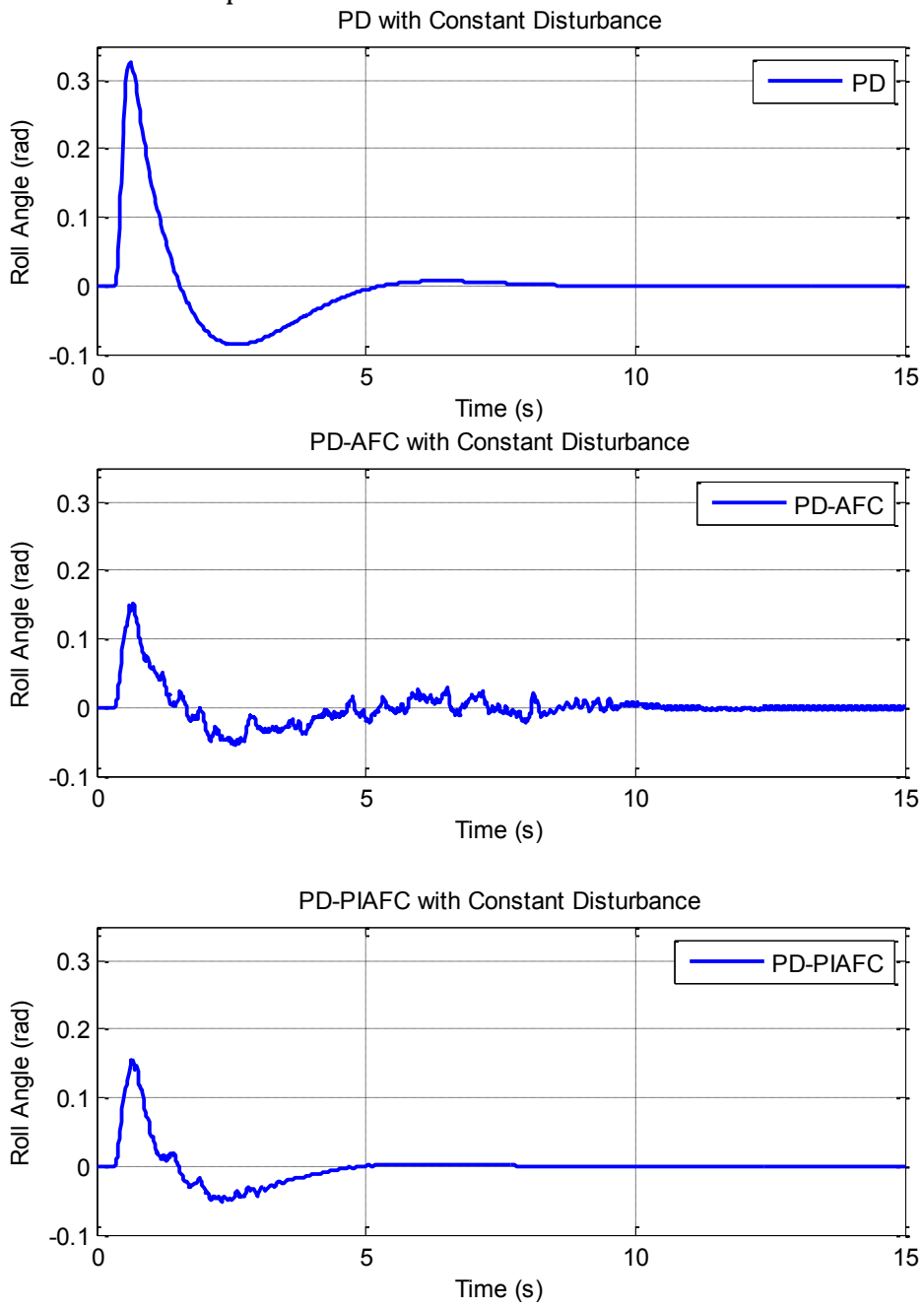

Figure 7. Constant disturbance simulation result

Figure 7 shows the comparison result of PD, PD-AFC, and PD-PIAFC method with constant disturbance. By using PD, maximum error is 0.325 radian and can stable at 5 seconds. PD-AFC and PD-PIAFC give smaller error, 0.15 radian. PD-AFC noise more than PD-PIAFC. PD controller has RMS value 0.059, PD-AFC is 0.041, and PD-PIAFC is 0.0389. From RMS value, we can conclude PD-PIAFC give best result of controller.

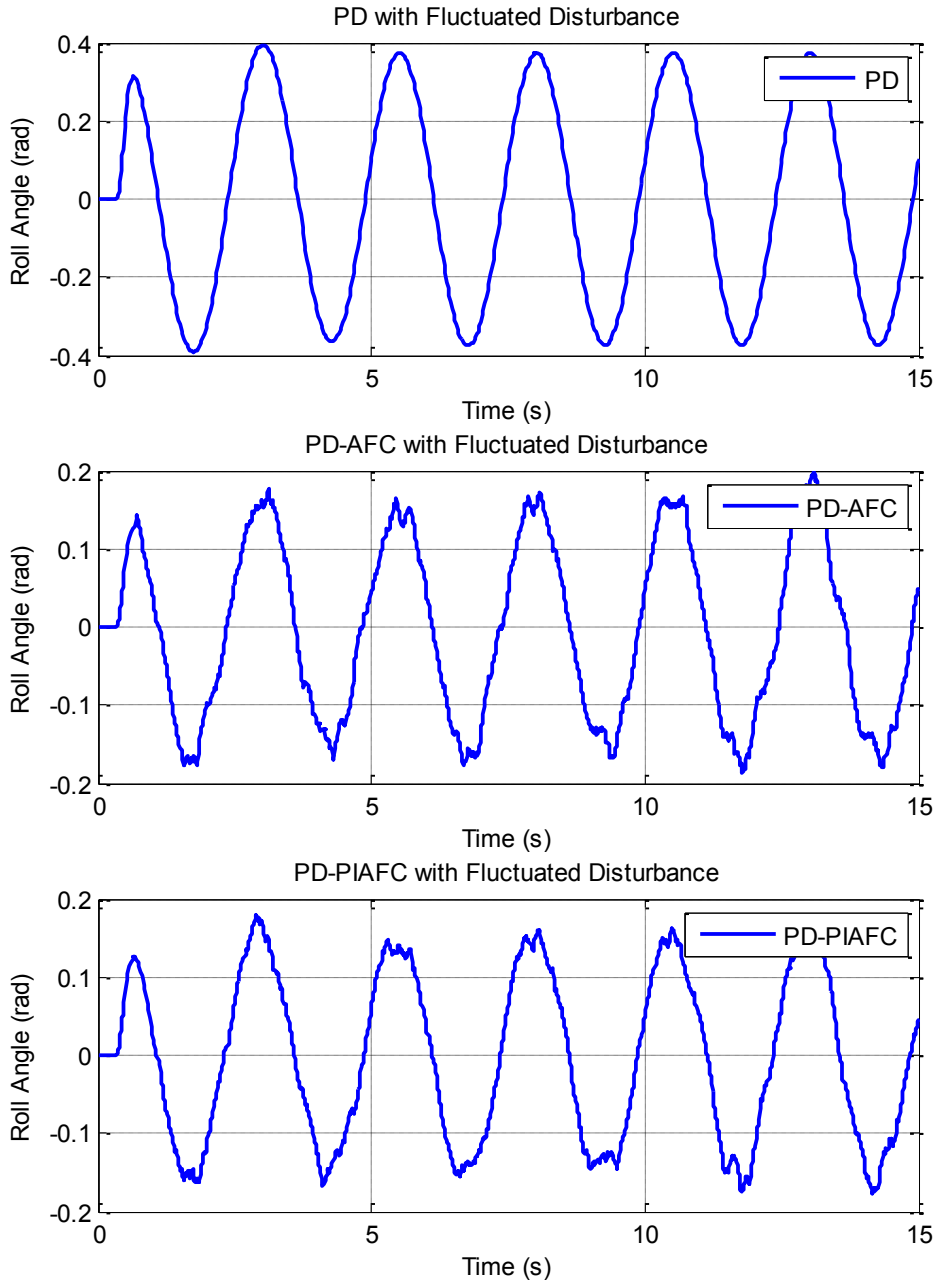

Figure 8. Fluctuated disturbance simulation result

Figure 8 shows the simulation result of PD method, PD-AFC, and PD-PIAFC method with fluctuated disturbance. In this simulation, PD maximum error is 0.4 radian. PD-AFC and PD-PIAFC give smaller error, 0.15 radian. PD-AFC noise more than PD-PIAFC. PD controller has RMS value 0.2586, PD-AFC is 0.1054, and PD-PIAFC is 0.1008. From RMS value, we can conclude PD-PIAFC give best result of controller.

From the simulation, PIAFC controller can minimize the effect of disturbance. In each simulation, PD-PIAFC gives best result. PD-PIAFC has lowest RMS value, 0.0389 for constant disturbance and 0.1008 for fluctuated disturbance.

6. CONCLUSION

An "x" configuration quadcopter has been succesfully modeled. Then, simulation results have been presented to show the controller performance. The simulation has succesfull give comparation about controller performance (PD, PD-AFC, PD-PIAFC) by calculate Root Mean Square (RMS) value. PD with AFC gives better result than PD. AFC optimization using PI (PD-PIAFC) give best result if compared with PD or PD-AFC. PD-PIAFC has lowest RMS value of result control signal, 0.0389 for constant disturbance and 0.1008 for fluctuated disturbance.

REFERENCES

[1] Gupte, Shweta, Paul Infant Teenu Mohandas, and James M. Conrad, **A survey of quadrotor Unmanned Aerial Vehicles**, *Proceedings of IEEE*. IEEE, , *Southeastcon*, pp. 1-6, 2012.

[2] Bouabdallah, Samir, Andre Noth, and Roland Siegwart, **PID vs LQ control techniques applied to an indoor micro quadrotor.** *Intelligent Robots and Systems, 2004.(IROS 2004). Proceedings. 2004 IEEE/RSJ International Conference on*. Vol. 3. IEEE, pp.2451-2456, 2004.

[3] Li, Jun, and Yuntang Li, **Dynamic analysis and PID control for a quadrotor**, *Mechatronics and Automation (ICMA), 2011 International Conference on*. IEEE, pp. 573-578, 2011.

[4] Mokhtari, Abdellah, and A. Benallegue, **Dynamic feedback controller of Euler angles and wind parameters estimation for a quadrotor unmanned aerial vehicle**, *Robotics and Automation, 2004. Proceedings. ICRA'04. 2004 IEEE International Conference on*. Vol. 3. IEEE, pp. 2359-2366, 2004.

[5] Erginer, Bora, and Erdinc Altug, **Modeling and PD control of a quadrotor VTOL vehicle**, *Intelligent Vehicles Symposium, 2007 IEEE*. IEEE, pp. 894-899, 2007.

[6] Pounds, Paul, Robert Mahony, and Peter Corke, **Modelling and control of a large quadrotor robot**, *Control Engineering Practice* 18.7 Elsevier, 2010, pp. 691-699, 2010.

[7] Sa, Inkyu, and Peter Corke, **Vertical infrastructure inspection using a quadcopter and shared autonomy control**, In *Field and Service Robotics*, pp. 219-232. Springer Berlin Heidelberg, 2014.
[8] Tayebi, A., and S. McGilvray, **Attitude stabilization of a four-rotor aerial robot**, *Decision and Control, 2004. CDC. 43rd IEEE Conference on*. Vol. 2. IEEE, pp. 1216-1221, 2004.
[9] Sumantri, Bambang, Naoki Uchiyama, Shigenori Sano, and Yuma Kawabata, **Robust Tracking Control of a Quad-Rotor Helicopter Utilizing Sliding Mode Control with a Nonlinear Sliding Surface**, *Journal of System Design and Dynamics* 7, no. 2, pp. 226-241, 2013.
[10] Ming Chen and Mihai Huzmezan, **A combined MBPC/2DOF H∞ controller for a quadrotor UAV**, *Proceeding of AIAA guidance, navigation, and control conference and exhibit*, Texas- USA, 11-14 August 2003.
[11] Estiko Rijanto, **Robust Control: Theory for Application**, ISBN: 979-9299-12-8, Bandung: ITB Press, 2000.
[12] Pitowarno, Endra, **An Implementation of A Knowledge-Based System Method to An Active Force Control Robotic Scheme**, *Master Thesis, Universiti Teknologi Malaysia,* 2006.
[13] Katsura, Seiichiro, Yuichi Matsumoto, and Kouhei Ohnishi, **Modeling of force sensing and validation of disturbance observer for force control**, *Industrial Electronics, IEEE Transactions on* 54, no. 1, pp. 530-538, 2007.
[14] Chen, Wen-Hua, **Disturbance observer based control for nonlinear systems**, *Mechatronics, IEEE/ASME Transactions on* 9, no. 4, pp. 706-710, 2004.
[15] Achtelik, Michael, Thomas Bierling, Jian Wang, Leonhard Höcht, and Florian Holzapfel, **Adaptive Control of a Quadcopter in the Presence of large/complete Parameter Uncertainties**, In *Infotech@ Aerospace 2011*, 2011.
[16] Bouabdallah, Samir, Pierpaolo Murrieri, and Roland Siegwart, **Design and control of an indoor micro quadrotor**, *Robotics and Automation, 2004. Proceedings. ICRA'04. 2004 IEEE International Conference on*. Vol. 5. IEEE, pp. 4393-4398, 2004.
[17] Benallegue, A., A. Mokhtari, and L. Fridman, **Feedback linearization and high order sliding mode observer for a quadrotor UAV**, *Variable Structure Systems, 2006. VSS'06. International Workshop on*. IEEE, pp. 365-372, 2006.
[18] Ni'am Tamami, Endra Pitowarno, I Gede Puja Astawa, **Modelling and PD Control for "x" Configuration Quadcopter**, *Indonesian Symposium on Robot Soccer Competition, 2013. Proceedings.* Dian Nuswantoro University. ISBN: 979-26-0264-X, Semarang: Dian Nuswantoro University Press, pp. 98-103, 2013.

EMITTER International Journal of Engineering Technology
Vol.2, No.1, June 2014
ISSN:2355-391X

Designing and Building of 3D Adventure Game "Tetuko: Childhood of Ghatotkacha" Using Kinect

Achmad Basuki, Jauari Akhmad NH, Jabbar Nendra Putra

Creative Industry Research Center
Politeknik Elektronika Negeri Surabaya
Kampus PENS, Jl. Raya ITS, Sukolilo, Surabaya
E-mail: basuki@pens.ac.id

Abstract

Nowadays, the young people are not interested in the local culture as a "wayang" puppet. This condition threatens the extinction of some of the local culture that should be a mainstay of the industry entering an era of creative industries. On the other hand, they are more interested in playing computer games as changing of people's lifestyles. It becomes our basic idea to produce a game as a creative product. The genre of this game is fighting-adventure. This game depictures a story of fighting between the baby Tetuko and giant Kala Pracona. The game uses Kinect and 3D platform technology to attract more players to feel their adventures. With Kinect technology, the player can control the character with his gesture. Thus, this game will increase the awareness of young people about the culture of Wayang.

Keywords: 3D game, kinect, kinect, adventure, local culture, creative industry.

1. INTRODUCTION

The "Wayang" puppet is a local culture that grows from generation to generation as part of Indonesian society. Puppet is a culture that consists of art, music and performances. Because of the two reasons above, the puppet can be one of the promising products in the creative industries in line with what is expressed by Marie Elka Pangestu [1].

In the story of Wayang, There is a famous figure. He is Ghatotkacha or Gatotkaca in Indonesian Language. Many people are familiar with this figure because he is strong and he can fly to the sky. Many young people do not know the story of Ghatotkacha's childhood. We conducted a small survey to find out how much the younger generations know Ghatotkacha figures. Our respondents were 20 students as a representative of young people on campus and the school. We asked about Tetuko, the childhood name of Ghatotkacha. It turned out that 19 of 20 respondents did not know this name.

This survey suggested that the culture of the puppet is not attractive to young people. It is our concern to try to make a product with Wayang background.

On the other hand, young children play computer games as the nowadays lifestyle. That's why the idea to include local cultural content in the game becomes an interesting research issue. Puput Windi [2] revealed that the RPG (Role Playing Game) games make players understand the story and the message conveyed in a game. RPG games could be a good choice to introduce the story of Wayang. Ayu Dyah Pramitasari [3] revealed that the classification of the game corresponding to the level of education would be a good approach to insert a value message. Mohammad Luthfi Folhalit [4] showed the 3D model of puppets with ARToolkit. The Augmented Reality had a huge potential in promoting the attaction of Wayang Kulit as one of the traditional art. Zainal [5] indicated that the level of one's knowledge about a culture may improve if he or she can get a chance to experience about that culture. So, the game with player experience is can be a promising way of preserving a culture.

Based on some of the review earlier, we propose to build a fighting-adventure game with 3D environment and the adventure story of Tetuko. This game has tittle "Tetuko: the childhood of Ghatotkacha". It contains an adventure story and fighting. With this genre, players feel the adventure Tetuko with his battles and plays according to the story. Finally, the player will get to know the story of Tetuko as the uniqueness of the story of Wayang. The young people will know the culture of Wayang as local culture [5].

This game uses the Kinect technology to control the character. Kinect technology is working on gesture recognition. Players control the character to perform movements. Kinect has affordances to create enjoyable, interesting interaction types, to boost player motivation, and to promote content via its multimedia and multi-sensory capacity [6]. In this game there are some basic movements to fight as hitting, kicking, jumping and defending. It makes the player feels a special sensation when plays this game.

2. RELATED WORKS

The educational history game is a kind of educational game that picked up the story in the history of the plot. This game generally will reconstruct and simulate historical story in the form of games so the user as if the actors were invited to witness even history. In this way the history of the material can be more easily absorbed by the user because it gives the impression that more than just reading books.

Galang W [7] proposed a board-game to lift folklore. In this game, the player can feel a social experience that is not found in many digital games. The key of this game is how the player experience to know the folklore. The game story has content about the story of the island of Java. The genre of this game is memory-game.

Fadilah Fahrul Hardiansyah [8] proposed JTME multiplayer game via Bluetooth to introduce Karapan Sapi. The multiplayer game has an advantage

in competitiveness between players. This game is an adventure game. Players play the avatar and get a pair of cows to be included in every game. The area represents the game with 4 cities of Madura such as Bangkalan, Sampang, Pamekasan, and Sumenep. To follow the race in town, players need to collect information from people who are in the city. With this game the player will know about the culture behind the story of Karapan Sapi.

Windi Puput [2] proposes a Role Playing Game (RPG) to introduce several kingdoms in Indonesian history as shown in figure 1. Target players are children. RPG genre makes players understand the storyline automatically while playing. This game requires the player character to play in accordance with the storyline. It makes this game is more successful in introducing the history of the kingdom because of the involvement of the players in the story.



Figure 1. RPG game of history of some kingdom on Indonesia

Dyah Ayu Pramitasari [3] proposed a multiplayer game of learning and the introduction of Indonesian culture for elementary school children grades 3-6 as shown in figure 2. This game offered a model approach the game in accordance with the level of education. This game trained the child's ability to master the Indonesian regions with wealth in it. Players can decide several options in resolving all game. The advantage of this game is the graphic model with cultural details.



Figure 2. Interface of cultural choices for playing

3. ORIGINALITY

Game "Tetuko's War" is a fighting-adventure game that tells the adventures and battles Tetuko, the childhood name of Ghatotkacha. This game uses the Kinect technology, so that the player can control the character Tetuko with gesture recognition. Thus the player really feel become Tetuko and his fights. Some movements adapted to the storyline in the story of Tetuko. Players can punch, kick and defend as Tetuko abilities.

This game is not only an alternative to introducing local cultural contents, but also provides an alternative user interface with attractive gesture recognition. This is a new trend that utilized several gaming companies to produce interactive and attractive games.

4. SYSTEM DESIGN

The system of game development is shown in figure 3. Games created using the Unity game engine, with Blender as a modeling engine, and ZDK Zigfu for the configuration of the character control. For general work process of the gameplay, the user must first perform a calibration of Kinect. The Kinect motion sensor which captures the user's body earlier, will be mapping it into rigging the character in gameplay that has been made.

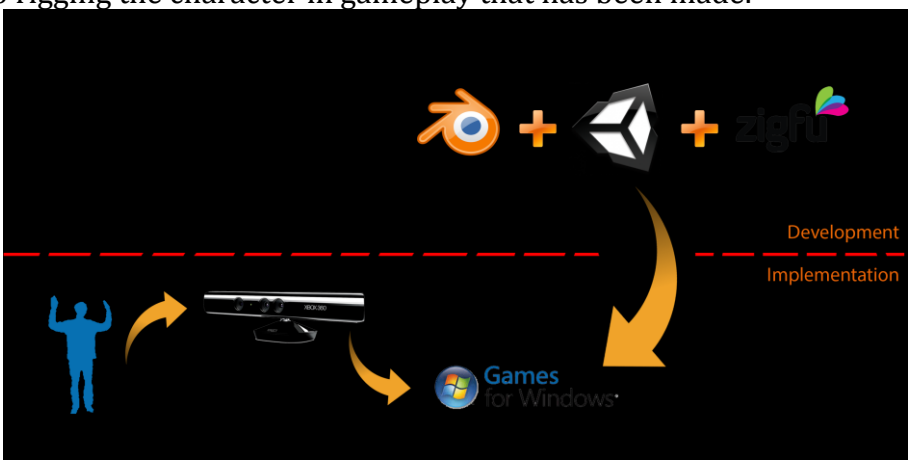

Figure 3. Game development

This game is a fighting-adventure game. There are two important points to make this game:

1. **Adventure**: the characters will interact with other characters to produce a story that can be understood by the player. At this stage, we build the characters and environments adapted on storyline of Tetuko.
2. **Battle**: Game uses gesture recognition to recognize and adjust to the movement of the player character movement based on the results of the calibration. Players can issue a motion offense and defense to defeat his enemies.

Tetuko's movement starts from the start point to the end point specified in the map. A player can not determine the route itself. The map

created in the form of terrain. In any terrain, there are some areas that have a Collider. Collider will call a certain function when passing through the region Tetuko character. Thus, the Collider is what will determine the route of a journey as shown in figure 4. Here is the Collider in question as shown in figure 5.



Figure 4. The entire map of journey

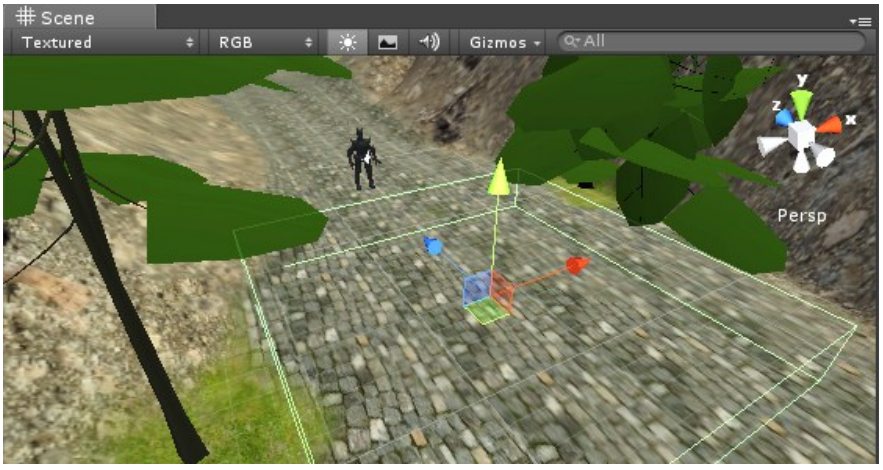

Figure 5. Collider when detect the enemy

The initial process of user-interaction of this game is the calibration process as shown in figure 6. The calibration process must be carried out prior to play. The distance between the player and the Kinect determine the success of the calibration process. In the calibration process the player to run some motion in the following order:

1. Systems detect the player (user detection).
2. Systems perform to detect the pose player.
3. The pose calibration system detects players.
4. Pose successful calibration.
5. Systems begin to detect the player's movements (user tracking).



Figure 6. Calibrating

There are two basic movements in the game, namely blocking and attacking. Blocking is done by moving the left hand. Attacking is done by moving the right hand.

1. **Blocking**: The part that should be exposed colliding first Tetuko is the left hand part, be exposed to new parts of the other. When exposed to enemy attack Tetuko left hand, automatically visible effects of particles. It shows that the character successfully blocking enemy attacks as shown in figure 7.



Figure 7. Blocking

2. **Attacking**: Doing attacking into the enemy, need a clear target. When the right-hand limb of the enemy character, will be seen the effects of fire-explosion particles as shown in figure 8. It shows that the character of successfully attacking the body toward the enemy.



Figure 8. Attacking

5. EXPERIMENT AND ANALYSIS

This experiment test all systems in this game. This game works with maximum performance when has the following specifications:

1) Intel(R) Core(TM) i3-238M CPU @ 2.30GHz (4 CPUs), ~2.3GHz
2) Memory 2048MB RAM
3) Windows 32 Bit
4) Kinect for Windows

5.1. Experiment on Calibration Process

The experiment result is shown in Table 1. It gives the results of the calibration column succeed/fail, whereas the results column will be filled with their effects on the results of the calibration of the character.

Table 1. Kinect's performance depend on disctance between player and kinect

#	Distance (m)	Status	Additional Description
1	0.8	Fail	No movement
2	1.0	Fail	No movement
3	1.2	Success	Character sways irregularly
4	1.4	Success	Character sways irregularly
5	1.6	Success	Character sways irregularly
6	1.8	Success	Hand difficult to move
7	2.0	Success	Hand difficult to move
8	2.2	Success	Ok
9	2.4	Success	Ok
10	2.6	Success	Ok
11	2.8	Success	Ok
12	3.0	Success	OK
13	3.2	Success	Hand difficult to move
14	3.4	Success	Hand difficult to move
15	3.6	Fail	No movement
16	3.8	Fail	No movement

The ideal distance between the player and Kinect sensor in order to capture the motion of the user's body is along the 1.2 - 3.4 m. Outside of that,

the Kinect motion sensor can not read the user's body. Meanwhile, at a distance of 1.2 - 3.4 m itself produces the mapping sensors to different characters also. The distance is too far or too close from the Kinect, kinect can not be made properly recognize the gesture.

5.2. User's Opinion

In this experiment, we perform the test with 10 people aged between 18-21 years old tester to give an opinion about this game. Tester unlimited game play, then we conduct direct interviews form of easy to control, the story, the quality of graphics and technology implementation. Interview results can be seen in Table 2.

Table 2. Interview results

#	Easy to control	Understanding of story	Graphic Quality	Implementation of Technology
1	Hard	Easy	Good	Interested
2	Hard	Easy	Good	Ordinary
3	Hard	Easy	Good	Ordinary
4	Hard	Normal	Good	Interested
5	Hard	Easy	Good	Interested
6	Middle	Easy	Good	Interested
7	Hard	Normal	Good	Interested
8	Hard	Easy	Good	Ordinary
9	Middle	Easy	Good	Interested
10	Hard	Difficult	Good	Ordinary

Based on interview data, 8 of 10 agree that this game is still hard to control properly. They stated that it is not easy to move according to the movement of the character in the story. But 9 out of 10 agree that this game managed to convey the message that there is a moral to the story. The moral of the story is a way of Tetuko. They become familiar figure Tetuko as one of the characters in Wayang culture. They agree that the quality of the graphics in this game is incredible. Lastly, they stated that the idea of the author to create a game with the Kinect technology can be quite interesting because the technology is still relatively new.

6. CONCLUSION

Based on the experiment, we conclude that:

1) Kinect on figthing-adventure game is a new way to play game.
2) The ideal distance for optimal gesture sensor from the player and Kinect is 1.2 – 3.4 m.
3) The Kinect makes the game becomes more difficult to control but still interesting.

REFERENCES

[1] Marie Elka Pangestu, **Pengembangan Indutri Kreatif Menuju Visi Ekonomi Kreatif Indonesia 2025**, Deperindag 2011.

[2] Puput Windi S, **Design of The RPG game for history of Indonesia's Kingdom With Java Language Learning For Kids and Teens**, Final Project, Politeknik Elektronika Negeri Surabaya, 2010.

[3] Ayu Dyah Pramitasari, **Multiplayer Game for Learning and Knowing The Indonesian Culture for 5-6th Elementary School**, Final Project, Politeknik Elektronika Negeri Surabaya, 2010.

[4] Mohamad Lutfi Dolhalit, Mohd Zulkhairul Hafiz Mat Jun, Ahmad Naim Hanapi and Farah Nadia Azman, **The Development of Shadow Play Wayang Kulit Using Augmented Reality**, International Journal of Interactive Digital Media, Vol. 1(2).

[5] Zainal A. Hasibuan, Yugo K.Isal, Baginda Anggun N.C., Mubarik Ahmad, and Nungki Selviandro, **Preservation of Cultural Heritage and Natural History through Game Based Learning**, International Journal of Machine Learning and Computing, Vol. 1, No. 5, December 2011.

[6] Hui-mei Justina Hsu, **The Potential of Kinect in Education**, International Journal of Information and Education Technology, Vol. 1, No. 5, December 2011.

[7] Galang W., **Perancangan Board-game Adaptasi Cerita Rakyat sebagai Media Edukasi Untuk Siswa Kelas 3 Sekolah Dasar**, Final Project, Desain Komunikasi Visual, Institut Seni Indonesia Yogyakarta, 2013.

[8] Fadiliah Fahrul Hardiansyah, **Karapan Sapi J2ME Multiplayer Game Via Blueetooth**, Final Project, Politeknik Elektronika Negeri Surabaya, 2011.

EMITTER International Journal of Engineering Technology
Vol.2, No.1, June 2014
ISSN: 2355-391X

Performance Analysis of an OFDM PHY Scheme with Zero Forcing Equalizer Using Software Defined Radio Platform and USRP

Ahmad Zainudin, Amang Sudarsono, I Gede Puja Astawa

Postgraduate Applied Engineering of Technology
Division of Electrical Engineering, Dept. of Electrical Engineering
Electronic Engineering Polytechnic Institute of Surabaya (EEPIS)
Kampus PENS, Jalan Raya ITS, Sukolilo 60111, Indonesia
Email : {zai, amang, puja}@pens.ac.id

Abstract

We present an implementation of Zero Forcing (ZF) equalizer in OFDM scheme using Software Defined Radio platform whereas NI USRP-2920 as the Radio Frequency (RF) front-end. ZF equalizer is employed to achieve reliable system at the receiver. Center frequency used for data transmission is 915 MHz. The reliability transmission and the performance of ZF equalizer are measured in term of different symbol mapping (i.e., M-PSK and M-QAM). The IQ rate determines the bandwidth available, whereas good performance is achieved with IQ rate less than 1 MHz. ZF equalizer achieves good performance when using BPSK, QPSK and 16-QAM modulation techniques. By applying ZF equalizer, bit error on BPSK and QPSK modulations can be reduced from 29,16% and 39,06% into 0%. This advantage of ZF equalizer also is able to press the bit error on 16-QAM and 64-QAM modulations into 3,125% and 8,85%, respectively.

Keywords: OFDM, SDR, USRP, Zero Forcing Equalizer

1. INTRODUCTION

Recently, demand of bandwidth is increasing, especially for mobile devices. Orthogonal Frequency Division Multiplexing (OFDM) is introduced as one of solutions to enable bandwidth efficiency and robustness due to intersymbol inteference (ISI) in the consequence of multipath fading environment [1]. The principle of OFDM is dividing high rate data stream into parallel low rate data streams using Fast Fourier Transform (FFT)[2]. Moreover, OFDM scheme is widely used in wireless communication system, such as IEEE 802.11 standard, cellular communication (e.g., WiMAX and LTE Advanced) and digital broadcasting standard (e.g., DVB-T). In addition, OFDM is combined by modulation with more bits per symbol to increase data

Copyright © 2014 EMITTER International Journal of Engineering Technology - Published by EEPIS

transmission throughput. OFDM has been successfuly implemented in wireless communication due to its advantages of reliability communication in multipath environment. However, OFDM system has the problem in dealing with ISI effect particularly for the high data rate transmission. An equalizer is required to combat intersymbol inteference when OFDM symbol time is larger than delay spread. The implementation of equalizer requires more hardware complexity. The used of Software Defined Radio (SDR) can reduce hardware investment, due to the hardware implementation is changed into a software configuration.

SDR is a choice of wireless implementation because of its easier, faster and cheaper implementation favored. SDR is able to change hardware components (i.e., modulator, demodulator, filter, detector, equalizer, multiplexing/demultiplexing, and amplifier) into a software configuration in personal PC or embedded system. This benefit is able to decrease hardware investment along with the complexity of wireless technologies. SDR comprises baseband processing, Analog to Digital Converter (ADC)/Digital to Analog Converter (DAC) and RF front end. Universal Software Radio Periperal (USRP) is front end part which can be used for good performance in wireless implementation. The main goal of SDR platform is not only cost reduction, but also increasing of the flexibility signal processing parameters [3].

In this paper, we introduce an implementation of ZF equalizer in OFDM system. The NI USRP-2920 tranceivers are used as RF front-end and LabVIEW SDR platform control system. The reliability system and the performance of ZF equalizer are observed. From experimental results, using ZF equalizer on BPSK and QPSK modulations can reduce bit error from 29,16% and 39,06% into 0%. This advantage also can press bit error on 16-QAM and 64-QAM modulations into 3,125% and 8,85%, respectively. The layout of this paper is organized as follows, firstly, we describe the introduction of OFDM. Then, SDR and USRP are described in the first Section. In Section 2, the implementation OFDM is detail explained. The experimental results and analysis are presented in Section 3. And finally, our conclusion is drawn in Section 4.

2. RELATED WORKS

Currently, several studies of OFDM implementation using SDR and USRP have been taken in account. An OFDM system by using BPSK and QPSK modulation techniques and utilizing GNU Radio and USRP are implemented by [4-7] with good performance be achieved by QPSK rather than BPSK modulation. In these experiments are used basic OFDM system. Data streams still are generated from random bits source. The reliability system is ignored. In the [7] Bit Error Rate (BER) performance versus Signal to Noice Ratio (SNR) is compaired between Matlab simulation and real implementation experimental result. The performance result of simulation and

implementation are not exactly the same. In the real experiment is difficult to measure the exact SNR value. The reliable transmission is offered [8] with employe Forward Error Correction (FEC). The performance of FEC is poor if the SNR lower than the threshold. Whereas, the noise environment are variants in real implementation system. The other algorithm is proposed [9] use a simple subcarrier blinding algorithm to compensate phase error. The worse performance is due to higher phase noise of the oscillator as internal reference clock. The performance of Zero Forcing equalizer with BPSK modulation is observed by [10] using matlab simulation. This equalizer can remove the effect of ISI when the channel is noiseless. The ZF equalizer performance is poor when the channel is noisly. ZF performance for single carrier and uncode OFDM is compared [11]. ZF-Single Carrier has better performance than the uncode OFDM.

3. ORIGINALITY

This paper presents a practical performance analysis of OFDM scheme. The OFDM transceiver is sucessfully contructed using LabVIEW platform and NI USRP-2920 as RF front-end. Reliability of the system is observed based on the symbol received constelation in the receiver side. The text file is sent over wireless medium with the 915 MHz. Moreover, a simple Zero Forcing (ZF) equalizer is employed on receiver side to combat for Inter Symbol Inteference (ISI). Unequalized and equalized data constellation are compared to determine equalizer performance used.

4. SYSTEM DESIGN

This system constructed OFDM scheme with employee Zero Forcing (ZF) equalizer in the receiver. Equalizer is used to combat ISI effect and can increase of reliable system. The algorithm is observed in real implementation system use USRP as RF front-end and SDR platform.

4.1 Orthogonal Frequency Division Multiplexing (OFDM) Scheme

OFDM is multiplexing scheme which divide data stream became more narrowband data channel to share the bandwidth available. Narrowband channel is called subcarrier which transmit phase or amplitude modulated data signal. Different with Frequency Division Multiplexing (FDM), OFDM have subcarrier that orthogonality. This orthogonality can reduce inteference between subcarrier and increase spectrum efficiency utilization. OFDM receiver require frequency synchonization to combat Inter-Carrier Interference (ICI). This inteference occurs caused by Doppler shift due the mobile device movement and multipath channel[2].

Data bits stream are converted from serial to parallel and each subcarrier is modulated using phase or amplitude modulation. Modulation prosses is called as symbol mapping. Each subcarrier is independently

modulated using. Then, all the modulated signal are carried by OFDM carrier use IFFT module to create complex signal containing all subcarrier. Data paraller stream is converted to serial stream and real and imaginer signal respectively are processed on Digital to Analog Converter (DAC). Both analog signal are multiplied by radio frequency with shift it's phase 90^0 and summing both. This signal will transmit over antenna. Figure 1 shows the diagram of OFDM system. The receiver will receive real and imaginer signal separately and they are processed by low pass filter to eliminate mirrored frequencies. Then, they are quantized by Analog to Digital Converter (ADC) block and the signal is calculated by Fast Fourier Transform (FFT) module. The data symbols are demodulated by symbol mapping block according to the modulation used. Parallel data stream is converted into data serial to obtain the desired data.

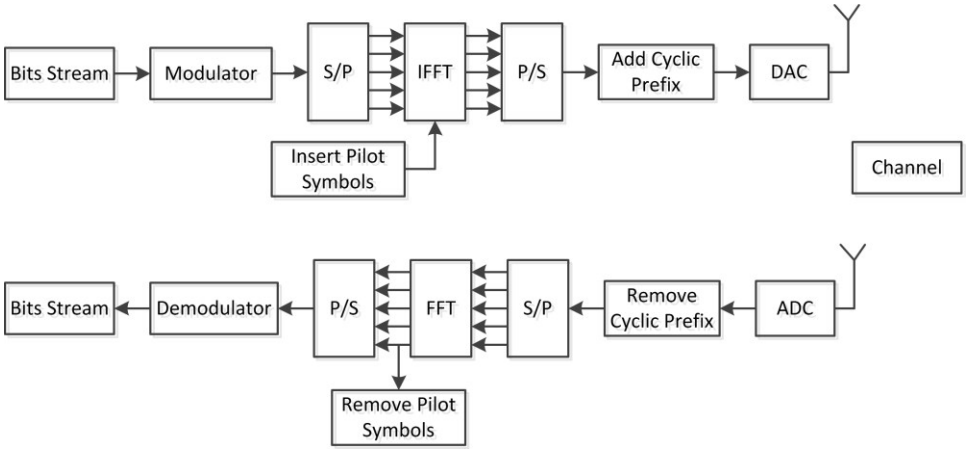

Figure 1. Block Diagram of OFDM Transmission System

Received signal will be received many times due multipath propagation specially in urban environment or mobile device are moving high speed. Line of sight and multipath signal have difference arrival time. It is called delay spread which can cause Inter Symbol Inteference (ISI). OFDM scheme proposes to reduce of ISI effect provided that can preserve orthogonality. Orthogonality OFDM subcarrier can be achieved with addition of guard time (guard interval). The OFDM guard time can be do by insert zero padding (ZP) or cyclic prefix (CP). CP is to extend the OFDM symbol by copying the last samples of the OFDM symbol into its front. CP is introduced before the OFDM symbol. Let T_G denote the length of CP and T_{sub} denote the duration of OFDM symbol without guard time. So, the extended OFDM symbols now have the duration of $T_{sym}=T_{sub}+T_G$. Guard time is selected longer than multipath delay so as not to cause inteference with the next OFDM symbol. The other advantage of CP is combating Inter Carrier Inteference (ICI) which is crosstalk between subcarriers.

OFDM system needs synchronization in the receiver side to find the beginning of each symbols corectly. Synchronization parameters include finding the right time delay, frequency deviation and phase shift of each symbols in the subcarrier. These parameters can be determined with addition redundancy in some of the subcarriers which transsmitted. The redundancy is called pilot symbol or preamble. The parameters are known by looking pilot signal from data received and will be calculated for synchronization and channel estimation process. The density of pilots detemine quality of synchronization but decrease of data rate transmission.

4.2 Zero Forcing (ZF) Equalizer

Equalization is employed to combat inter symbol inteference which occur if OFDM symbol time is larger than delay spread. Equalizer is a filter that use an approximated inverse of channel frequency response or channel estimation[2]. ZF is a simple frequency domain equalizer can reduce of ISI effects, but it will greatly affected of inhancing the noise power. The ZF employ channel estimation (H_{est}) and generally based on pilot subcarrier frequency. Let $s(n)$ denote the bits squence from text file and the $\hat{s}(n)$ denote the data estimation. The equation of ZF can expresed as

$$\hat{s}(n) = s(n) * \frac{1}{H_{est}} \quad (1)$$

4.3 Software Defined Radio (SDR)

SDR is block communication system such as modulation, demodulation, filter, encoding and decoding, source coding, channel coding, ect, are provided as software code in the PC or embedded systems. These technologies help the researcher and provider to reduce the hardware investment to implement and examine the new standard communication or algorithm enhancement[12]. The implementation is more flexible, all radio paramaters are set through software configure for same radio device to be operated with any type of waveform. This contributes to development and research easier, faster and cheaper. There are several type SDR platform which widely implemented in the wireless communication research community, such as LabVIEW and opensource GNU Radio. LabVIEW is a data flow graphical programming language designed fo several application (i.e. control, measurement and RF communication)[13]. GNU Radio is an open source software for digital signal processing (DSP) function that was developed using C++ (low-level code) and python (high-level code) programming. SDR architecture for transmitter and receiver is illustrated as Figure 2.

For transmit the data computer host generate complex digital baseband signal. Wideband data converters cannot support the processing bandwidth and dynamic range required across different wireless standards. As a result, the analog-to-digital converter (ADC) and the digital-to-analog converter

(DAC) are usually operated at intermediate frequency (IF). In digital IF block there are three processes before through the DAC block. The first DUC (Digital Upconverter) process which baseband signal is filtered and interpolated before it is quadrature modulated with a tunable carrier frequency. Second process is Crest Factor Reduction (CFR) and then Digital Predistortion (DPD) which is linearization techniques. High-speed mobile data versions employ non-constant envelope modulation techniques such as quadrature phase shift keying (QPSK) and quadrature amplitude modulation (QAM), so linearity is needed on the power amplifiers. Digital IF is converted to analog signal through DAC block. Then, the signal is multiplied by local oscillator and through Power Amplifier (PA) then transmitted over antenna.

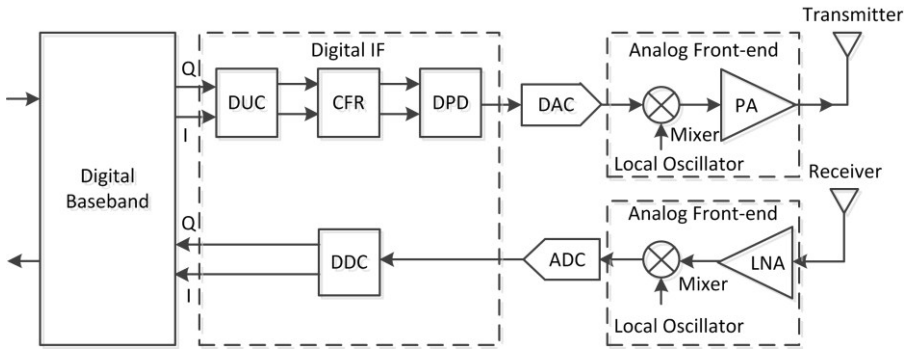

Figure 2. SDR Architecture for Transmitter and Receiver

4.4 Universal Software Radio Peripheral (USRP)

SDR implementation use USRP which hardware device that as a RF front end. USRP is now supported in Simulink and LabVIEW [14]. The USRP consist of an FPGA, A/D and D/A, RF daugther board, and an interface to the host port. USRP devices are manufactured by Ettus Research and National Instrumen (NI). Ettus issue several of USRP's types, such as USRP bus serries (first generation), embedded serries and network serries (second generation). The first generation if USRPs use USB 2.0 connection with PC host which provides up to ≈ 30 MHz. But the second generation use gigabit ethernet up to 50 MHz and is powered by a 6 VDC[15]. The second generation widely used for real time implementation wireless communication such as USRP2 and USRP N210. For So with same device can be used for several band frequencies.

Recently, NI has manufactured several USRP's types. USRP NI-2920 and USRP NI-2921 widely implemented with combining LabVIEW software. The NI-2920 can be used for several wireless applications including white space, broadcast FM, public safety, land-mobile, low-power unlicensed device (ISM) bands, sensor networks, cell phones, amateur radio and GPS. The NI USRP-2920 has frequency range of 50 MHz to 2,2 GHz. On other hand, USRP NI-2921 has frequency range of 2.4 to 2.5 GHz and 4.9 to 5.9 GHz, for

implemention of low-power unlicensed devices on industrial, scientific and medical (ISM) bands at 2.45 GHz or 5.8 GHz[16].

5. IMPLEMENTATION

OFDM PHY is contructed in this system. OFDM transceiver are implemented use NI USRP-2920 and LabVIEW platform. On transmitter side, the initalize process begins with open the session of USRP hardware. In this process is determined USRP IP's used. After that, configuring the signal such as determining IQ rate, carrier frequency, gain and active antenna. The next step is encodig the file source. Read from binary file function is used to read text file with the return string data form. String data is converted became byte array data. Byte array is unpacked to obtain bits 0's and 1's with decide 8 bits per integer. Bit stream 0's and 1's through mapper symbols appropriate modulation used. BPSK symbol consists 1 bit, 2 bits for QPSK, 4 bits form 16-QAM and 6 bits for 64-QAM. Mapping symbol is determined considered a type modulation scheme.

The OFDM symbols are constructed from 48 data symbols (48 pts per OFDM symbol). The pilot symbols are inserted after every 12th data symbol (52 pts per OFDM symbol). Pilot symbols are used to handle channel estimation. Zero padding are placed at the edges (6 zeroes as start symbol and 5 zeroes as stop symbol respectively) and 1 zero at DC carrier (64 pts per OFDM symbol). Performe a Inverse FFT to convert the frequency domain signals to the time domain. Insert a ¼ cyclic prefix by duplicating the last 16 point OFDM symbol and are placed at beginning (80 pts per OFDM symbol). Then the digital signals are converted to analog signals. Transmit the signals using a USRP as RF front end. The transmission process can be seen at figure 3 and 4.

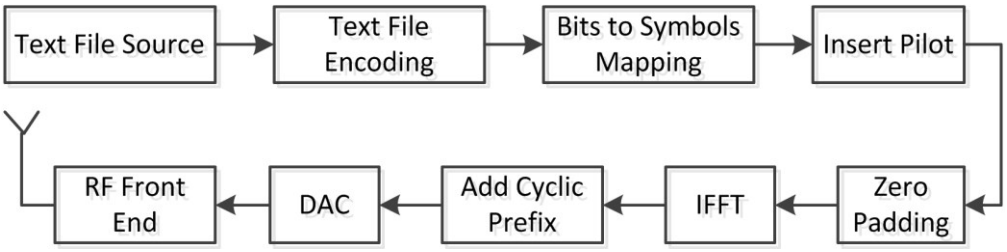

Figure 3. Transmission process at transmitter side

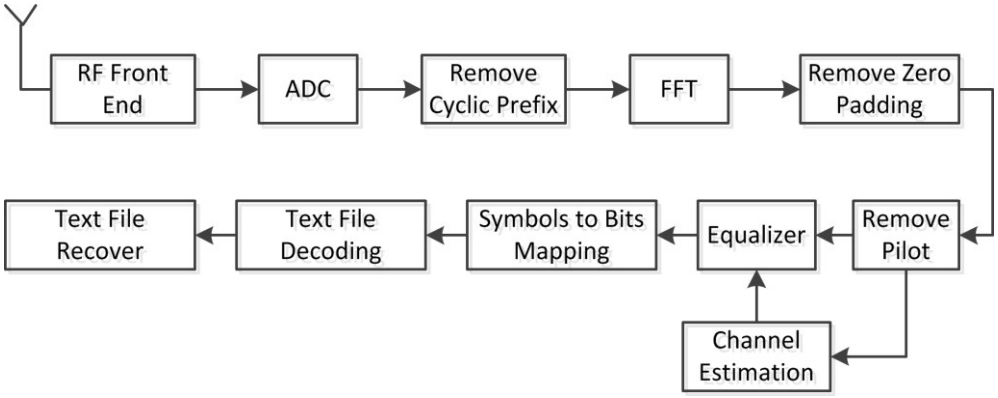

Figure 4. Transmission process at receiver side

The signals are received and converted to digital signals. In this process begins USRP initalize with open Rx session and signal configure. USRP IP's, gain and active antenna are determined. IQ rate and carrier parameters are same with transmitter configure. The cyclic prefix and offset frequency are removed and the signals are converted to frequency domain through FFT process. Guard band (zero padding) are remove at OFDM symbol edges, respectively. Pilot symbols removing is used as channel estimation reference. The multiple of data and channel estimation invers will obtain equalized data. Bits stream be obtained after through symbols to bits mapping block. The sum of bits generated corresponding with modulation mapping used. The binary file is read and create text file use text file decoding. The OFDM parameters is shown at Table 1.

Table 1. Parameters of OFDM PHY design

Parameter	Value
FFT size (N_{FFT})	64
Number of data subcarrier	48
Number of pilot subcarrier	4
Number of start zero padding subcarrier	6
Number of stop zero padding subcarrier	5
Number of DC carrier subcarrier	1
Cyclic prefix (CP) ratio	¼
Number of total subcarrier	80
Center frequency	915 MHz

6. EXPERIMENT AND ANALYSIS

The performance measurement of OFDM system which is constructed includes : the reliability of image transmission using several modulation (i.e BPSK, QPSK, 16-QAM and 64-QAM), the data rate transmission and the performance of Zero Forcing (ZF) equalizer is observed based on constellation diagram on the receiver side. The text file is sent with file size 1 KB.

6.1 The reliability of text file transmission measurement

The purpose of this step to observe the reliability of OFDM system which cronstructed. The text file be sent from one NI USRP-2920 to another use 915 MHz center frequency wit FFT length 64. The system is observed on indoor enviroment. The OFDM spectrum can be seen at figure 3. The frequency band of the spectrum depending on In phase and Quadrature IQ rate used. IQ sampling rate is sampling frequency ($\frac{F_s}{2}$) and determine of bandwidth avalible. In this experiment is used IQ rate 2 MHz. The figure shows that DC carrier is in the middle on carrier ($\frac{N}{2}$) where N is FFT length used. If the IQ rate is incresed, spectrum bandwidth will go up too. Figure 4 shows the spectrum with different IQ rate. The greater of the IQ rate used, the computation of computer host is increasing too. This phenomenon will be felt when one computer host control several USRP (e.g. transmitter and receiver).

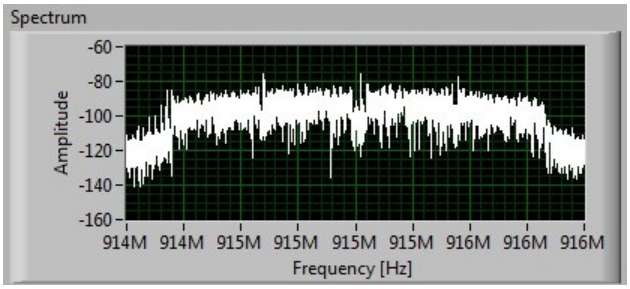

Figure 3. The spectrum of OFDM signal with IQ rate 2 MHz

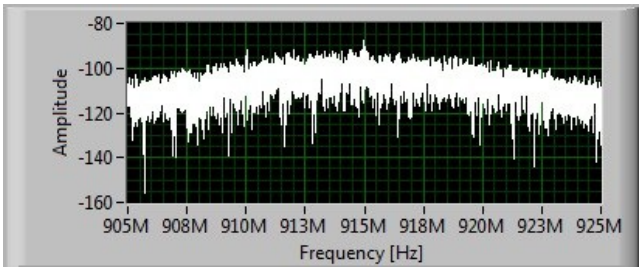

Figure 4. The spectrum of OFDM signal with IQ rate 20 MHz

The NI USRP-2920 has available bandwidth up to 40 MHz[21]. The next step will be observed of comparison the IQ rate with the reliability of transmission. The IQ rate is increased and the data accuracy is observed based on constellation diagram. The Table 2 shows the constellation diagram with different IQ rate and are modulated using QPSK. The reliability system is achieved when use IQ rate less than 1MHz. When the IQ rate is more than 1 MHz, the error data which received increase. Although the NI USRP-2920 support transmits and receives bandwidth up to 40 MHz.

Table 2. Comparison of constellation diagram with different IQ rate

IQ rate	Constellation	IQ rate	Constellation
50kHz	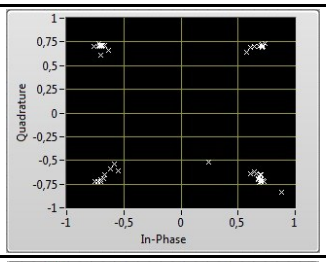	2MHz	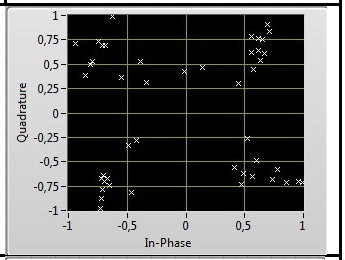
100kHz	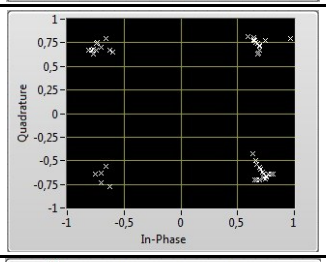	5MHz	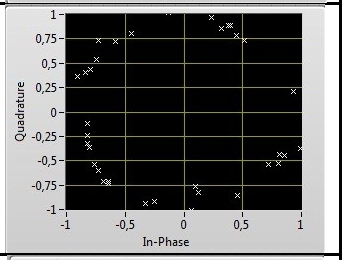
200kHz	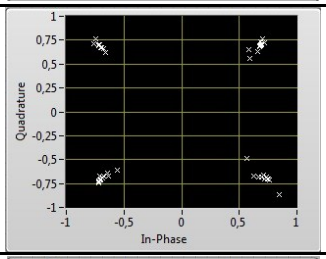	10MHz	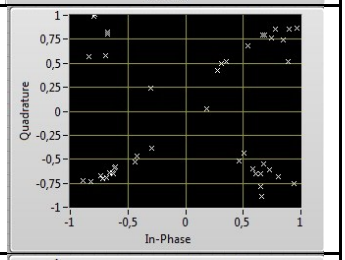
500kHz	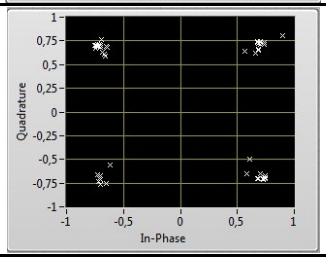	20MHz	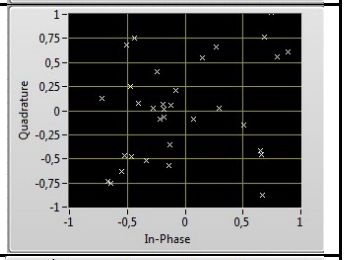
1MHz	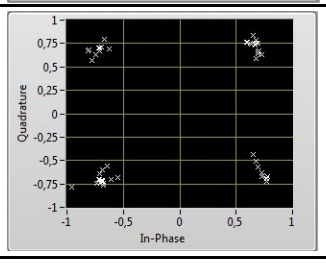	40MHz	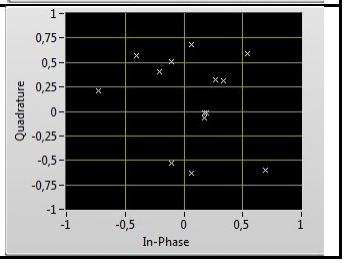

6.2 The performance of Zero Forcing (ZF) equalizer

The equalizer is used to combat ISI which making the communication less reliable. The performance of equalizer can be observed based on the accuracy of contellation diagram on the receiver side. In this experiment use IQ rate 200kHz. Comparison of contellation diagram for several modulation is shown in Table 3. The good performance of ZF equalizer is achieved when is modulated using BPSK, QPSK and 16-QAM. The good performance is achieved because these modulation are resistant with noise. The poor performance

occur when use 64-QAM. The more error data are received when this modulation is used. The performance system can be increasing with more complexity equalizer or non linear equalizer.

Table 3. Comparison of constellation diagram using ZF equalizer for several modulation

Modulation	Transmitter	Unequalized	ZF equalizer
BPSK	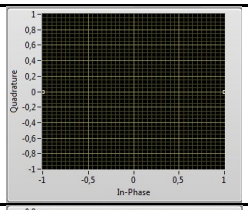	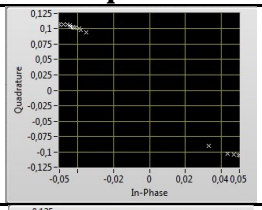	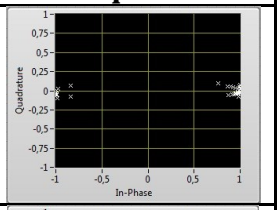
QPSK	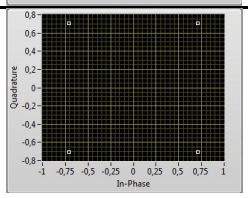	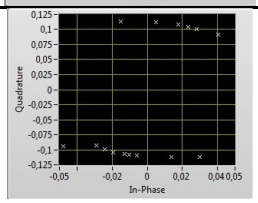	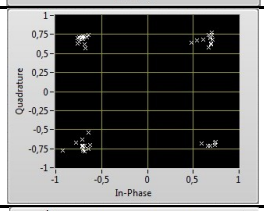
16-QAM	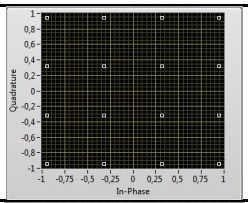	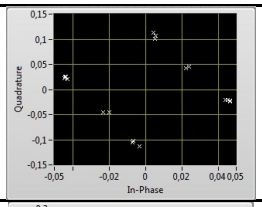	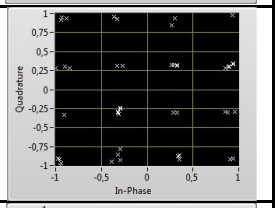
64-QAM	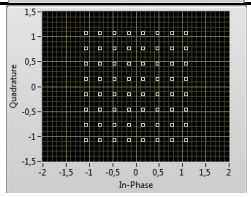	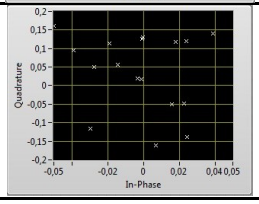	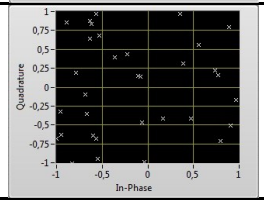

The ZF equalizer can be used for error correction of the data. The performance of ZF equalizer is also observed based on bit error of text file sent for several modulation. The bit error be obtained with comparing of text file source and text file recover. The compairing of bit error for unqualized data and use ZF equalizer with several modulation is shown at figure 5. With use ZF equalizer can reduce bit error from 29,16% into 0% when use BPSK modulation. As well as when use QPSK modulation, bit error can be pressed with same value from 39,06 %. Whereas, the bit error began to increase when 16-QAM and 64-QAM modulation used, became 3,125% and 8,85%. But this error is not so large when compared with unequalized on same modulation. The bit error achieve 44,79% and 53,125% when equalizer is not used.

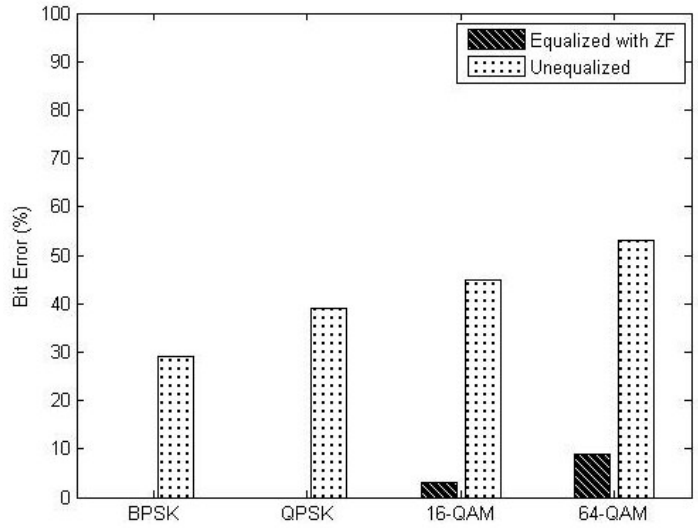

Figure 5. The compairing of bit error for unequalized data and use ZF equalizer

7. CONCLUSION AND FUTURE WORK

A LabVIEW application has been developed to implement OFDM communication system use BPSK, QPSK, 16-QAM and 64-QAM modulation. Moreover, ZF equalizer is employed to achieve reliable system. The IQ rate determine the bandwidth available, but in this experiment good performance is achieved with IQ rate less than 1 MHz. BPSK, QPSK and 16-QAM are more resistant with noise enviroment than 64-QAM. The good performance of ZF equalizer is achieved when is modulated using BPSK, QPSK and 16-QAM. By applying ZF equalizer can reduce bit error from 29,16% and 39,06% into 0% when use BPSK and QPSK modulation. Whereas, the bit error can be pressed became 3,125% and 8,85% when 16-QAM and 64-QAM modulation be used. Next experiment will constructed OFDM PHY scheme with MMSE equalizer to increase the reliability OFDM system which be implemented use USRP as RF front end.

REFERENCES

[1] Y. Sun, **Bandwidth-Efficient Wireless OFDM**, IEEE Journal on selected area in Communication, Vol. 19, No. 11, November 2001

[2] M. Ergen, **Mobile Broadband Including WiMAX and LTE**, pp109, ISBN: 978-0-387-68189-4, New York, USA, Springer Science+Business Media, LLC 2009

[3] S. Costanzo, F. Spadafora, A. Borgia, H. O. Moreno, A. Costanzo, G. Di Massa, **High Resolution Software Defined Radar System for Target Detection**, Journal of Electrical and Computer Engineering, Volume 2013

[4] A. Marwanto, M. A. Sarijari, N. Fisal, S. K. S. Yusof, R. A. Rashid, **Experimental Study of OFDM Implementation Utilizing GNU Radio and USRP-SDR**, Procceding of the 2009 IEEE 9th Malaysia International Conference on Communication, pp. 132-135,ISSN:978-1-4244-5532-4, Kuala Lumpur, Malaysia,15-17 December 2009

[5] Abirami M, Gandhiraj R, Soman K. P, **Performance Analysis of Real Time OFDM Based Communication System Using GNU Radio and USRP,** International Journal of Advanced Research in Computer Science and Software Engineering, ISSN : 2277 128X, Volume 3, June 2013

[6] A. Y. F. Youssef, K. M. H. Hassan, M. G. Mostafa, M. T. Saad, M. Khairy, **Implementation of a wireless OFDM system using USRP2 and USRP N210 Kits**,Graduation Project Report,Faculty of Engineering,Cairo University,Giza,Egypt,July 2012

[7] I. Kardaras, A. Liavas, **Software-Defined Radio Implementation of an OFDM Link**, Master of Science, Technical University of Crete, Department of Electronic and Computer Engineering, 2010

[8] A. Kaschub, C. Muller, M. Proebster, T. Werthmann, M. Schmidt, **Design and implementation of an OFDM-based communication system for the GNU Radio platform**, Master Thesis, Institut fur Kommunikationsnetze und Rechnersysteme, Universitat Stuttgart. Germany, 2009

[9] G. Berardinelli, P. Zetterberg, O. Tonelli, **An SDR Architecture for OFDM Transmission over USRP2 Boards,** Signals, Systems and Computers IEEE Conference, pp 965-969, ISSN : 1058-6393, Pacific Grove, CA, 6-9 Nov 2011

[10] A. Kanchan, S. Dwivedi, **Comparison of BER Performance in OFDM Using Different Equalization Techniques,** International Journal of Engineering and Advanced Technology (IJEAT), ISSN:2249-8958, Volume-1, Issue-6, August 2012

[11] S. Ohno, **Performance of Zero-Forcing Equalizer for Single-Carrier Zero-Padded Transmissions Over Multipath Fading Channels,** IEEE International Conference on Acoustics, Speech, and Signal Processing (ICASSP '04), pp IV-1017-IV-1020,ISSN:1520-6149,2004

[12] A. Zainudin, A. Sudarsono, I. G. P. Astawa, **Reliability Analysis of Digital Communication for Various Data Types Transmission Using GNU Radio and USRP**, Industrial Electronic Seminar (IES) 2013,pp 91-96, ISBN 978-602-9494-87-7, Electronics Engineering Polytechnic Institute of Surabaya,2013

[13] A. Gupta, A. Forenza, R. W. Hearth Jr., **Rapid MIMO-OFDM Software Defined Radio System Prototyping**, pp 182-187, Signal Processing System IEEE Conference,2004

[14] E. Grayver, **Implementing Software Defined Radio**,pp 145,Springer Science + Business Media, New York,2013

[15] **Ettus Research Data sheet**, USRP, USRP N210, http:www.ettus.com, accessible April, 2014

[16] **National Instrument Data sheet**, NI USRP-2920, NI USRP-2921, http:indonesia.ni.com, accessible April, 2014

EMITTER International Journal of Engineering Technology
Vol.2, No.1, June 2014
ISSN:2355-391X

Reinforced Intrusion Detection Using Pursuit Reinforcement Competitive Learning

Indah Yulia Prafitaning Tiyas, Ali Ridho Barakbah, Tri Harsono, Amang Sudarsono

Postgraduate Applied Engineering of Technology
Division of Information and Computer Engineering, Department of Information and Computer Engineering, Electronic Engineering Polytechnic Institute of Surabaya
EEPIS Campus, Jalan Raya ITS, Sukolilo 60111, Indonesia
Email: indahyuliap@yahoo.com, ridho@eepis-its.edu, trison@eepis-its.edu, amang@eepis-its.edu

Abstract

Today, information technology is growing rapidly, all information can be obtained much easier. It raises some new problems, one of them is unauthorized access to the system. We need a reliable network security system that is resistant to a variety of attacks against the system. Therefore, Intrusion Detection System (IDS) required to overcome the problems of intrusions. Many researches have been done on intrusion detection using classification methods. Classification methods have high precision, but it takes efforts to determine an appropriate classification model to the classification problem. In this paper, we propose a new reinforced approach to detect intrusion with On-line Clustering using Reinforcement Learning. Reinforcement Learning is a new paradigm in machine learning which involves interaction with the environment. It works with reward and punishment mechanism to achieve solution. We apply the Reinforcement Learning to the intrusion detection problem with considering competitive learning using Pursuit Reinforcement Competitive Learning (PRCL). Based on the experimental result, PRCL can detect intrusions in real time with high accuracy (99.816% for DoS, 95.015% for Probe, 94.731% for R2L and 99.373% for U2R) and high speed (44 ms). The proposed approach can help network administrators to detect intrusion, so the computer network security system become reliable.

Keywords: Intrusion Detection System, On-Line Clustering, Reinforcement Learning, Unsupervised Learning.

1. INTRODUCTION

Based on data compiled by CERT [11], the number of intrusions from year to year is increase. From 1995 to 2008, the total attack was summarized by CERT is 46.156, as illustrated in figure 1.a.

Copyright © 2013 EMITTER International Journal of Engineering Technology - Published by EEPIS

Meanwhile, according to data analyzed by Carnegie Mellon University (2002) and Idaho National Laboratory (2005), intruder technical knowledge decreases, as illustrated in Figure 1.b.

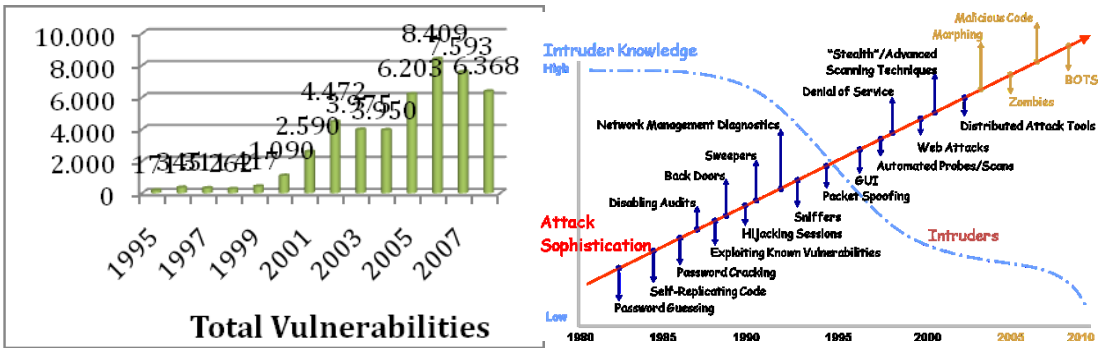

a. The number of intrusions summarized by CERT[11]

b. Decreasing intruder technical knowledge[12]

Figure 1. The number of intrusions and intruder technical knowledge

Therefore, Intrusion Detection System (IDS) required to overcome the problems of intrusion. The system that detects and logs illegal access is called as intrusion detection system [7]. Intrusion detection system consists of three categories, there are host-based, network-based and vulnerability assessment-based. Host-based where information is found on a single or multiple host systems. Network-based that examines the information captured from network communications. Vulnerability assessment-based identify vulnerabilities in internal networks and firewall. The functionality intrusion detection classified into two as anomaly detection and misuse detection.

Misuse detection is a system that works by comparing the packet traffic on the computer network with signature database. The weakness of misuse detection is not able to detect any new attacks because the attack was not found in the signature database such that late in detecting the attack. In addition, the administrator must manually update signature database. Anomaly detection is a system that comparing the packet traffic on the computer network with a normal traffic pattern, but it has the disadvantage of sending a lot of false positives and can be fooled by the actual attack. Anomaly detection will identify how much bandwidth, protocol, ports that are normally used. If the system detects an abnormal, it will send alerts to the administrator.

There are four categories of attacks, namely Denial Of Service (DOS), Remote to local (R2L), User to Root (U2R) and Probe with the following explanation [7]:

- Denial of Service (DOS) Attacks: DOS attack is an attack where as the attacker creates a few calculations or memory resource completely engaged or out of stock to handle authentic requirements, or reject justifiable users the right to utilize a machine.
- User to Root (U2R) Attacks: These are a category of attack where an attacker begins by accessing normal user account in the system (maybe attained by hunting the passwords, by social engineering or by attacking dictionary) and get advantage of several vulnerability to accomplish root entrée to the system.
- Remote to local (R2L) Attacks: R2L attack occurs when an intruder who has the potential to send packets to a system/machine over a network without having an account in that system/machine, makes use of a few vulnerability to accomplish local access as a client of that system/machine.
- Probes (PROBE) Attack: Probing is a collection of attacks where an attacker scrutinizes a network to gather information or to conclude prominent vulnerabilities.

2. RELATED WORKS

Many researches in intrusion detection have been done using various techniques. A brief description of some researches that inspire us, such as:

A. M. Chandrashekhar and K. Raghuveer [7], "Fortification of Hybrid Intrusion Detection System Using Varians of Neural Networks and Support Vector Machines" (January, 2013) proposed hybrid intrusion detection system which combining Fuzzy C-Means, Neuro-Fuzzy Classifier (NF), SVM Vector Generator and Radial Basis Function (RBF) SVM. The accuracy rate reaches 98.94% for DOS attack and 97% for the other attack types (Probe, U2R, R2L).

A. S. Aneetha and Dr S. Bose [5], "The Combined Approach for Anomaly Detection using Neural Networks and Clustering Techniques" (August, 2012) proposed hybrid intrusion detection system which combining Self Organizing Map (SOM that has been modified) with Fuzzy K-Means Clustering. The accuracy rate reaches 98.5% for DOS attack.

Prof. Dr. Kais Said Al-Sabbagh [6], "Development an Anomaly Network Intrusion Detection System Using Neural Network" (December, 2012) proposed Self Organizing Map (SOM) to improve payload anomaly detector (PAYL). The proposed system improve the models recognition ability in the PAYL detector, for a filtered unencrypted HTTP subset traffic of DARPA 1999 dataset, from 55.234% in the PAYL system alone to 99.94% in the proposed system. In addition, SOM decreases the ratio of false positive from 44.676% in the PAYL stand alone system to 5.176% in the proposed system.

Shaker Reyadh Namh Naoum and Zainab Al-Sultani [8], "Hybrid System of Learning Vector Quantization and Enhanced Resilient Back-propagation Artificial Neural Network Classification for Intrusion" (February, 2013) proposed a hybrid intrusion detection system that combines methods Learning Vector Quantization (LVQ) and Enhanced Resilient Back-

propagation Artificial Neural Network. The level of accuracy reached 98.4 % for DoS , 99.59 % for Probe , 96.4 % for R2L , 70.3 % for U2R.

Amir Azimi Alasti Ahrabi, Kaveh Feyzi, Zahra Atashbar Orang, Hadi Bahrbegi, and Elnaz Safarzadeh [2], "Using Learning Vector Quantization in Alert Management of Intrusion Detection System" (2012) proposed a new alert management system by using Learning Vector Quantization (LVQ).

Reyadh Shaker Naoum and Zainab Namh Al-Sultani[3], "Learning Vector Quantization (LVQ) and k-Nearest Neighbor for Intrusion Classification" (2012) proposed hybrid intrusion detection system which combining Learning Vector Quantization artificial neural network with k-Nearest Neighbor approach to detect intrusion. Hybrid (LVQ-kNN) was able to classify the datasets into five classes at learning rate 0.09 using 23 hidden neurons with classification rate about 89%.

Kyaw Thet Khaing [1], "Enhanced Features Ranking and Selection using Recursive Feature Elimination (RFE) and k-Nearest Neighbor Algorithms in Support Vector Machine for Intrusion Detection System" (June, 2010) proposed hybrid intrusion detection system which combining enhanced SVM, Recursive Feature Elimination (RFE) and k-Nearest Neighbor (KNN) to detect intrusion. The improvement precision is only 0.4% on average, but the improvement for false negative rate are between 16.2% and 28.8%. The experimental results are precision = 99.91%, false negative = 5.49%, time execution = 77.85 second.

Nitin Mohan Sharma, Tapan P. Gondaliya [9], "Enhance IDS False Alarm Filtering Using KNN Classifier" (May, 2013) proposed k-Nearest Neighbor (KNN) classifier to reduce the number of false alarms. KNN classifier successfully reduces up to 93% of false alarms generated by famous IDS.

3. ORIGINALITY

Intrusion Detection System (IDS) is a software or hardware used to detect unauthorized access of a computer system or network [4]. Many research have done using classification method. Classification methods have high precision, but need appropriate classification model and need long time to classify intrusions.

In this paper we propose a new reinforced approach for detecting intrusions using On-Line Clustering which can perform clustering in real-time with high accuracy in detecting intrusions. We use Pursuit Reinforcement Competitive Learning (PRCL) [10] to perform On-Line Clustering.

PRCL proposed by Ali Ridho Barakbah & Kohei Arai [10], is expected to detect new attacks in realtime with higher speed and higher accuracy than previous research and can help network administrators to detect intrusion, so the computer network security system become reliable.

4. SYSTEM DESIGN

The proposed system consists of 3 phases: (1) Data pre-processing phase, (2) PRCL algorithm and (3) Performance evaluation phase.

Here is a Block Diagram System shown in Figure 2.

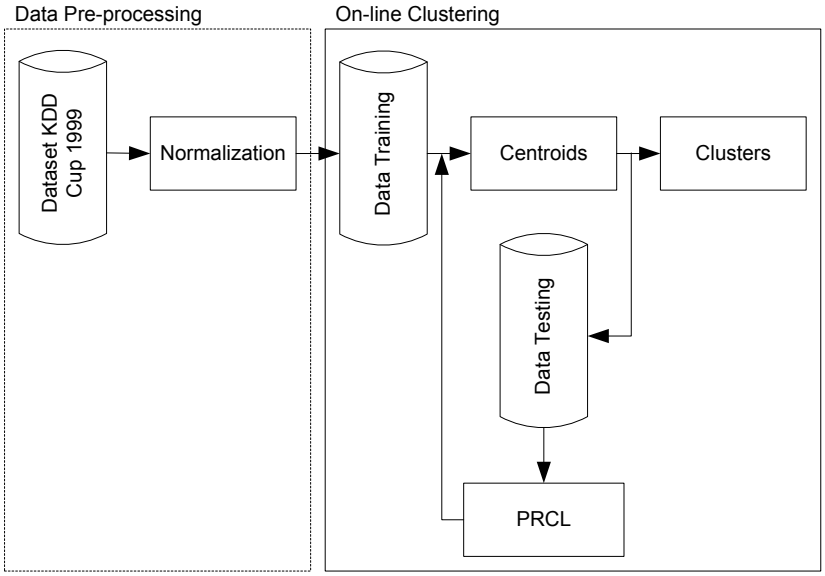

Figure 2. Block diagram system

4.1. Data Pre-processing Phase

The proposed system will be trained using 10% KDD Cup 1999 dataset. The total dataset of 10% KDD Cup is 494.021 with composition (DOS=391.458, Normal=97.278, Probe=4.107, R2L=1.126, U2R=52). KDD Cup 1999 dataset consists of moderately around 5 million vectors single correlation vectors, where each single connection vector consisting of 41 features and is marked as a normal or an attack, through accurately one particular attack type [7].

4.2. PRCL Algorithm

In this phase, we use Pursuit Reinforcement Competitive Learning (PRCL) to detect intrusions. The algorithm of PRCL is described as follows [4]:

a. First of all, we determine the winning unit i^* from:

$$d_{i^*} = \arg\min_i d(x, w_i) \quad (1)$$

b. Update the reward track of x for all weights, as follows:

$$r(x, w_{ij}) = r(x, w_{ij}) + \beta\,(1 - r(xj, w_{ij})) \text{ if } i = i^*$$

and $$r(x, w_{ij}) = r(x, w_{ij}) + \beta\,(0 - r(xj, w_{ij})) \text{ if } i \neq i^* \quad (2)$$

c. Select the winning i^* from maximizing the reward as :

$$w_{i^*} = \arg\max_i r(x, w_i) \quad (3)$$

d. Update the weight vectors as follows:

$$\Delta w_{ij} = a\,(x_j - w_{ij}) \quad \text{if } i = i^*$$

and $$\Delta w_{ij} = 0 \quad \text{if } i \neq i^* \quad (4)$$

where a is learning rate, β is reward rate, d is distance, r is reward, x is new data.

4.3. Performance Evaluation Phase

We use accuracy to evaluate the performance of the proposed system. Firstly, we calculate confusion matrix, such as: True Positive (TP), False Negative (FN), True Negative (TN) and False Positive (FP). The table 1.a explains the confusion matrix. Table 1.b explains the definition of TP, TN, FP, FN.

Table 1. Confusion matrix and definition [1]

a. Confusion matrix

Confusion Matrix			
		Predicted Class Intrusion	
		Yes	No
Actual Class Intrusion	Yes	True Positive	False Negative
	No	False Positive	True Negative

b. Definition

Definitions
TP and TN: True Positive and True Negative are correct classifications.
FP: False Positive occurs when the result is envisaged as positive when it is actually negative.
FN: False Negative occurs when the result is envisaged as negative when it is actually positive.

The performance of a binary classification test is statistically measured by precision and recall. The proportion of actual positives which are correctly recognized is calculated by recall. The overall accuracy is calculated by using precision, recall and F-measure which are generally used to estimate the rare class prediction. It is advantageous to achieve a high recall devoid of loss of precision. Harmonic mean of precision and recall is called as F-measure. The equation used for Recall, Precision, F-measure and overall Accuracy is described as follows [7]:

$$\text{Accuracy} = (TN+TP) / (TN+TP+FN+FP) \quad (5)$$

5. EXPERIMENT AND ANALYSIS

In this paper we compare PRCL with Learning Vector Quantization (LVQ), Reinforcement Guided Competitive Learning (RGCL), and Sustained Reinforcement Guided Competitive Learning (SRGCL).

Vector quantization is one example of competitive learning [4]. Vector quantization is a method used to have the network "discover" structure in the data by finding how the data is clustered.

Reinforcement Guided Competitive Learning (RGCL), proposed by A. Likas, is a new method to solve on-line clustering problem using Reinforcement Learning [10].

Sustained RGCL is the modification of RGCL that employs the above weight update scheme. It will be called the SRGCL algorithm (Sustained RGCL) [10].

PRCL, LVQ, RGCL, SRGCL, and SVM will be trained using 10% KDD Cup 1999 dataset. We use 100000 data points with composition: normal=25000 and intrusion= 75000 (DOS=69715, Probe=4107, R2L=1126, U2R=52). The number of cluster=5 (0=Normal, 1=DoS, 2=Probe, 3=R2L, 4=U2R).

PRCL, LVQ, RGCL, SRGCL, and SVM will be tested using learning rate (alpha) = 0.1, 0.05, 0.01, 0.005, 0.001, 0.0005, and 0.0001. The following are the results of an experiment of PRCL, LVQ, RGCL, and SRGCL using learning rate (alpha) = 0.1, 0.05, 0.01, 0.005, 0.001, 0.0005, 0.0001 and data composition = Random-Minimum, Sequential, Random-Maximum.

The accuracy of intrusions detection between LVQ, RGCL, PRCL, and SRGCL with data composition (Random–Minimum, Sequential, Random–Maximum) illustrated in Figure 3.

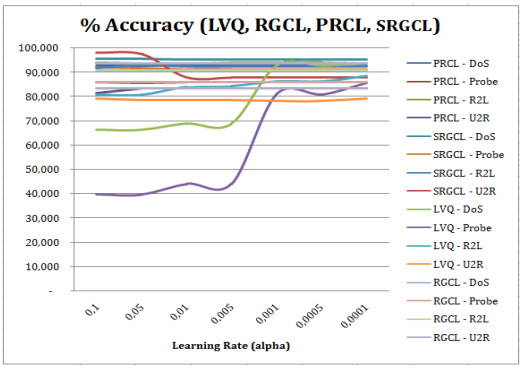

a. Random – Minimum

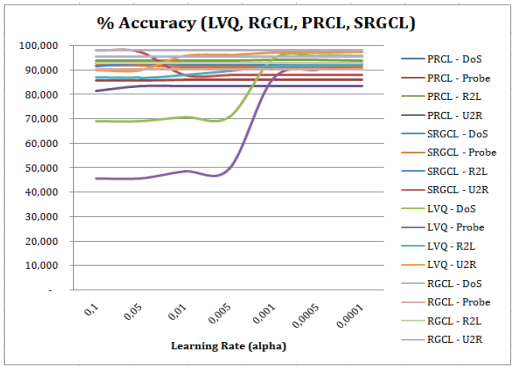

b. Random - Sequential

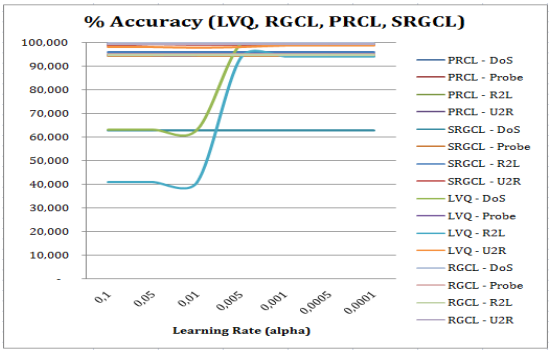

a. Random – Maximum

Figure 3. Accuracy of intrusions detection between LVQ, RGCL, PRCL, and SRGCL

The experimental results of random - minimum explain that almost all algorithms stable when alpha = 0.0001 (Figure 3.a). The experimental results of random - sequential explain that almost all algorithms stable when alpha = 0.0001, 0.0005 (Figure 3.b). The experimental results of random – maximum explain that almost all algorithms stable when alpha = 0.0001, 0.0005, 0.001 (Figure 3.c). The experimental results of random – minimum, random – sequential, random - maximum explain that the smaller learning rate (alpha), the accuracy will be better.

The accuracy of intrusions detection using PRCL higher than SRGCL but SRGCL more stable than PRCL. PRCL stable when beta=0.0001 and learning rate=0.0005, 0.0001, while SRGCL stable when beta=0.0001 and learning rate=0.001, 0.0005, 0.0001. The accuracy of intrusions detection using PRCL almost same with LVQ, but PRCL more stable than LVQ when learning rate=0.0005, 0.0001. The accuracy of intrusions detection using PRCL almost same with RGCL but RGCL more stable than PRCL. PRCL stable when learning rate (alpha)=0.0005, 0.0001, while RGCL stable when learning rate (alpha)=0.01, 0.005, 0.001, 0.0005, 0.0001.

The following are the results of a comparison between LVQ, RGCL, SRGCL, PRCL, SVM with data composition = Random-Maximum illustrated in Table 2.

Table 2. Comparison accuracy and processing time measurement (ms) of intrusions detection between LVQ, RGCL, SRGCL, PRCL, and SVM

Technique	DoS (%)	Probe (%)	R2L (%)	U2R (%)	Time (ms)
LVQ (On-Line Clustering)	99.843	95.038	94.174	98.847	39
RGCL (On-Line Clustering)	99.844	95.042	94.659	99.373	60
SRGCL (On-Line Clustering)	62.946	94.424	95.974	99.263	83
PRCL (On-Line Clustering)	99.816	95.015	94.731	99.373	44
SVM (Classification)	99.996	99.804	99.690	99.836	5050

The experimental results shown in Table 2 explain that smaller learning rate (alpha), the accuracy of LVQ, RGCL, SRGCL, PRCL will be better. PRCL achieves high accuracy (99.816% for DOS, 95.015% for Probe, 94.731% for R2L and 99.373% for U2R) when learning rate (alpha) = 0.0001, beta=0.001, 0.0005, 0.0001 and data composition=Random-Maximum. SRGCL achieves high accuracy (62.946% for DOS, 94.424% for Probe, 95.974% for R2L and 99.263% for U2R) when learning rate (alpha)=0.0001, beta=0.0001 and data composition=Random-Maximum. LVQ achieves high accuracy (99.843% for DOS, 95.038% for Probe, 94.174% for R2L and 98.847% for U2R) when learning rate (alpha)=0.0001 and data composition=Random-Maximum. RGCL achieves high accuracy (99.844% for DOS, 95.042% for Probe,

94.659% for R2L and 99.373% for U2R) when learning rate (alpha)=0.0001 and data composition=Random-Maximum. SVM achieves high accuracy (99.996% for DOS, 99.804% for Probe, 99.690% for R2L, and 99.836% for U2R).

The result of a comparison explains that :

- ✓ The accuracy of intrusions detection using PRCL almost same with LVQ but PRCL more stable than LVQ, beside LVQ faster than PRCL.
- ✓ The accuracy of intrusions detection using PRCL almost same with RGCL but PRCL faster than RGCL.
- ✓ The accuracy of intrusions detection using PRCL higher and faster than SRGCL.
- ✓ The accuracy of intrusions detection using PRCL lower than SVM but PRCL faster than SVM.

6. CONCLUSION

This paper presents a new reinforced approach to detect intrusion using On-Line Clustering which can perform clustering in real-time with high accuracy in detecting intrusions. We use Pursuit Reinforcement Competitive Learning (PRCL) to perform On-Line Clustering.

This proposed approach was examined with KDD Cup dataset. From experimental study, the proposed approach achieves high accuracy (99.816% for DOS, 95.015% for Probe, 94.731% for R2L and 99.373% for U2R) and high speed (44 ms) when learning rate (alpha) = 0.0001, beta=0.001, 0.0005, 0.0001. SRGCL achieves high accuracy (62.946% for DOS, 94.424% for Probe, 95.974% for R2L and 99.263% for U2R) and high speed (83 ms) when learning rate (alpha)=0.0001, beta=0.0001. LVQ achieves high accuracy (99.843% for DOS, 95.038% for Probe, 94.174% for R2L and 98.847% for U2R) and high speed (39 ms) when learning rate (alpha)=0.0001. RGCL achieves high accuracy (99.844% for DOS, 95.042% for Probe, 94.659% for R2L and 99.373% for U2R) and high speed (60 ms) when learning rate (alpha)=0.0001. SVM achieves high accuracy (99.996% for DOS, 99.804% for Probe, 99.690% for R2L, and 99.836% for U2R) and low speed (5050 ms). Data composition of all algorithms=Random–Maximum.

The accuracy of intrusions detection using PRCL higher than SRGCL but SRGCL more stable than PRCL. The accuracy of intrusions detection of LVQ almost same with RGCL but RGCL more stable than LVQ. The accuracy of intrusions detection PRCL almost same with LVQ but PRCL more stable than LVQ. In this paper, we also compare PRCL (On-Line Clustering) with SVM (Classification). The experimental results explain that the accuracy of intrusions detection using PRCL lower than SVM but PRCL faster than SVM.

In this paper our proposed reinforced approach to detect intrusion with PRCL perform shown high performance in speed and accuracy comparing to the other algorithm.

REFERENCES

[1] Kyaw Thet Khaing, **Enhanced Features Ranking and Selection using Recursive Feature Elimination(RFE) and k-Nearest Neighbor Algorithms in Support Vector Machine for Intrusion Detection System**, *International Journal of Network and Mobile Technologies* Vol. 1, Issue 1, pp. 1832-6758, June 2010.

[2] Amir Azimi Alasti, Kaveh Feyzi, Zahra Atashbar Orang, Hadi Bahrbegi, Elnaz Safarzadeh, **Using Learning Vector Quantization in Alert Management of Intrusion Detection System**, *International Journal of Computer Science and Security (IJCSS),* Vol. 6, Issue. 2, 2012.

[3] Reyadh Shaker Naoum, Zainab Namh Al-Sultani, **Learning Vector Quantization (LVQ) and k-Nearest Neighbor for Intrusion Classification**, *World of Computer Science and Information Technology Journal (WCSIT),* Vol. 2, No. 3, pp. 105-109, 2012.

[4] Manoj Sharma, Keshav Jindal, Ashish Kumar, **Intrusion Detection System using Bayesian Approach for Wireless Network**, *International Journal of Computer Applications*, Volume 48– No.5, pp. 0975 – 888, June 2012.

[5] A. S. Aneetha and Dr. S. Bose, **The Combined Approach for Anomaly Detection using Neural Networks and Clustering Techniques**, *Computer Science & Engineering An International (CSEIJ)*, Vol.2, No.4, pp. 37-46, August, 2012.

[6] Prof. Dr. Kais Said Al-Sabbagh, Assist. Prof. Hamid M. Ali, Elaf Sabah Abbas, **Development an Anomaly Network Intrusion Detection System Using Neural Network**, *Journal of Engineering*, Vol. 18, No. 12, pp. 1325-1334, December, 2012.

[7] A. M. Chandrashekhar, K. Raghuveer, **Fortification of Hybrid Intrusion Detection System Using Variants of Neural Networks and Support Vector Machines**, *International Journal of Network Security & Its Applications (IJNSA)*, Vol.5, No.1, pp. 71-90, January, 2013.

[8] Reyadh Shaker Naoum, Zainab Namh Al-Sultani, **Hibrid System of Learning Vector Quantization and Enhanced Resilient Backpropagation Artificial Neural Network for Intrusion Classification**, *International Journal of Research and Reviews in Applied Sciences (IJRRAS)*, Vol. 14, No. 2, February 2013.

[9] Nitin Mohan Sharma, Tapan P. Gondaliya, **Enhance IDS False Alarm Filtering Using KNN Classifier**, International Journal of Emerging Research in Management & Technology, Vol. 2, Issue 5, pp. 2278-9359, May 2013.

[10] Ali Ridho Barakbah, Kohei Arai, **Pursuit Reinforcement Competitive Learning,** *Information and Communication Technology Seminar (ICTS)*, 2006.

[11] http://www.cert.org/stats/ [accessed on July 28th, 2013] .

[12] www.cert.org/archive/pdf/CERTCC_**Vulnerability_Discovery**.pdf [accessed on July 28th, 2013].

EMITTER International Journal of Engineering Technology
Vol.2, No.1, June 2014
ISSN:2355-391X

Centronit: Initial Centroid Designation Algorithm for K-Means Clustering

Ali Ridho Barakbah[1] and Kohei Arai[2]

[1]Electronic Engineering Polytechnic Institute of Surabaya
Jalan Raya ITS Surabaya 60111, Indonesia
E-mail: ridho@pens.ac.id

[2]Department of Information Science
Saga University, 1 Honjo, Saga 840-8502, Japan
E-mail: arai@is.saga-u.ac.jp

Abstract

Clustering performance of the K-means highly depends on the correctness of initial centroids. Usually initial centroids for the K-means clustering are determined randomly so that the determined initial centers may cause to reach the nearest local minima, not the global optimum. In this paper, we propose an algorithm, called as Centronit, for designation of initial centroid optimization of K-means clustering. The proposed algorithm is based on the calculation of the average distance of the nearest data inside region of the minimum distance. The initial centroids can be designated by the lowest average distance of each data. The minimum distance is set by calculating the average distance between the data. This method is also robust from outliers of data. The experimental results show effectiveness of the proposed method to improve the clustering results with the K-means clustering.

Keywords: K-means clustering, initial centroids, K-means optimization.

1. Introduction

Clustering is an effort to classify similar objects in the same groups. Cluster analysis constructs good cluster when the members of a cluster have a high degree of similarity each other (internal homogeneity) and are not like members of other clusters (external homogeneity) [1][2]. It means the process to define a mapping $f:D \rightarrow C$ from some data $D=\{d_1, d_2, ..., d_n\}$ to some clusters $C=\{c_1, c_2, ..., c_n\}$ on similarity between d_i. The applications of clustering is diversely in many fields such as data mining, pattern recognition, image classification, biological sciences, marketing, city-planning, document retrievals, etc.

The most well known, widely used and fast methods for clustering is K-means clustering developed by Mac Queen in 1967. The simplicity of K-means clustering made this algorithm used in various fields. K-means

Copyright © 2013 EMITTER International Journal of Engineering Technology - Published by EEPIS

clustering is a partitioning clustering method that separates data into k mutually excessive groups. Through such the iterative partitioning, K-means clustering minimizes the sum of distance from each data to its clusters. K-means clustering is very popular because of its ability to cluster a kind of huge data, and also outliers, quickly and efficiently. It remains a basic framework for developing numerical or conceptual clustering systems because various possibilities of distance and prototype choice [3].

However, K-means clustering is very sensitive to the designated initial starting points as cluster centers. K-means clustering generates initial clusters randomly. If a randomly designated initial starting point close to a final cluster center, then K-means clustering can find the final cluster center. It, however, is not always. If a designated initial point is far from the final cluster center, it will lead to incorrect clustering results [4]. Because of initial starting points generated randomly, K-means clustering does not guarantee the unique clustering results [5]. K-means clustering is difficult to reach global optimum, but only to one of local minima [6].

2. RELATED WORKS

Several methods proposed to solve the cluster initialization for K-means clustering. A recursive method for initializing the means by running K clustering problems is discussed by Duda and Hart (1973). A variation of this method consists of taking the entire data into account and then randomly perturbing it *k* times [5]. Bradley and Fayyad [7] proposed an algorithm that refines initial points by analyzing distribution of the data and probability of data density. Penã et al. [8] presented empirical comparison for the initialization methods for K-means clustering and concluded that the random and Kaufman initialization method outperformed the other two methods with respect to the effectiveness and the robustness of K-means clustering. Shehroz and Ahmad [5] proposed Cluster Center Initialization Algorithm (CCIA) to solve cluster initialization problem. CCIA is based on two observations, which some patterns are very similar to each other. It initiates with calculating mean and standard deviation for data attributes, and then separates the data with normal curve into certain partition. CCIA uses K-means and density-based multi scale data condensation to observe the similarity of data patterns before finding out the final initial clusters. The experimental results of CCIA performed the effectiveness and robustness of this method to solve the several clustering problems.

3. ORIGINALITY

In this paper, we propose a new approach, called as Centronit, to designate initial centroids for K-Means clustering. Centronit is based on the calculation of data density inside the certain range of data distribution. Centronit does not involve probabilistic variables at all so that it produces the constant clustering results. Moreover, because of reflecting the data distribution, Centronit is robust for outliers.

4. DESIGN SYSTEM

4.1 Basic Theory of K-means Clustering

Let $A=\{a_i \mid i=1, ..., n\}$ be attributes of n-dimensional vector and $X=\{x_i \mid i=1, ..., r\}$ be each data of A. The K-means clustering separates X into k partitions called clusters $S=\{s_i \mid i=1, ..., k\}$ where M∈X is $M=\{m_i \mid i=1, ..., n(s_i)\}$ as members of S. Each cluster has cluster center of $C=\{c_i \mid i=1, ..., k\}$.

K-means clustering algorithm can be described as follows:

1. Initiate its algorithm by generating random starting points of initial centroids c_k.
2. Calculate the distance $d(x,c)$ between vector x_i to cluster center c_k. Euclidean distance used to be used to express the distance.
3. Separate x_i into s_k which has minimum $d(x,c)$.
4. Determine the new cluster centers defined as:

$$c_i = \frac{1}{p}\sum_{j=1}^{p} m(s_i, j), \qquad where\ p = n(s_i) \tag{1}$$

5. Go back to step 2 until $c_i = c_i$-1

To calculate the distortion of K-means clustering, let E:$X \rightarrow S$ be encode function to cluster X into S, and D:$S \rightarrow X$ be the decode function. The distortion of clustering can be defined as:

$$Distortion = \left|\sum_{i=1}^{r}(x_i - D[E(x_i)])\right| \tag{2}$$

The correct clustering has $x_i=D[E(x_i)]$, so that *Distortion* is 0. A good clustering performs minimum *Distortion*. Therefore, it try to make *Distortion* as minimum as possible. Referring Eq.1 and $M \in X$, the effort to minimize *Distortion* can be set by minimizing P as:

$$P = \left|(m(s_i, j) - c_j)\right| \tag{3}$$

where c_k is the cluster center of $m(s_i,k)$. Therefore, the determining of initial centroids for K-means is very important because it can determine the distortion and/or the precision of clustering results.

4.2 Basic Concept of our proposed Centroit

It is common that the ideal initial cluster center resides near average gravity of the cluster members. It means that it absolutely depends on the data distribution of them. For a simple case which has only 1 cluster, if the cluster center $\bar{x}$ of the clusters assumed as one of the members, it performs:

$$\frac{1}{n}\sum_{j=1}^{n}\left|\bar{x} - x_j\right| < \frac{1}{n}\sum_{j=1}^{n-1}\left|x_i - x_j\right| \tag{4}$$

where $x_i \neq x_j$. Eq. 4 expresses that $\bar{x}$ is the lowest average distance to the other members. Because the cluster center is unknown in a priori, Eq. 4 can be modified in order to look for the nearest members from $\bar{x}$ that can be analyzed it as below:

$$T_i = \frac{1}{n-1}\sum_{j=1}^{n-1}\left|x_i - x_j\right| \quad (5)$$

where $x_i \neq x_j$. From Eq. 5, the nearest members from desired cluster center which show the most minimal T_i can be determined.

4.3 Capturing certain area

Starting from Eq. 5, we then expand the case, which consists more than one cluster. The differential distance $|x_i - x_j|$ can be calculated because it has scalability factor in the certain area. Let we apply the circular region with diameter λ to appoint the certain range of area as shown in Figure 1.

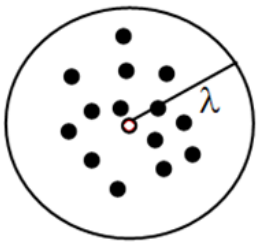

Figure 1. Certain area showed by circular region with diameter λ

Then, Eq. 5 can be modified as follows:

$$T_i = \frac{1}{n_i-1}\sum_{j=1}^{n_i-1}\left|x_i - x_j\right| \quad (6)$$

where $|x_i - x_j| \leq \lambda$ and n_i is number of points inside the circular area which point *i* is its center.

Based on Eq. 6, the most minimum T as the nearest members from desired cluster center is determined. This implies that the most minimum T can express the good initial centroids.

It can be explained that the nearest point to cluster center, assumed as *a*, can relatively cover calculation of all points which make n_a close to total points. On the contrary, the furthest point to cluster center, assumed as *b*, can just cover calculation of some points because the distance to furthest point is relatively ≤ λ . Figure 2(a) and 2(b) illustrates the different coverage calculation between two points. Therefore, it makes $n_a > n_b$, so that it causes $T_a < T_b$.

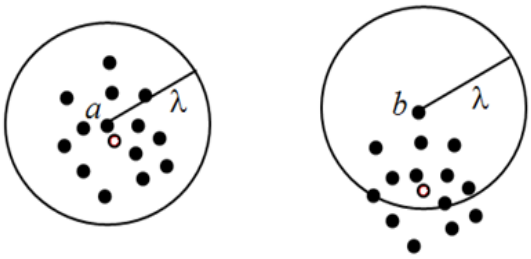

(a) (b)

Figure 2. Illustration of different coverage calculation between point *a* in (a) and point *b* in (b), with $n_a = 14$, $n_b = 10$.

Now, we can apply Eq. 6 for clustering cases more than one cluster by setting the appropriate value λ. Figure 3 shows use of λ for capturing the certain area of clustering.

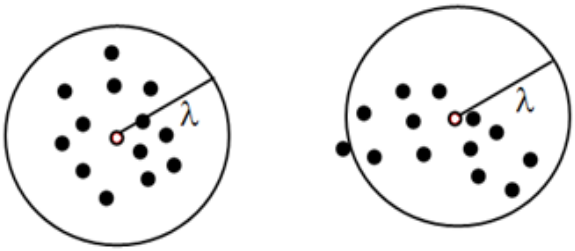

(a) (b)

Figure 3. Capturing two areas of clustering cases

Because it just applied one value of λ, it could be n_m lower than total members of cluster, as is shown in Figure 3 that there is certain point outside the circular range. It will also make that the nearest point to the cluster center can be represented by the lowest minimal value of T_i. Meanwhile, it also can answer why this approach can be robust from outlier of data.

4.4 Setting appropriate λ

The most critical point is how to set the appropriate λ. It will be difficult if we set manually because the clustering cases are very various. If the dimension of data is more than three, it is difficult to imagine the visualization of the data distribution. In this paper, we try to overcome with the automatic setting of value λ.

Referring the case in Figure 3, the ideal λ can be determined by half of differential distance between the cluster centers, as is shown in Figure 4.

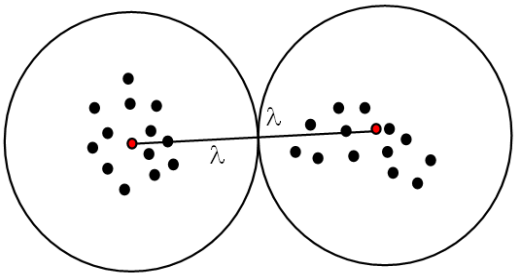

Figure 4. Determining λ with differential distance between the cluster centers.

It may cause the certain points those are near to the boundary involve some members of the other clusters, as is shown in Figure 5. That is what we aim because it will make T_i bigger, so that it has low chance to be initial cluster center.

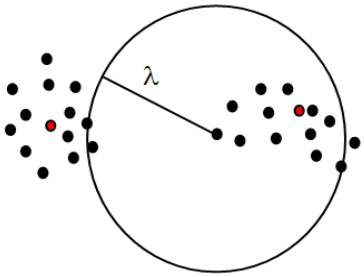

Figure 5. Illustration of a point which is involving some members of the other clusters.

The desired cluster centers of the clustering cases are not known in a priori so that the value of λ from differential distance between cluster centers has not been determined. The following approach to solve this problem is proposed. The distribution of the data actually can express the average distance among them. Based on Eq. 5, it is possible to determine λ by calculating the average distance between all data points as follows:

$$\lambda = \frac{1}{2n(n-1)} \sum_{i=1}^{n} \sum_{j=1}^{n-1} \sqrt{|x_i - x_j|} \quad (7)$$

where $x_i \neq x_j$. From Eq. 7, the value of λ can be set automatically. It expresses the average distance among separated clusters.

4.5 Execution steps

In this subsection the following execution steps of our proposed Centronit for initial centroids of *K*-means clustering is proposed,

1. Set $X=\{x_i \mid i=1, ..., r\}$ as each data of A where $A=\{a_i \mid i=1, ..., n\}$ is attribute of *n*-dimensional vector.

2. Set K as the predefined number of clusters.
3. Compute diameter of circular area λ as Eq. 7.
4. Compute n_i as number of points inside the circular area λ for x_i which point i is its center. Execute for i=1…n where n is total number of points.
5. Compute differential distance T_i for each point as Eq. 6.
6. Init p=0 as a counter to compute number of initial centroids that will be designated.
7. Find T_m as the most minimum value of T.
8. Increment p=p+1
9. Assign c_p = T_m as designated initial cluster center
10. Set T_m with a defined big value
11. Repeat to step 7 until p=K

After processing, it will generate the designated initial centroids c_p where p=1, 2, ..., K. Then, we can apply it as initial centroids for K-means clustering. The experiment results will perform the accuracy of the proposed method.

5. EXPERIMENT AND ANALYSIS

Two experimental data, normal random data distribution datasets and real world datasets are used for evaluation of the proposed Centronit for K-means clustering.

5.1 Normal random distributed data

In order to evaluate an ability of the proposed method for well-separate case of clustering, two dimensional normal random data distribution datasets are used. We make 1000 experiments, then clustering performance of the proposed method is compared with Hierarchical methods (Single Linkage, Centroid Linkage, Complete Linkage and Average Linkage), Fuzzy C-means and K-means clustering using random initialization. For Fuzzy C-means clustering, 1.5 for degree of fuzziness is used as an example. For K-means clustering, we take the average results of 100 experiments.

The following variance factors V is defined as a performance measure in the experiments. Variance constraint [9] can express the density of the clusters with variance within cluster and variance between clusters [10][11]. The ideal cluster has minimum variance within clusters (V_w) to express internal homogeneity and maximum variance between clusters (V_b) to express external homogeneity [12].

$$V = \frac{V_w}{V_b} \tag{8}$$

Table 1 shows the variance factor comparison among the aforementioned methods. From Table 1, the variance factor of the proposed method shows the lowest V, same as V of the Hierarchical methods so that it

is concluded that the proposed method does work so well for the well-separated clustering cases.

Table 1. Comparison of variance factor for normal distributed random dataset

Clustering Algorithm	V
Hierarchical Clustering	0.002997
Fuzzy c-means	0.005898
K-means (random init.)	0.0164869
K-means using Centronit	0.002997

5.2 Real world datasets

The real world datasets used are Iris data, Wine data, Fossil data, Ruspini data, Letter Recognition data and New Thyroid data which are widely used and well known datasets for evaluation of clustering algorithms.

The raw data of the real world datasets are used because comparison of clustering performance between the proposed method and the other existing methods is concerned. If we normalize the data, even though it is usual to get the better clustering results, the clustering results are not only dependent on clustering methods, but also are dependent on normalization methods.

Clustering performance of Single Linkage, Centroid Linkage, Complete Linkage, Average Linkage, Fuzzy c-means, *K*-means clustering with random designated initial cluster center is compared to the proposed method. The same datasets as CCIA [5] is used are utilized for the comparison, even though its clustering result computed after normalizing the data ranges from 0 to 1. For Fuzzy c-means clustering, 1.5 for degree of fuzziness is again used. For *K*-means clustering using random initialization, 100 iteration times is used and take the average results.

The following error percentage which is calculated from the number of misclassified patterns and the total number of patterns in the datasets is evaluated.

$$Error = \frac{Numberofmisclassified}{Numberofpatterns} x100\% \quad (9)$$

5.2.1 Iris dataset

This dataset is from the UCI Repository [13]. This dataset contains information about Iris flowers. There are three classes of Iris flowers, namely Iris Setosa, Iris Versicolor and Iris Virginica. The dataset consists of 150 examples with 4 attributes. One class is well separable against the other two. The others have a large overlap. Table 2 shows the comparison of error ratio between our proposed Centronit and other clustering algorithm for Iris dataset.

Table 2. Comparison of Error ratio for Iris dataset

Clustering Algorithm	Error (%)
Single Linkage	32
Centroid Linkage	9.3333
Complete Linkage	16
Average Linkage	9.3333
Fuzzy C-means	13.524
K-means (random init.)	17.7507
K-means using CCIA	11.33
K-means using Centronit	10.6667

5.2.2 Wine dataset

We also obtained this dataset from UCI Repository [13]. The data is the result of a chemical analysis of wines grown in a region in Italy but derived from three different cultivars. There are three classes. The dataset consists of 178 examples each with 13 continuous attributes. The dataset contains distribution 59 examples of class 1, 71 examples for class 2 and 48 examples for class 3. Table 3 shows the comparison of error ratio between our proposed Centronit and other clustering algorithm for Wine dataset.

Table 3. Comparison of Error ratio for Wine dataset

Clustering Algorithm	Error (%)
Single Linkage	57.3034
Centroid Linkage	38.764
Complete Linkage	32.5843
Average Linkage	38.764
Fuzzy c-means	30.3371
K-means (random init.)	32.6197
K-means using CCIA	5.05
K-means using Centronit	29.7753

The high error happened with *K*-means clustering using Centronit compared with CCIA because the raw data actually has far difference scale among attributes. There is an attribute that has high scale of value compared to the others. For this case, the data is usually better to standardize before clustering. Table 4 performs the error of *K*-means clustering using Centronit after normalizing the data using 4 different normalization methods.

Table 4. Error of *K*-means using Centronit after normalizing wine dataset

Normalization Method	Error (%)
Min-Max (0-1)	5.618
Z-Score	2.809
Sigmoid	2.809
Softmax	2.809

5.2.3 Fossil dataset

The Fossil data is obtained from Chernoff [14]. It consists of 87 nummulitidae specimens from Eocene yellow limestone formation of northwestern Jamaica. There are three 6 attributes with 3 classes which the distribution is 40 examples of class 1, 34 examples of class 2 and 13 examples of class 3. Table 5 shows the comparison of error ratio between our proposed Centronit and other clustering algorithm for Fossil dataset.

Table 5. Comparison of Error ratio for Fossil dataset

Clustering Algorithm	Error (%)
Single Linkage	13.7931
Centroid Linkage	11.4943
Complete Linkage	14.9425
Average Linkage	9.1954
Fuzzy c-means	11.5057
K-means (random init.)	8.5931
K-means using CCIA	0
K-means using Centronit	4.5977

K-means clustering using CCIA showed the smallest error compared to the others as is shown in Table 5. However, if any of the normalization is taken into account, then *K*-means clustering with Centronit shows the smallest errors as is shown in Table 6.

Table 6. Error of *K*-means using Centronit after normalizing Fossil dataset

Normalization Method	Error (%)
Min-Max (0-1)	0
Z-Score	12.6437
Sigmoid	4.5977
Softmax	12.6437

5.2.4 Ruspini dataset

The Ruspini dataset represents a simple, well-known example that is commonly used as a benchmark problem in evaluating clustering methods and is widely available, incorporated as a built-in data object in both R and S-plus statistics packages [15]. The dataset consists of 75 bi-variate attribute vectors. There are fthe classes. The dataset contains 23, 20, 17 and 15 in classes 1, 2, 3 and 4, respectively. Table 7 shows the comparison of error ratio between our proposed Centronit and other clustering algorithm for Ruspini dataset.

Table 7. Comparison of Error ratio for Ruspini dataset

Clustering Algorithm	Error (%)
Single Linkage	0
Centroid Linkage	0
Complete Linkage	4

Clustering Algorithm	Error (%)
Average Linkage	0
Fuzzy c-means	0
K-means (random init.)	13.7787
K-means using CCIA	4
K-means using Centronit	0

5.2.5 Letter recognition dataset

This dataset obtained from UCI Repository [13]. The objective is to identify each of a large number of black-and-white rectangular pixel displays as one of the 26 capital letters in the English alphabet. The character images were based on 20 different fonts and each letter within these 20 fonts was randomly distorted to produce a file of 20,000 unique stimuli. Each stimulus was converted into 16 primitive numerical attributes (statistical moments and edge counts), which were then scaled to fit into a range of integer values from 0 through 15. The training data consists of first 16000 items and then used the resulting model to predict the letter category for the remaining 4000. For experimental purpose we have taken 595 patterns of letter A and 597 patterns of letter D from the training dataset, as CCIA has done. Table 8 shows the comparison of error ratio between our proposed Centronit and other clustering algorithm for Letter Recogniton dataset.

Table 8. Comparison of Error ratio for Letter Recognition dataset

Clustering Algorithm	Error (%)
Single Linkage	49.8322
Centroid Linkage	48.1544
Complete Linkage	42.7852
Average Linkage	6.8792
Fuzzy c-means	13.1711
K-means (random init.)	8.2326
K-means using CCIA	8.55
K-means using Centronit	8.2215

5.2.6 New thyroid dataset

The new thyroid dataset is also obtained from UCI Repository [13]. The dataset contains information about classification whether a patient's thyroid to the class euthyroidism, hypothyroidism or hyperthyroidism. The diagnosis (the class label) was based on a complete medical record, including anamnesis, scan etc. The dataset consists 5 attributes, with 215 examples. The distribution is 150 of class euthyroidism, 35 of class hypothyroidism and 30 of class hyperthyroidism. Table 9 performs the comparison of error ratio between our proposed Centronit and other clustering algorithm for New Thyroid dataset.

Table 9. Comparison of Error ratio for New Thyroid dataset

Clustering Algorithm	Error (%)
Single Linkage	29.7674
Centroid Linkage	27.907
Complete Linkage	28.3721
Average Linkage	26.0465
Fuzzy c-means	14.4186
K-means (random init.)	20.9842
K-means using Centronit	13.9535

6. CONCLUSION

It is widely reported that the K-means clustering algorithm suffers from initial centroids. The main purpose is to optimize the designation of the initial centroids for K-means clustering. Therefore, in this paper we proposed Centronit as a new algorithm of initial centroid designation algorithm for K-Means Clustering. This algorithm is based on the calculating the average distance of the nearest data inside region of the minimum distance. The initial centroids can be designated by the lowest average distance of each data. The minimum distance is set by calculating the average distance between the data. This algorithm creates the unique clustering results because it does not involve the probabilistic calculation. Moreover, because of observing the data distribution, Centronit is robust for outliers. Experimental results with normal random data distribution and real world datasets perform the accuracy and improved clustering results as compared to some clustering methods.

REFERENCES

[1] G.A. Growe, **Comparing Algorithms and Clustering Data: Components of The Data Mining Process**, Thesis, Department of Computer Science and Information Systems, Grand Valley State University, 1999.

[2] V.E. Castro, **Why so many clustering algorithms-a position paper**, *ACM SIGKDD Explorations Newsletter*, Volume 4, Issue 1, pp. 65-75, 2002.

[3] H. Ralambondrainy, **A conceptual version of the K-means algorithm**, *Pattern Recognition Letters 16*, pp. 1147-1157, 1995.

[4] YM. Cheung, ***k**-Means: A new generalized k-means clustering algorithm***, *Pattern Recognition Letters 24*, pp. 2883-2893, 2003.

[5] S.S. Khan, A. Ahmad, **Cluster center initialization algorithm for K-means clustering**, *Pattern Recognition Letters*, 2004.

[6] B. Kövesi, JM. Boucher, S. Saoudi, **Stochastic K-means algorithm for vector quantization**, *Pattern Recognition Letters 22*, pp. 603-610, 2001.

[7] P.S. Bradley, U.M. Fayyad, **Refining initial points for K-means clustering**, *Proc. 15th International Conference on Machine Learning (ICML'98)*, 1998.
[8] J.M. Penã, J.A. Lozano, P. Larrañaga, **An empirical comparison of fthe initilization methods for the K-means algorithm**, *Pattern Recognition Letters 20*, pp. 1027-1040, 1999.
[9] C.J. Veenman, M.J.T. Reinders, E. Backer, **A maximum variance cluster algorithm**, *IEEE Transactions on Pattern Analysis and Machine Intelligence*, Vol. 24, No. 9, pp. 1273-1280, 2002.
[10] S. Ray, R.H. Turi, **Determination of number of clusters in K-means clustering and application in colthe image segmentation**, *Proc. 4th ICAPRDT*, pp.137-143, 1999.
[11] W.H. Ming, C.J. Hou, **Cluster analysis and visualization**, *Workshop on Statistics and Machine Learning, Institute of Statistical Science*, Academia Sinica, 2004.
[12] Ali Ridho Barakbah, Kohei Arai, **Identifying moving variance to make automatic clustering for normal dataset**, *Proc. IECI Japan Workshop 2004 (IJW 2004)*, Musashi Institute of Technology, Tokyo, 2004.
[13] UCI Repository (http://www.sgi.com/tech/mlc/db/)
[14] C. Yi-tsuu, **Interactive Pattern Recognition**, *Marcel Dekker Inc*., New York and Basel, 1978.
[15] R.K. Pearson, T. Zylkin, J.S. Schwaber, G.E. Gonye, **Quantitative evaluation of clustering results using computational negative controls**, *Proc. 2004 SIAM International Conference on Data Mining*, Lake Buena Vista, Florida, 2004.

EMITTER International Journal of Engineering Technology
Vol.2, No.1, June 2014
ISSN:2355-391X

Hybrid Modeling KMeans – Genetic Algorithms in the Health Care Data

Tessy Badriyah

Electronics Engineering Polytechnic Institute of Surabaya Indonesia
Jl. Raya ITS - Kampus ITS Sukolilo Surabaya 60111, INDONESIA
E-mail: tessy@pens.ac.id

Abstract
K-Means is one of the major algorithms widely used in clustering due to its good computational performance. However, K-Means is very sensitive to the initially selected points which randomly selected, and therefore it does not always generate optimum solutions. Genetic algorithm approach can be applied to solve this problem.
In this research we examine the potential of applying hybrid GA-KMeans with focus on the area of health care data. We proposed a new technique using hybrid method combining KMeans Clustering and Genetic Algorithms, called the "Hybrid K-Means Genetic Algorithms" (HKGA). HKGA combines the power of Genetic Algorithms and the efficiency of K-Means Clustering. We compare our results with other conventional algorithms and also with other published research as well. Our results demonstrate that the HKGA achieves very good results and in some cases superior to other methods.

Keywords: Machine Learning, K-Means, Genetic Algorithms, Hybrid KMeans Genetic Algorithm (HGKA).

1. INTRODUCTION

Clustering can be considered the most important unsupervised learning problem. It deals with finding a structure in a collection of unlabeled data. A clustering could be defined as the process of organizing objects into groups whose members are similar in some way. A cluster is therefore a collection of objects which are similar between them and are dissimilar to the objects belonging to other clusters. The goal of clustering is to determine the intrinsic grouping in a set of unlabeled data [1].

Among the various clustering algorithms, K-Means (KM) is one of the most popular methods used in data analysis due to its good computational performance. However, it is well known that KM might converge to a local optimum, and its result depends on the initialization process, which randomly generates the initial clustering. In other words, different runs of KM on the same input data might produce different results [2].

Copyright © 2013 EMITTER International Journal of Engineering Technology - Published by EEPIS

In this research, we explored the use of machine learning techniques for health care modeling. A major problem in the health care modeling is a guarantee to get the best model in order to improve the diagnostic with regard to speed, accuracy and reliability.

The main emphasis of this research is combining some techniques in machine learning to improve a classification performance. We propose a hybrid modeling techniques which combines the power of Genetic Algorithms with K-Means Clustering. Our results demonstrate that the Genetic K-Means algorithm is a very competitive and in some cases superior with results from other methods. The performance and efficiency of our approach is investigated using the classification accuracy when compared with conventional method and published results from other researcher.

This paper is organized as follows : in section 2 we review some related works, in section 3 we present our proposed, in section 4 we discuss the experimental results and section 5 is the conclusions.

2. RELATED WORKS

Many papers have been published on the subject of machine learning and cancer which the majority being concerned with using machine learning methods to identify, classify, detect, other malignancies or disease, especially for diagnosis and prognosis activity. In the following section we summarize selected papers in different research areas of medical data analysis and health care data modeling.

Decision Tree is one of the most well-established classification methods. a very well-known decision tree classifier developed by Ross Quinlan [4]. Many researchers have been used decision tree for classifying medical-related data. Adam et. al. [5] applied decision-tree learning to mass spectra of prostate cancer patients. Another researcher [6] applied an improve decision tree algorithm called T3 for mining stroke related medical data.

Neural Network (NN) are well suited to tackle problems that people are good at solving, like prediction and pattern recognition. Furthermore, NN have been applied within the medical domain for clinical diagnosis [7] and drug development [8].

Many clustering algorithms such as K-Means, K-Nearest Neighbour, Fuzzy C Mean and more advance techniques have been successfully applied to various medical task [9]. Joseph Cruz [10] reported several examples of clustering approaches in medical data.

Ensemble methods consist of a set of models and certain model fusion criteria. Statistical, computational and representational reasons have been presented to explain the success of ensemble methods [6]. The fundamental idea is that assuming each classifier's accuracy is better than random. Combining multiple classifiers can improve classification performance if each individual classifier's performance is above an acceptable level (at least

better than random) and their outputs are diverse (ideally statistically independent but in practice different enough such that their errors would not coincide).

3. ORIGINALITY

In this research, we proposed a new technique using hybrid method combining KMeans Clustering and Genetic Algorithms, called the "Hybrid K-Means Genetic Algorithms" (HKGA).

Our new proposed technique HKGA combines the powerful of GA and the simplicity and efficiency of K-Means. Combination between K-Means and GA can be done in two ways. The first method is running GA and then put the results into KMeans. The second method is running KMeans and then use the results as an initial population of GA. Based on published research by [2] the second method is better than the first. By using initial centroid value from GA, at least KMeans clustering start a good first step. We use the second method as the main idea behind our proposed technique for combine KMeans Clustering and GA. The uniqueness of this research can be identified by using GA as initialization centroid value to optimize KMeans clustering.

4. SYSTEM DESIGN

First, we are going to overview two existing methods: KMeans Clustering and Genetic Algorithms, and then give a detail explanation about proposed techniques : a Hybrid KMeans Genetic Algorithms (HKGA).

4.1 K-Means Clustering

KMeans algorithm is relatively faster, simpler and needs less computation, but it has some weaknesses. The disadvantages K-Means algorithm is that it is sensitive to the initially selected points, and therefore it does not always generate the same results. This algorithm also does not guarantee to find the global optimum.

KMeans Algorithms can be explained in detail in the following algorithm [Algorithm 1.].

Algorithm 1. K-Means Clustering
Input:
k: the number of clusters,
D: a data set containing n objects.
Output: A set of k clusters.
Method:
(1) arbitrarily choose k objects from D as the initial cluster centers;
(2) repeat
(3) (re)assign each object to the cluster to which the object is the most similar, based on the mean value of the objects in the cluster;
(4) update the cluster means, i.e., calculate the mean value of the objects for each cluster;
(5) until no change;

4.2 The Genetic Algorithms

The Genetic Algorithm (GA) technique was originally proposed by Holland [12]. GA has been applied to many function optimization problems and is shown to be good in finding optimal or near optimal solutions. The GA can be explained in detail in the following algorithm (Algorithm 2)

```
Algorithm 2. Genetic Algorithms
begin
  t = 0;
  initialize P(t);
  evaluate structures in P(t);
  while termination condition not satisfied do
  begin
   t = t + 1;
   select_repro C(t) from P(t-1);
   recombine and mutate structures in C(t) to C'(t);
   evaluate structures in C'(t);
      select_replace P(t) from C'(t) and P(t-1);
   end
end
```

4.3 Framework of Proposed Technique

The originality of this research has been explained in section 3, and the following we will give a detail explanation about our proposed techniques : a Hybrid modelling KMeans Genetic Algorithms (HKGA).

The Hybrid KMeans Genetic Algorithms is explained in the following detail (Algorithm 3)

```
Algorithm 3. Framework of Hybrid KMeans Genetic Algorithms
Stage 1 : Generate Initial Population from KMeans
Input:
D: a data set
S : size of  population (number of chromosome)

Output: A set of N chromosome.
Method :
(1) Determine number of chromosome (population size) as S
(2) repeat
(3)     randomly choose initial cluster centers;
(4)    running KMeans Algorithm on Dataset D
(5) until S;

Stage 2 : Optimize using Genetic Algorithm
Input:
D: a data set
Genetic Parameter : crossoverrate, mutationrate, size of population
maxIter : maximum iteration
Algorithm 3. Framework of Hybrid KMeans Genetic Algorithms (continued)
```

……..

Output: The best chromosome.
Method :
(1) repeat
(2) parent selection using roulette wheel based on fitness function
(3) crossover process;
(4) mutation process
(5) survivor selection, pass the selected chromosome to the next generation\
(6) until maxIter;

We will describe in detail, the elements of GA in our proposed techniques.

4.3.1. Chromosome Representation

In our approach, each chromosome represents sequence number of centroid representation. For example, the problem which have two classes (benign or malignant), the chromosome consists of 2 centroids (number of clusters or classes). The length of chromosomes indicates the number of gen in the chromosomes. For example, the dataset consist of 9 attribute and have 2 classes, we can calculate the length of the chromosome is = 9 x 2 = 18 genes.

Cluster-1	Attribute 1	Attribute 2	Attribute 3		Attribute-n
Cluster-2	Attribute 1	Attribute 2	Attribute 3		Attribute-n
	……	……	……		……
Cluster-k	Attribute 1	Attribute 2	Attribute 3		Attribute-n

k = number of clusters
n = number of attributes

Figure 1. Structures of the chromosomes for HKGA

4.3.2. Initial Population

In the initialization phase, initial population of N chromosomes is generated. N is the size of population means the number of solution (number of chromosome) in population. To generate chromosomes (c1; c2; . . . ; cn), we employ the KMeans Clustering.

4.3.3. Fitness value calculation

The following is the pseudo code to calculate fitness value In this pseudo code, we need total fitness value when use roulette wheel selection to choose which parent involved in crossover or mutation process.

```
Algorithm 4. Fitness value calculation
total_fitness=0;
for i=1: number_of_chrom,,
   [1] get accuracy between output and datatarget
   [2] set accuracy as fitness value
   [3] total fitness value is sum up of all fitness value
end;
```

4.3.4. Selection

We use Roulette Wheel Selection in the Selection process, which the pseudo code in explained below :

```
Algorithm 5. Roulette Wheel Selection
function individu=Selection(number_of_chrom,kromosom,V)
[1] total_fitness=0;
[2] Accumulate fitness value from all the chromosome
    Save to total_fitness
[3] for i=1:number_of_chrom,
          Calculate the proportion each of fitness value to
Algorithm 5. Roulette Wheel Selection (continued)
……
           total_fitness
    end;
[4] for j=1:number_of_chrom,
            Generate random number and see the position
             based on proportion of
             fitness value of each chromosome.
             taken in accordance with the individual
             chromosome selected
    end;
```

4.3.5. Crossover

We use 2-point crossover to generate 2 offspring. (2 point obtained at random).

4.3.6. Mutation

For mutation operator we use changes in the small value on gen values in the chromosomes. The mutation process is described as follows:

```
Algorithm 6. Mutation Process
[1] for i=1:number_of_chrom,
          Let (a1,a2, …, ank) denote gen of the chromosome;
[2]     for i=i:length_of_chrom,
[3]           v = generate random number between [0,1]
[4]           if (v<=mutation_rate) then do
[5]         Generate random number between [0,1]
[6]         For the i-th point of the chromosome;
                      Increment/Decrement aj with the smallest
                      number (0.1)
          End;
       End;
     End;
```

4.3.7. Survivor Selection

We believe that diversity plays an important role in the Genetic Algorithms, thus maintaining diversity in the population is a point we can conclude. In the following, pseudo code in Selection process :

```
Algorithm 7. Selection process
Pseudo code for Survivor Selection :
[1] listing the parent chromosome and pick the best one.
[2] Sorting chromosome combine parent and child (offspring)
[3] Pick the remain (N-1) from the top after sorting
```

5. EXPERIMENT AND ANALYSIS

5.1. Dataset

In this section, we describe dataset used to evaluate the proposed method. We use the following dataset :

(1) Breast Cancer from MATLAB
There are 9 attributes used to determine whether a patient classified into benign or malignant (2 classes), and there are 699 cases in the dataset.

(2) Thyroid dataset from MATLAB
This data set has 3 classes, contains information related to thyroid dysfunction. The problem is to determine whether a patient has a normally functioning thyroid, under functioning (hypothyroid), or over-active functioning hyperthyroid. There are 7200 cases in the data set, with 21 attributes used to determine to which of the three classes the patient belongs.

(3) Lung Cancer
The dataset is taken from UCI Machine Learning Repository [15]. There are 56 attributes and 2 classes with 32 instances.

(4) Wisconsin Breast Cancer (WBC) Dataset
The breast cancer data set is also available in UCI Lab [15] and it was obtained from the University of Wisconsin Hospitals, Madison

from Dr. William H. Wolberg. This dataset is widely used among researchers to test the effectiveness of classification algorithms. The aim of the classification is to distinguish between benign and malignant cancers (2 classes) based on 9 attributes, and there are 683 instances.

5.2. Experiment Procedure

For the experiment, we use cross validation methods. In cross-validation, a data set is randomly divided into a number of subsets of roughly equal size. Ten-fold cross validation, in which the data set is divided into 10 subsets, is most commonly used. The system is trained and tested for 10 iterations. In each iteration, 9 subsets of data are used as training data and the remaining set is used as testing data. In rotation, each subset of data serves as the testing set in exactly one iteration. The accuracy of the system is the average accuracy over the 10 iterations [6]. We execute every algorithms on four different dataset ten times and taken the average value and standard deviation.

5.3. Experimental Results

The following tables show the comparison results between the conventional algorithms and the hybrid algorithm. Table 1 shows the results of experiments with KMeans Algorithm.

Table 1. KMeans Algorithms Results

No	Dataset Name	Best Result	Worse Result	Average ± standard deviation
1	Breast Cancer	95.85	95.70	95.74±0.06
2	Thyroid	86.51	51.90	72.35±10.65
3	Lung Cancer	77.78	51.85	65.93 ± 8.87
4	WBC Dataset	98.98	96.49	96.74 ± 0.79

We used the same input parameters for HKGA: number of chromosomes=10, probability of crossover= 0.95, probability of mutation = 0.7 and maximum iteration = 50. There is no reason to set parameters like that. We just set it up randomly.

Table 2 shows the experiment by using genetic algorithms.

Table 2. Experiment Results using Genetic Algorithm

No	Dataset Name	Best Result	Worse Result	Average ± standard deviation
1	Breast Cancer	96.99	92.56	95.11 ± 1.52
2	Thyroid	92.61	92.53	92.58±0.02
3	Lung Cancer	92.59	74.07	83.33 ± 5.59
4	WBC Dataset	99.85	96.78	99.27 ± 0.93

Table 3 uses a hybrid scenario 1 in which the genetic algorithm is run first and then KMeans, called by HGAK (Hybrid Genetic Algorithms - KMeans)

Table 3. Experiment Results using Hybrid Genetic KMeans (HGAK)

No	Dataset Name	Best Result	Worse Result	Average ± standard deviation
1	Breast Cancer	95.85	95.71	95.84 ±0.05
2	Thyroid	92.61	92.53	92.58±0.02
3	Lung Cancer	88.89	74.07	84.81 ± 4.43
4	WBC Dataset	99.12	98.98	99.06±0.076

Table 4 uses a hybrid scenario 2 where the KMeans algorithm run first and then the results are used as an initial population for the next run of Genetic Algorithm.

Table 4. Experiment Results using Hybrid KMeans Genetic Algorithm (HKGA)

No	Dataset Name	Best Result	Worse Result	Average ± standard deviation
1	Breast Cancer	97.14	95.85	96.22 ± 0.50
2	Thyroid	99.61	94.36	96.69 ± 1.77
3	Lung Cancer	96.3	92.59	93.70 ± 1.79
4	WBC Dataset	99.71	99.27	99.46 ± 0.22

Table 5 shows that our proposed method Hybrid KMeans Genetic Algorithms (HKGA) achieved the best result compare to other convensional algorithms. These results show that the combination of KMeans algorithms and Genetic Algoritms give better results than each algorithm run independently. Only in one case (in WBC dataset), Genetic Algorithms performs better then Hybrid Genetic Algorithms KMeans (HGAK). In Table 5 we also can see that the accuracy between GA and HGAK is the same in the thyroid dataset.

Table 5 : Comparison between conventional methods and hybrid method

No	Dataset Name	KMeans	GA	HGAK	HKGA
1	Breast Cancer	95.74±0.06	95.11±1.52	95.84±0.05	96.22±0.50
2	Thyroid	72.35±10.65	92.58±0.02	92.58±0.02	96.69±1.77
3	Lung Cancer	65.93±8.87	83.33±5.59	84.81±4.43	93.70±1.79
4	WBC Dataset	96.74±0.79	99.27±0.93	99.06±0.076	99.46±0.22

Using the same dataset, we compare our proposed algorithm Hybrid KMeans Genetic Algorithm (HKGA) with other published research. All of the algorithms given in Table 6 used the same dataset (the Wisconsin Breast Cancer Dataset).

Table 6. Classification Accuracy Benchmark for Wisconsin Breast Cancer Dataset

No	Researchers	Methods	Accuracy
1	Biying Zhang [16]	Novel Neural Network	97.24%
2	A. Verikas, et.al [17]	fuzzy derivative	97.10%±0.75
3	Akay, MF. [18]	F-score + SVM	99.51%
4	Our Result	HKGA	99.46%±0.22

Table 6 shows that our proposed method (HKGA) has a better accuracy (99.46%) than Novel Neural Network method (97.24%) proposed by [16] and Fuzzy Derivative method (97.1) proposed by [17]. Unfortunately our method is still below F-score & SVM method (99.51) proposed by [18].

6. CONCLUSION

In this research we have presented two scenario of a new machine learning approach using hybrid method combining KMeans Clustering and Genetic Algorithms, called the the "Hybrid Genetic Algorithms - KMeans (HGAK)" and "Hybrid KMeans - Genetic Algorithms" (HKGA).

The proposed method can be characterized by the design of its operators, including encoding, crossover, mutation and selection survivor. Among the two hybrid modeling scenarios proposed in this study, HKGA shows a better performance than HGAK. In HKGA, we treated the KMeans Clustering to generate initial population in Genetic Algorithm and used GA to solve the problem in order to obtain global optimal solution.

Hybrid Genetic Algorithms KMeans (HGAK) does not always improve the result of conventional algorithms, it can produce similar result or even worse. It's depends on the characteristics of the data itself.

Similar to KMeans, GA are also having problems trapped in premature convergence. To avoid the convergence process of the algorithm, we used survivor selection strategy to keep diversity in the population of GA. The element of GA that proposed in this research has worked well.

Based on experimental results, we can conclude that HKGA that proposed in this research provides a satisfactory performance compared with the other algorithm (KMeans, Genetic Algorithms, and HGAK), and outperform compared with some algorithms from the other researchers.

There are two important issues in GA: exploitation and exploration. When we get the better offspring which have better fitness value that means exploitation, sometime some of the good chromosome dominates the population, than GA will trapped to premature convergence. So the most important thing is to keep the diversity in the process of survivor selection to give the population of GA have a chance to do an exploration to find a global optimum.

In the future works, we have a plan to combine GA with other techniques in Machine Learning that never done before. More investigations

should be done and considered to carry out a comprehensive and comparative study on hybrid modelling techniques in the health care data..

REFERENCES

[1] Boncheva, V.M., **Using the Agglomerative Method of Hierachical as a Data Mining Tool in Capital Market**, International Journal Information Theories & Applications, Vol. 15, 2008.

[2] Al-Shboul, B., Myaeng, S.H., **Initializing K-Means using Genetic Algorithms, World Academy of Science**, Engineering and Technology 54, 2009.

[3] Delen, D. W., **Predicting breast cancer survivability : a comparison of three data mining methods**, Artificial Intelligence in Medicine, 2004.

[4] Quinlan, J., **Improved use of continuous attributes in C4.5**. AI Research , 77-90, 1996.

[5] Adam B-L, Qu Y, Davis JW, Ward MD, Clements MA, Cazares LH et al.. **Serum protein fingerprinting coupled with a pattern-matching algorithm distinguishes prostate cancer from benign prostate hyperplasia and healthy men**, Cancer Research, 2002.

[6] Tjortjis,C., Saraee,M., Theodoulidis,B., Keane, J.A.,. **Using T3, an Improved Decision Tree Classifier for mining stroke related medical data**, University of Manchester, 2005.

[7] Guan W, Zhou M., Hampton C. Y., Benigno B., **Ovarian Cancer Detection from Metabolomic Liquid Chromatography/Mass Spectrometry Data by Support Vector Machine**, BMC Bioinformatics, 2000.

[8] Weinstein J, K. Kohn and M. Grever, et. al.. **Neural Computing in Cancer Drug Development : Predicting Mechanism of Action**, Information Science , 447-451, 1992.

[9] Dhiraj, K., Rath, S. K., **Gene Expression Analysis Using Clustering**. International Journal of Computer and Electrical Engineering, 2009.

[10] Cruz, J. A., David S. Wishart, **Applications of Machine Learning in Cancer Prediction and Prognosis**, Journal on Cancer Informatics , pp. 59-78, 2006.

[11] Jiawei Han, M. K., **Data Mining: Concepts and Techniques**, Morgan Kaufmann Publishers, 2000.

[12] Holland, J. H., **Adaptation in Natural and Artificial Systems**, AnnArbor, MI: Univ. of Michigan Press, 1975.

[13] De Jong, K.A., **Evolutionary Computation: A Unified Approach**, MIT Press, Cambridge, MA, 2006.

[14] Chen, H.; Fuller, S. S.; Friedman, C.; Hersh, W., **Knowledge Management and Data Mining in Biomedicine**. Medical Informatics, 2005.

[15] UCI Machine Learning Repository: http://archive.ics.uci.edu/ml/machine-learning-databases/

[16] Zhang, B,. **A Joint Evolutionary Method Based on Neural Network For Feature Selection**, Second International Conference on Intelligent Computation Technology and Automation(IEEE), 2009.
[17] A. Verikasa,M. Bacauskiene, D. Valincius, A. Gelzinis, **Predictor output sensitivity and feature similarity-based feature selection**, Science Direct : Fuzzy Sets and Systems, 2008 .
[18] Akay, M. F., **Support vector machines combined with feature selection for breast cancer diagnosis**, Science Direct : Expert Systems with Applications, 2009.

EMITTER International Journal of Engineering Technology
Vol.2, No.1, June 2014
ISSN:2355-391X

Impression Generation of Indonesian Cultural Paintings for Mobile Application with Culture Dependent Color-Impression Metric Creation Contents

Devira Nanda Kuswhara, Ali Ridho Barakbah, Nur Rosyid Mubtadai, Yuliana Setiowati

Electronic Engineering Polytechnic Institute of Surabaya
Jalan Raya ITS Surabaya 60111, Indonesia
E-mail: devira@student.eepis-its.edu, ridho@pens.ac.id, rosyid@pens.ac.id, yuliana@pens.ac.id

Abstract

Painting is one of complex image reflecting observations and feelings of the artist to the environment. This condition extends the need of painting impression generation system since common people with lack of art experience would have difficulties to interpret the painting. From this point of view we presents a new model to provide representative impressions of paintings by providing a color-impression metric taken from public survey and implement it for mobile application. The new model provides analytical functions to generate the representative impression of the image query. The functions consist of two main section: (1) The cultural-dependent color-impression metric creation which consist of conducting survey, applying normalized 3D color vector quantization to image dataset, generating image-impression metric, and generating color-impression metric; and (2) Impression generation of image query which consist of applying normalized 3D color vector quantization to image query and measuring the similarity between image query and color-impression metric. To perform our proposed impression generation system, we examine our system with Indonesian cultural image dataset and 5 different mobile devices. Our proposed system performs main color impression precision result with average precision of more than 60%. Brightness intensity and zooming affects the retrieved impressions. Rotating captures of an image generate the same retrieved impressions. The system also performs average response time vary in range 41263 to 117434 milliseconds from all devices.

Keywords: impression generation system, color based impression, cultural computing, mobile application.

Copyright © 2013 EMITTER International Journal of Engineering Technology - Published by EEPIS

1. INTRODUCTION

Painting is a living artistic tradition which integrates respected philosophy, aesthetics, and cultural values and beliefs. Appreciating painting means to understand the languages that all people speak that cut across racial, cultural, social, educational, and economic barriers and to enhance cultural appreciation and awareness. Irrespective of the precious values contained on it, painting is one of complex images to human which is often expressed in abstract way. It needs more sensibility and sensitivity of human to interpret since visual impression may differ in each person. Unless having lot of experiences in appreciating art, common people will have difficulties to get the impression of the painting.

2. RELATED WORKS

We refer to several works about discovering impression of cultural property using computational method on representative color and color feature as related works. Barakbah et al. [1] have been proposed a method called 3D color vector quantization where the color information of the image is extracted using the histogram from RGB color space and then quantized in 5x5x5 size of RGB color space to 125 positions in the RGB color spaces. Shiranita et al. [2] presented an impression-word-giving system for images based on colors extracted using Lab Color Space. The main color is determined by 85% of all pixels in the image. Then they calculated the minimum distance and the average distance to 160 impressions used. Comparisons are determined in accordance with the impression of the source image. Suhardijanto et al. [3] presented a model explaining the relation between culture and emotion-oriented color which is used for image retrieval system with aspects of human emotion. Sasaki et al. [4] presented a dynamic image-query creation and metadata extraction method with semantic correlation computation between color-combinations and impressions of multiple image data. This image-query creation method representing impression of color makes it possible to expand the range of image retrieval for a large number of image data of cultural property in digital archives.

3. ORIGINALITY

This paper proposes an impression generation system of Indonesian cultural painting images with a new model for selecting and representing the image impressions by creating culture dependent color-impression metric obtained from public survey and implementing the system to a mobile application. The objective of the proposed system in this paper is to apprehend user intention to get the representative impressions of the paintings related to human emotional sense. We implement 231 Indonesian cultural images consisting five categories of painting stream: abstractionism, naturalism, expressionism, realism, and romance; in our survey to collect impressions. The architecture of our proposed system is shown in Figure 1.

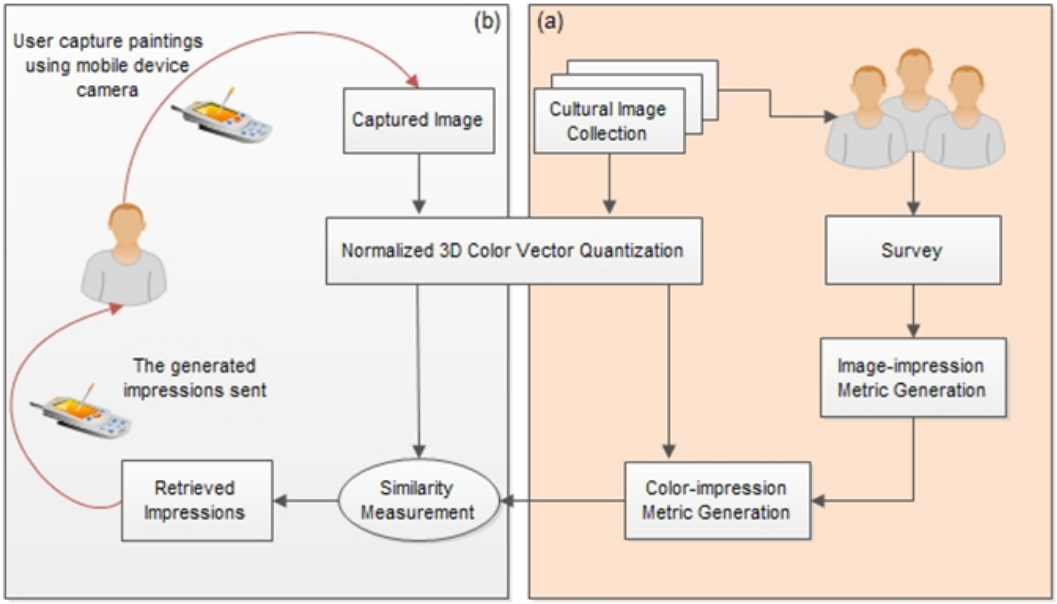

Figure 1. The architecture of the proposed impression generation system: (a) The cultural-dependent color-impression metric creation, and (b) Impression generation of image query

Our proposed system presents a supporting tool to ease user experience in appreciating cultural painting by providing representative impressions of the captured painting. This system will bring a significant contribution especially to help communicating the ideas between the artists and the painting observers. Furthermore, the system will develop human aesthetic experience in order to be able to appreciate art that encompass social and cultural meanings and implications.

4. IMPRESSION GENERATION ANALYTICAL FUNCTION

4.1 The Cultural-dependent Color-Impression Metric Creation

The function consists of several steps to create culture dependent color-impression metric creation: (1) Impression Survey, (2) Normalized 3D Color Vector Quantization, (3) Image-impression metric generation, and the last (4) Color-Impression metric generation.

(1) Impression Survey

Figure 2 shows the design of a web-based polling system, where users fill the polling by choosing at least one of 30 impressions related to Indonesian culture that have been provided on the list. The result of the survey will be converted to a raw user-impression metric.

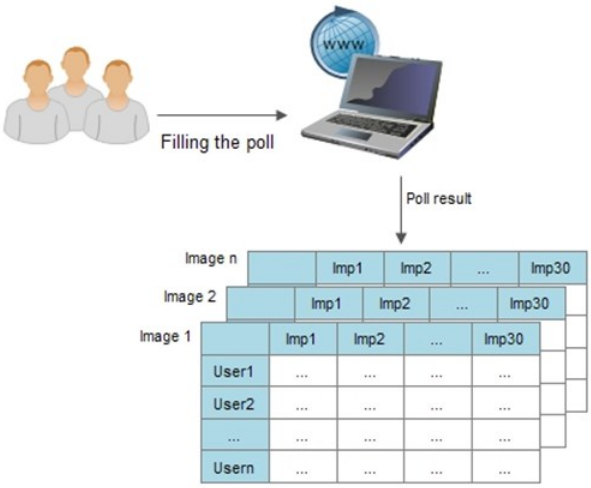

Figure 2. Polling system design

Image Dataset

In this process, each user will finish the polling of 8 images of Indonesian cultural painting which are randomly generated among the 231 images dataset consist of 5 categories: naturalism, expressionism, abstract, realism and romance. There are 34 paintings of abstract, 28 paintings of naturalism, 57 paintings of expressionism, 20 of paintings romance and 109 paintings of realism. Those are all painted by Indonesian painters.

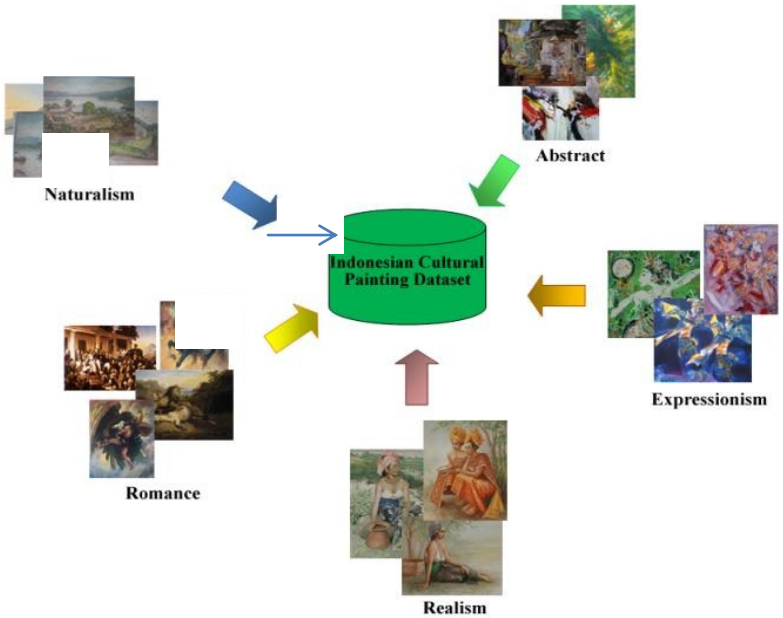

Figure 3. Painting Categories

Impressions List

The Japanese impression set which is known as Kansei have 180 impressions related to colors. A recent study [5] presented research about method to classify those color-impressions based on cultural perception. The

research worked using 17 impressions out of 180. In our proposed system, we implement 30 impressions out of 50 from recent work [6] which is inspired from the Kansei list. The selected impressions are considered suitable with Indonesian culture. The Impression list is shown at Table 1.

Table 1. Impressions list

Impressions List		
Aman	Curiga	Letih
Bersemangat	Sopan	Ragu
Bingung	Khawatir	Sepi, sunyi
Khilaf	Cinta	Menarik
Malu, segan	Sombong, angkuh	Damai, tenteram, tenang
Kejam, marah	Cantik, indah	Putus asa
Suci, mulia	Romantis	Kacau
Dengki, cemburu	Nekad	Mengagumkan, mempesona
Sedih, perih	Sabar	Resah, risau
Ikhlas	Sensual	Gembira, senang

The impression polling had been started since 15th October to December 10th 2013 with 120 voters filling the poll. The polling process is described by following points.

1. The voters access the web address of polling system and click the start button.
2. The system automatically generates 8 random images out of 231 image collections in sliding template.
3. Each image is displayed with a set of check boxes containing the impression word.
4. The voters must choose at least one impression for each image.
5. The polling process is ended by clicking the finish button.

(2) Normalized 3D Color Vector Quantization

This step is used for extract the color features of image dataset and image query given by users. The In this step, the color information of the image dataset and the image query is extracted using the histogram from 3D-Color Vector Quantization of RGB color space. According to the recent study [1], 3D color vector quantization is 64x64x64 quantization size of the RGB color space so that it can be represented with 125 positions in the RGB color space.

Considering that the sizes of image dataset could be various, calculation of the local average is needed to normalize the features. In case of two images below that have different size of pixels, the colors histogram shows that the second image produces a bigger value than the first one. This can cause an error while generating representative colors because a large number of non-dominant colors are generated from second image. Figure 4 shows the process of the normalized 3D vector quantization.

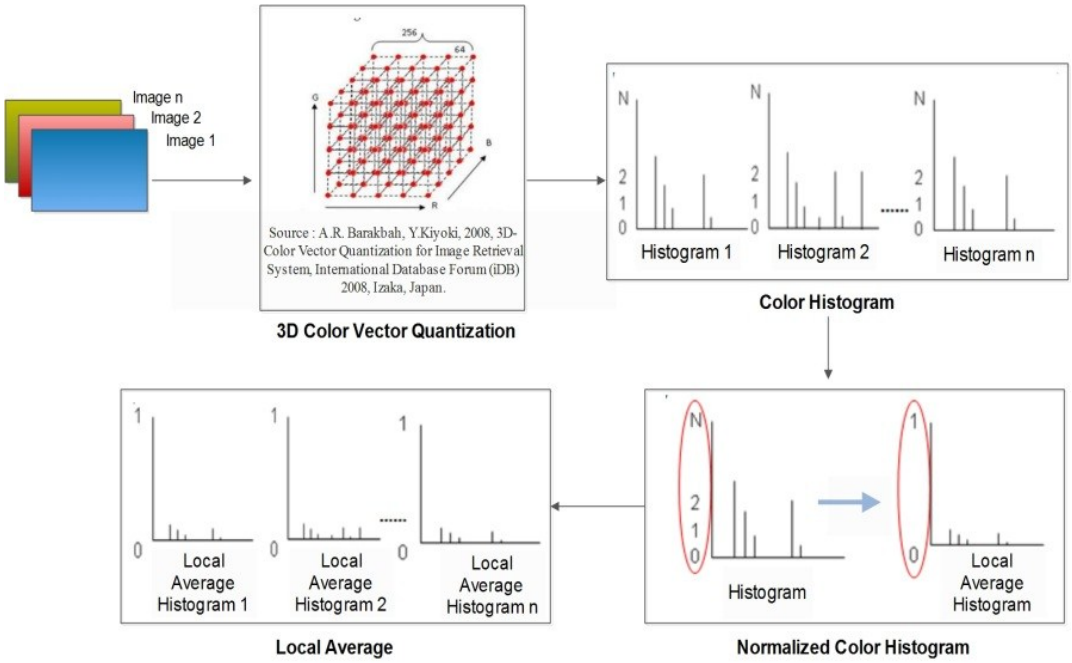

Figure 4. Normalized 3D color vector quantization of image dataset process: process of generating image histogram, histogram output, process of normalized image histogram, histogram final output.

The outcome of normalized 3D color vector quantization of all image dataset processes is a set of local average histograms. The local average of each image dataset will be indexed into an image color feature metric. The metric contains information of color features of multiple images. The table of image color feature metric is shown in Table 2.

Table 2. Image color feature metric

Image	f_1	...	f_{25}	...	f_{50}	...	f_{75}	...	f_{100}	...	f_{125}
Img_1	$n_{1,1}$	...	$n_{1,25}$	...	$n_{1,50}$	...	$n_{1,75}$	...	$n_{1,100}$	...	$n_{1,125}$
...	$n_{..,1}$	...	$n_{..,25}$	...	$n_{..,50}$	...	$n_{..,75}$	...	$n_{..,100}$	...	$n_{..,125}$
Img_n	$n_{n,1}$	...	$n_{n,25}$	...	$n_{n,50}$	...	$n_{n,75}$	...	$n_{n,100}$	...	$n_{n,125}$

Where f_i is color feature, i is color feature cluster index of 125 positions in the RGB color space, and n is total number of image pixels grouped by color feature cluster, and Img is image query of image dataset.

(3) Image-Impression Metric Generation

In the web-based polling system, users are asked to fill the polling by choosing at least one of 30 impressions related to Indonesian culture that have been provided on the list. The result of the survey will be converted to a raw user-impression metric. The next step is classifying similar objects in the same groups with optimal centroid. The automatic clustering is used to determine optimum cluster number. Then we use approach of combining the k-means and hierarchical algorithm which is described in [7] as the centroid k-means model is good to optimize the initial centroids. The raw user image impression metric would be dataset for the clustering. All of the processes needed to generate cultural-dependent image-impression metric of image are shown in Figure 5.

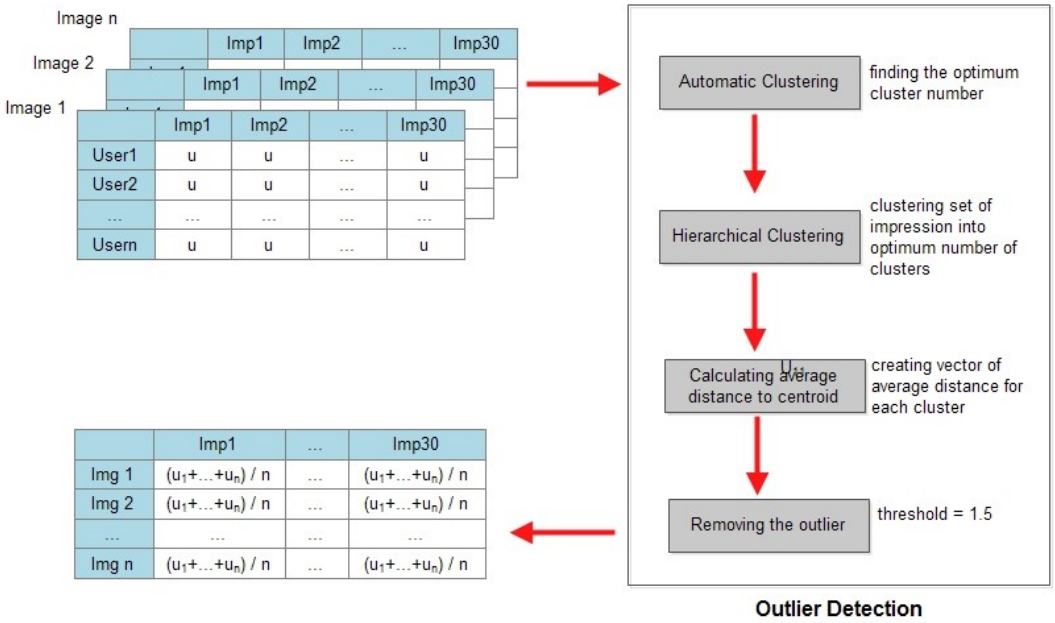

Figure 5. The Image-impression metric generation process

The attribute we need to obtain next is the average distance of cluster member to the centroid. The average can be obtained by calculating mean of dataset distance to centroid within the same cluster. We define a threshold t = 1.5 to take the value of a specified outlier detection function.

We examine each data using the specified outlier detection function. The function compares the data distance to its centroid to the multiplication of threshold t and average distance a. The outlier detection function takes values 1 if value of d exceeds given threshold multiplication function and takes the value 0 otherwise. The value of outlier detection function is taken to decide whether the data is an outlier or not. where value 1 means outlier and otherwise.

After removing the outlier, the normalization is applied by calculating sum of the total number of impressions for each image. The final value is taken from total number divided by the total user who gives the impression.

The normalized user image impression vector would be taken to develop image impression metric. The all 231 normalized user image impression vectors of image dataset would be indexed into an image-impression metric.

(4) Color-Impression Metric Generation

In this subsection, we already have image color feature metric and image impression metric of 231 images dataset. Both metric have important role in creating color-impression metric. We work with both metric to obtain metadata association by using inner product multiplication. The process of color-impression metric generation is shown at Figure 6.

The image impression metric needs to be transposed first due to inner product condition. The inner product multiplication could be implemented only if the number of first metric total column equals with the number of second metric total row. It results a matrix of size *n* x *p*, where *n* is the number of rows in the first matrix (left) and *p* is the number of columns in the second matrix (right). The equation for implementing inner product function is shown at Eq. 1.

$$\boldsymbol{M_1} \times \boldsymbol{M_2} = \sum_{i=1}^{n} \boldsymbol{M_{1_i}} \times \boldsymbol{M_{2_i}} \quad (1)$$

where M_1 is the first metric and M_2 is the second metric and the size or the result metric depends on number of column of M_1 and number of row of M_2.

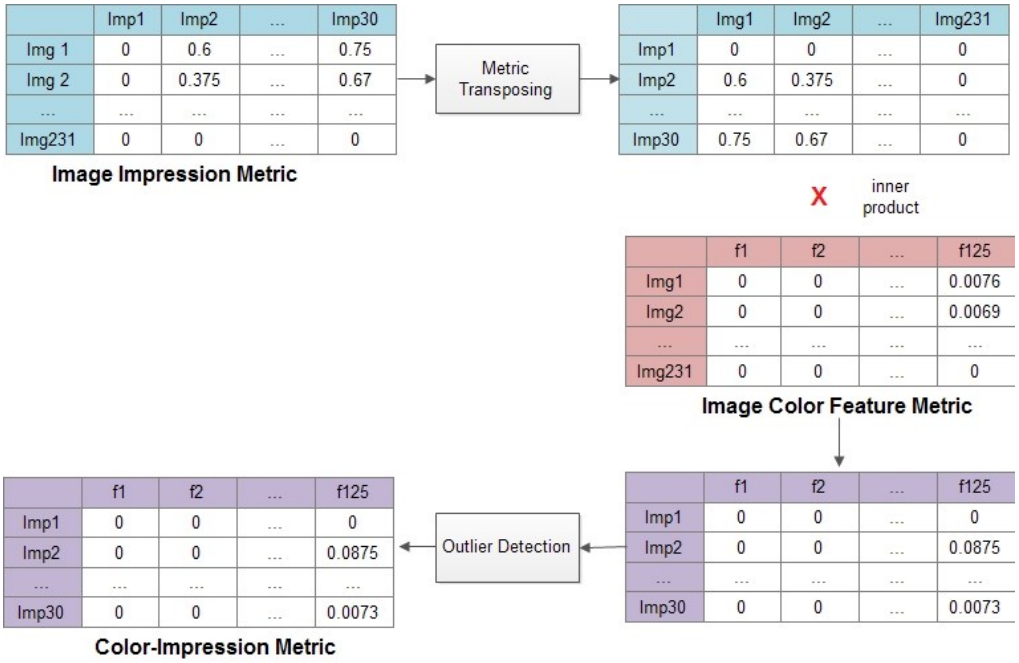

Figure 6. Process of color-impression metric generation

The inner product of both metric results a new metric which classifies the representative color feature related to impression based on impression polling on Indonesian cultural painting. Thus we call the metric as cultural-

dependent.

Like the previous step, after multiplying both metric, we examine each data using the specified outlier detection function. The function compares the data distance to centroid *d* to the multiplication function of threshold *t* and average distance *a*. The outlier detection function takes values 1 if value of d exceeds given threshold multiplication function and takes the value 0 otherwise. The value of outlier detection function is taken to decide whether the data is an outlier or not in which value 1 means outlier and otherwise.

The generated color-impression metric needs to be normalized to prevent the impression dominating the computed dissimilarity and variables that are measured in small valued units and contributing very little. The normalization is applied by calculating sum of the total number of impressions for each impression (each row). The determinant *dt* value is taken from total number of each row like shown in Eq. 2.

$$dt = \sum_{i=1}^{k} n_i \quad (2)$$

where *n* refers to value specified on the color feature cluster and *i* refers to index of the cluster. If the determinant values 0, it means the specified impressions contribute very little in the computing. Therefore, the specified impression should be removed.

4.2 Impression Generation of Image Query

In this section, we build the main function which specified our system objective. The cultural-dependent color-impression metric would be implemented to the mobile application to measure the similarity between each impression metadata and image query captured by user. We implement the function to device with Android operating system.

(1) Normalized 3D Color Vector Quantization

Since the size of image pixels captured by mobile device is large in number, we resize the image to 150 x 200 pixels to optimize the mobile computing and response time. Larger size of pixels may cause long time in computing especially in clustering color features. The illustration of the resizing process is shown at Figure 7.

The resized picture is taken to implement the color feature extraction. The conversion from user's image query to color feature metadata equals with the same previous color vector quantization process on image dataset. The resized image query is extracted using the histogram from 3D-Color Vector Quantization of RGB color space. According to the recent study [1], 3D color vector quantization is 64x64x64 quantization size of the RGB color space so that it can be represented with 125 positions in the RGB color space.



Figure 7. The illustration of resizing image

(2) Similarity Measurment

The distinct function on this section is measuring similarity between image query and impression metadata on cultural-dependent color-impression metric. In recent work [8], Qian et. al. analyzed those two distance measures based on feature vectors normalized by image size and experiment with them in the context of color image database. The research concluded that the cosine angle distance, in general, works equally well for image databases. We can use the cosine similarity between the image query vector and color-impression vector as a measure of the score of the representative impression for the image query. The resulting scores can then be used to select the top-scoring impressions for a query. The implementation is shown at Eq. 3.

$$\text{Similarity}=\cos\theta \frac{A.B}{||A||\,||B||} = = \frac{\sum_{i=1}^{n} A_i \; x \; B_i}{\sqrt{\sum_{i=1}^{n}(A_i)^2}\sqrt{\sum_{i=1}^{n}(B_i)^2}} \quad (3)$$

where n is the number of color metadata clusters, A is representative color of image query, and B is representative color of impression. The result will be ranked in descend to find the most similar impression for the image query.

5. EXPERIMETAL STUDY

To perform our proposed impression generation of cultural painting system, we examine our system with Indonesian cultural painting dataset consisting of 2 multicolor red dominant paintings, 2 multicolor blue dominant paintings, and 2 multicolor blue dominant paintings. Several experiments are applied for each category of dominant color. To analyze the precision, we compare the similarity of impressions retrieved from application testing and impressions retrieved from the highest color feature of the image. To analyze the performance, we compare the application performance running in several devices. We examine our system with several collections of Indonesian cultural painting. Example of paintings are shown at Figure 8.



Figure 8. Example of paintings for experiments

5.1 Experiment in Measuring Impression Precision

Here we conduct an experimental study to analyze the precision of the generated impression. Performance comparison is obtained from comparing image retrieved impressions to its main color-impression. Ground-truthing of a large image dataset is a resource and cost intensive work. The only way to present performance objectively is through precision, which is defined in Eq. 4.

$$\text{Precision} = \frac{\text{Number of relevant main color impressions}}{\text{Total number of retrieved main color impressions}} \quad (4)$$

The words inside Table 3 show a set of impressions generated by application from Painting 1.

Table 3. Experiment result of painting 1

Rank	Retrieved Impressions
1	Cantik, indah
2	Ikhlas
3	Suci, mulia
4	Cinta
5	Sabar
6	Merangsang
7	Bersemangat
8	Damai, tenteram, tenang
9	Sopan
10	Gembira, senang

We investigated the main colors of the images by looking at the clustering result of color feature extraction on step color vector quantization. The rank of main colors was determined by the sum of pixels of the main colors in order. The main color feature is shown at Table 4. We compare the impressions of 3 main colors of image and the retrieved impressions from Table 3. All main color impressions matched the retrieved impressions list.

Table 4. Main color feature of painting 1

Rank	Main Color			Main color impression
	R	G	B	
1	127	127	127	Bersemangat
2	191	191	127	Cinta
3	191	127	127	Cantik-indah

Table 5. Average impression precision of painting collections

Painting	Retrieved Impressions	Main color-impressions	Precision
1	Cantik-indah, suci-mulia, sabar, bersemangat, cinta, ikhlas, damai-tenteram-tenang, khawatir, mengagumkan-mempesona. gembira-senang	Bersemangat, cinta, cantik-indah	100%
2	Cantik-indah, cinta, suci-mulia, menggoda, mengagumkan-mempesona, kacau, sabra, ikhlas, damai-tenteram-tenang, sopan	Cantik-indah, cinta, cantik-indah	100%
3	Ikhlas, menarik, suci-mulia, khawatir, damai-tenteram-tenang, gembira-senang, bersemangat, putus asa, aman, sabar	Ikhlas, putus asa, khawatir	100%
4	Ikhlas, suci-mulia, bersemangat, gembira-senang, aman, sabar, damai-tenteram-tenang, menarik, cantik-indah, khawatir	Sabar, cantik-indah, mengagumkan-mepesona	66.67%
5	Gembira-senang, khawatir, menarik, damai-tenteram-tenang, suci-mulia, bersemangat, sedih-perih, aman, putus asa, malu-segan	Sedih-perih	33.33%
6	Gembira-senang, khawatir, menarik, damai-tenteram-tenang, suci-mulia, bersemangat, sedih-perih, aman, putus asa, malu-segan	-	0%

From the experiment results, the impression precision was measured by comparing the top three main color impressions to the retrieved impressions provided by the application. Main color was determined by the highly count of color feature clusters. The centroid cluster represents the main color, and the main color impression is determined by impression which has the highest count of color feature on the certain cluster. The experiments showed that the three main color impressions matched the top ten retrieved impressions averagely for more than 60%.

5.2 Experiments in Various Captures

Here we conducted an experimental study to analyse the generated impressions taken from several way of capturing. We select top ten high rank impressions and measure the similarity of each capture mode to the normal mode of the capture category. Our system was examined to brightness based captures, rotating captures, zooming capture. We obtained the similarity value by calculate the relevant retrieved impressions divided by total number of retrieved impressions.

Brightness intensity did affect and bring significant difference in retrieved impressions. The color feature of each captured image is different to each other due to the different intensity of brightness. Thus, the generated impressions of one capture are different to the other. The retrieved impressions of bright mode have similarity to the retrieved impressions normal mode for averagely 50%. The retrieved impressions of dark mode have similarity to the retrieved impressions normal mode for less than 20%. The experiments results are shown at Table 6.

Table 6. Similarity of impressions generated from brightness based captures

Painting	Similarity of impressions by Bright mode	Similarity of impressions by Dark mode
1	50 %	10 %
2	40 %	10 %
3	60 %	20 %
4	50 %	10 %
5	50 %	10 %
6	50 %	20 %

In other experiment, we analyze that rotating capture of painting does not affect and bring no difference in retrieved impressions. This was caused by while captured image is being rotated, the new image had the same color features with previous image. The retrieved impressions of each position have similarity to the retrieved impressions of other positions exactly 100%. The experiments results are shown at Table 7.

Table 7. Similarity of impressions generated from rotating captures

Painting	Similarity of impressions by 90° capture mode	Similarity of impressions by 180° capture mode	Similarity of impressions by 270° capture mode
1	100 %	100 %	100 %
2	100 %	100 %	100 %
3	100 %	100 %	100 %
4	100 %	100 %	100 %
5	100 %	100 %	100 %
6	100 %	100 %	100 %

We also found that zooming capture bring small difference in retrieved impressions. The difference in retrieved impression caused by the different color feature of each captured image. Though having different color feature, the retrieved impressions were quite similar to each other. From the results, the retrieved impressions of zoom 1 capture have similarity to the retrieved impressions normal mode for averagely above 80%. The retrieved impressions of zoom 2 capture have similarity to the retrieved impressions normal mode for more than 80%. The experiments results are shown at Table 8.

Table 8. Similarity of impressions generated from zooming captures

Painting	Similarity of impressions by zoom 1 capture mode	Similarity of impressions by zoom 2 capture mode
1	80%	80 %
2	80%	80%
3	90 %	70 %
4	90 %	100 %
5	80 %	80 %
6	70 %	80 %

5.3 Experiments in Device Performance

Here we conducted an experimental study to analyze the response time of the device to generate impression. We examined our system with one collection of Indonesian cultural painting and five devices. The specification of the devices is shown at Table 9.

We examine our system to all devices to three of six paintings used on previous experiments. The result is shown at table 4. In Table 4, we perform device performance on executing 3 main processes: (1) RGB Extraction, (2) Color Vector Quantization, and (3) Similarity Measurement. Where D refers to device we used in experiments. Device 1 refers to Huawei Ascend Y300, 2 refers to Samsung Galaxy Ace 2 I8160, 3 refers to Samsung Galaxy Tab 2 7.0 P3100, 4 refers Huawei Mediapad 7 Vogue to and 5 refers to Samsung Galaxy Note 8.0 N5100.

Table 9. Device specifications

Spec	Device1 (D1)	Device2 (D2)	Device3 (D3)	Device4 (D4)	Device5 (D5)
Type	Huawei Ascend Y300	Samsung Galaxy Ace 2 I8160	Samsung Galaxy Tab 2 7.0 P3100	Huawei Mediapad 7 Vogue	Samsung Galaxy Note 8.0 N5100
OS	Android 4.1	Android 2.3	Android 4.0.3	Android 4.1	Android 4.1.2
CPU	Dual-core 1 GHz Cortex-A5	Dual-core 800 MHz	Dual-core 1 GHz	Quad-core 1.2 GHz	Quad-core 1.6 GHz Cortex-A9
Memory	512 MB RAM	768 MB RAM	1 GB RAM	1 GB RAM	2 GB RAM

Table 10. Device response time

Process	D1 (ms)	D2 (ms)	D3 (ms)	D4 (ms)	D5 (ms)	Avg (ms)
1	96	102	74	40	27	67.8
2	107172	116259	65299	62086	40850	78333
3	13	12	10.5	8	7	10.1
Total	108255	117434	65959	62714	41263	79125

The system finished in range of 41263 to 117434 milliseconds. From the comparison, Samsung Galaxy Note which has highest specification in CPU have the fastest average response time among all. The rank of the average time response is similar with the rank of device CPU qualification.

5. CONCLUSION

In this paper, we have presented an impression generation system of Indonesian cultural painting with cultural-dependent color metric creation for mobile application. Our proposed system is built to apprehend user intention to get the representative impressions of the paintings related to human emotional sense. From four experimental studies, our proposed system performed main color impression precision result with average effectiveness of more than 60%. Brightness intensity affected the retrieved impressions, but the main color impression precision result was quite stable. The process of public impression polling conducted on this system opens big impression outliers, because the impression of every person is different so it cannot obtain a perfect score in the creation of color-impression metric. From device performance experimental studies, our proposed system performed the average response time vary in range 41263 to 117434 milliseconds. The process of clustering of thousands of image color features in color vector quantization leads the time consuming and core processing. Therefore, the system requires high qualification of CPU above 1GHz on mobile device to run efficiently.

REFERENCES

[1] Ali Ridho Barakbah, Yasushi Kiyoki, **3D-Color Vector Quantization for Image Retrieval System**, *International Database Forum (iDB)* 2008, Izaka, Japan, 2008.

[2] Kazuhiko Shiranita, Kenichiro Hayashi, Akifumi Otsubo, **An Impression-word-giving System for Images Based on Colors**, http://www.idemployee.id.tue.nl/g.w.m.rauterberg/conferences/CD_doNotOpen/ADC/final_paper/056.pdf (The journal was accessed on August 2, 2013).

[3] Totok Suhardijanto, Kiyoki Yasushi, Ali Ridho Barakbah, **A Culture-Dependent Metadata Creation Method for Color-based Impression Extraction with Cultural Color Spaces**, *International Journal of Information Modelling and Knowledge Bases*, Vol. XXII, IOS PRESS, March, 2011.

[4] S. Sasaki, Y. Itabashi, Y. Kiyoki, X. Chen, **An Image-Query Creation Method for Representing Impression by Color-based Combination of Multiple Images**, *Information Modeling and Knowledge Bases*, Vol. XX, pp. 105-112, 2009.

[5] K. G. D. Tharangie, K. G. K. Kumara, I. Jayasinghe, C. A. Marasinghe, Koichi Yamada, **Kansei Color Associations for an Interactive Learning Environment for Children**, http://kjs.nagaokaut.ac.jp/yamada/papers/TH-B2-4.pdf (The journal was accessed on September 2, 2013)

[6] Syamsiar Ferdiansyah, Ali Ridho Barakbah, Nana Ramadijanti, **Impression Based Batik Decoration with Culture-dependent Color Impression**, D4 Program, Electronic Engineering Polytechnic Institute of Surabaya, 2012.

[7] Kohei Arai and Ali Ridho Barakbah, **Hierarchical K-means: An Algorithm for Centroid Initialization for K-means**, *Reports of the Faculty of Science and Engineering*, Saga University, Vol. 36, No.1, 2007.

[8] Gang Qian, Sural, S., Pramanik, S., **A Comparative Analysis of Two Distance Measures in Color Image Databases**, *Proc. International Conference on Image Processing*, Vol.1, pp.I-401 - I-404, 2002.

EMITTER International Journal of Engineering Technology
Vol.2, No.1, December 2014
ISSN:2355-391X

Automatic Backup System for Virtualization Environment

Idris Winarno, Muzaki Nurus Sani

Politeknik Elektronika Negeri Surabaya
Kampus PENS, Jl. Raya ITS Sukolilo, Surabaya, 031-5947280
E-mail: idris@pens.ac.id, vnyx14@gmail.com

Abstract

Virtualization is a technology lately much discussed and considered as the proper way to cut costs in the construction of a data center. One example of the implementation of virtualization technologies is to using VMware. Another tools for virtualization are Xen and OpenVZ, but VMware is more flexible than Xen or OpenVZ because VMware can run a variety of operating systems. Although it has the advantage, virtualization technology also has a vital weakness, virtualization technologies could be analogous by putting all the eggs in a basket. This means that if the master server problem, all systems inside the virtual machine can not be used. However, it can be anticipated by provide backup facilities that run continually and automatically. VMware itself has had an application to backup/replicate virtual machines. However, that application is not free yet.
This research has been design and creates a web-based software for backing up virtual machines on VMware. So it made easier for users and admins to perform periodic backups of virtual machines.
From the test results has been done, it can be seen that used disk type thin or zeroed thick make process backup faster, system can't work well when virtual machine has snapshot, scheduling system and restoring system has worked well, physical ability data storage influence system.

Keywords: Virtual machine, virtualization, Vmware, Backup, Data Center.

1. INTRODUCTION

The data center is a facility used for the placement of a set of servers or computer systems and storage which is conditioned by the power supply , air - conditioning , fire prevention and is usually equipped with physical security system [1]. At first, the data center is always built in a large room to assist the operation of a company. The super computers are still too complex for the maintenance and operation. Until in the 1960s IBM introduced a mainframe virtualization technology in its products, which can be built on a mainframe

Copyright © 2014 EMITTER International Journal of Engineering Technology - Published by EEPIS

virtual machines - virtual machine by utilizing the resources of a very large IBM mainframe. Virtualization itself can be interpreted as the creation of a virtual version of a form or something physical, such as operating systems, storage devices / data storage or network resources [2]. With virtualization technology makes it easier to implement data center on company facilities. Virtualization technology has many advantages such as [2] :

- **Efficiency**, by using the concept of virtualization, an agency can cut procurement costs for servers.

- **Security**, concept of virtualization has protection on various system resources, namely by eliminating the division of resources directly, so there is no problem of protection in virtualization technology. Virtualization technology is a perfect vehicle for operating systems research and development. With virtualization technology, if there is a change in one part of the machine, it is guaranteed not to change other components.

- **Recovery**, virtualization solutions can be used for system recovery plan that requires portability and flexibility across platforms.

In addition to the above advantages of virtualization technology also has drawbacks, virtualization technologies could be analogous to putting all the eggs in one basket. This means that if the master server problem, all systems inside the virtual machine can not be used. It can be anticipated by providing automatic backup facility and periodically or by applying the principle of fail over / clustering.

VMware itself has had an application to backup / replicate virtual machines that Veeam Backup & Replication. However, these applications are still paid.

Through this research, is expected to be a tool to facilitate the users especially network admin perform backups automatically and periodically.

2. RELATED WORKS

Reviewing of several papers that there is:

Xiaoying Wang , Zhihui Dua, Yinong Chen, Sanli Li (2007) [1], in a paper entitled "Virtualization-based autonomic resource management for multi-tier Web applications in shared data center". The paper explains that they develop a new architecture of resource management framework for multi-tier applications based on virtualization mechanisms to isolate different application environments for security reasons and to provision shared resources effectively and efficiently to meet different service quality targets with The minimum operating costs.

Xiangzhen Kong, Chuang Lin, Yixin Jiang, Wei Yan, Xiaowen Chu (2010) [2], in a paper entitled "Efficient dynamic task scheduling in virtualized the data centers with fuzzy prediction". The paper explains that the virtualization also brings some challenges, particularly for resource management and task scheduling. This paper proposes an efficient dynamic task scheduling scheme for virtualized data centers. Considering the availability and responsiveness performance, the general model of task scheduling for virtual data centers is

built and formulated as a two-objective optimization. Procedure graceful fuzzy prediction method is given to model the uncertain workload and the vague availability of the virtual server nodes, by using type I and type-II fuzzy logic systems.

Hai Jin, Wei Gao, Song Wua, Xuanhua Shi, Xiaoxin Wub, Fan Zhou (2010) [3], in a paper entitled "Optimizing the live migration of virtual machine by CPU scheduling". This paper explains that they are addressing the problem of downtime during the migration of virtual machine by designing optimization scheme for live migration, which according to pre-copy speed, vCPU operating frequency can be reduced so that at certain phases of memory pre-copy the remaining dirty can achieve the desired small amount . VM downtime during the migration can be limited. This scheme works for the scenario where the migrated application has a high memory writing speed or the pre-copy speed is slow for example, due to low network bandwidth between the migration.

3. Method

GhettoVCB is backup agent used to backup the virtual machine server ESX (i). GhettoVCB created using the basic shell programming so it can work on UNIX OS. These scripts perform backups of virtual machines residing on ESX (i) server 3.5/4.x/5.x using methodology similar to VMware VCBtool. The script takes a snapshot of the virtual machine is running, backing up the master VMDK (s) and then when you're done, delete the snapshot until the next backup process. The only caveat is that it utilizes the resources available to the Service Console of ESX server or Busybox Console (Tech Support Mode) from the ESXi server running the backups as opposed to following the traditional method of offloading virtual machine backups through a VCB proxy [6].

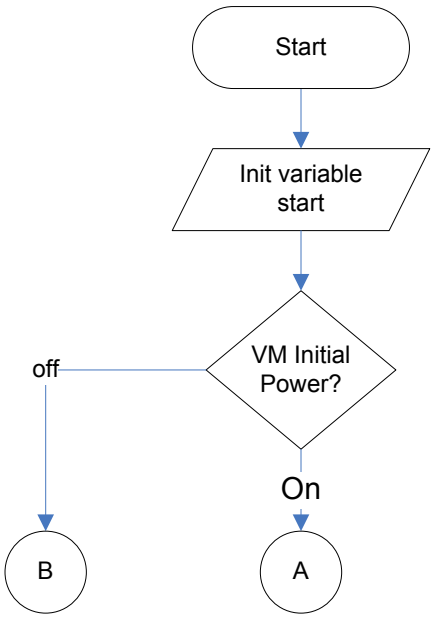

Figure 1. Flowchart GhettoVCB

This script has been tested on ESX and ESXi 3.5/4.x/5.x 3.5/4.x/5.x and supports the following backup media: LOCAL STORAGE, SAN and NFS[7]. Script is a non - interactive and can be setup to run via cron. Currently, this script accepts a text file that lists the names of the virtual machine display (s) to be supported. Moreover, one can specify the folder that contains the configuration data on a per VM basis for granular control over backup policies.

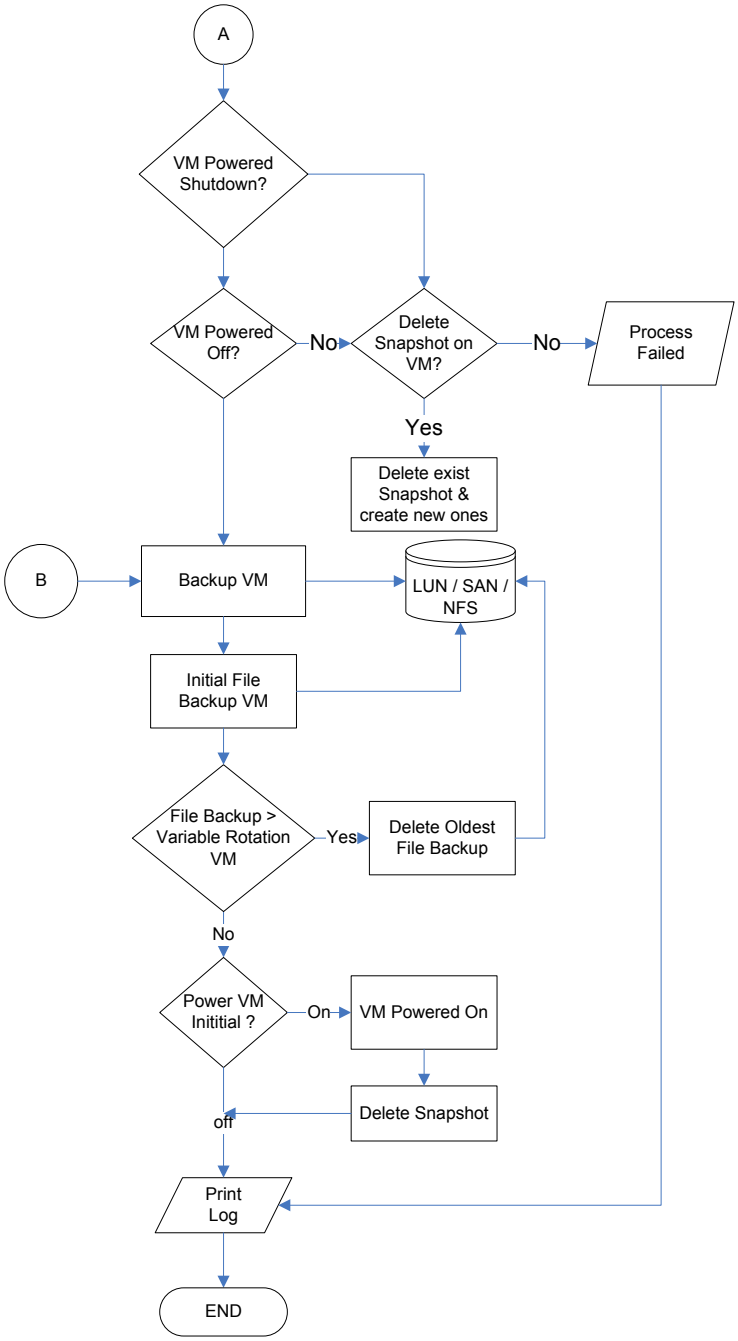

Figure 2. Flowchart GhettoVCB

Explanation of the flowchart (figure 1 and figure 2) such as:

- When running the agent, the script will initialize variables-variables that have been entered.
- After that, the agent will check whether the VMs to be backed up alive / dead. If you die, then the agent directly to backup VMs.
- If the VMs are alive then the agent will see the variable that has been entered to determine whether to turn off or not. If still on the agent will do the snapshotting process on the VMs.
- Then the agent will perform backups and store them into a predetermined storage.
- Agent will check the amount of rotation in the variable and the number of files stored on the storage. If more of the storage agent will remove the oldest data.

4. SYSTEM DESIGN

There is a design of the whole process in the manufacture of the system. As we know, before a system previously made sure no idea of the background to make such a system, it has been described by the authors in the introduction. Then to make a sketch of the system also needed a system that would be made, the authors have translate the planning system. Once the idea and design of existing.

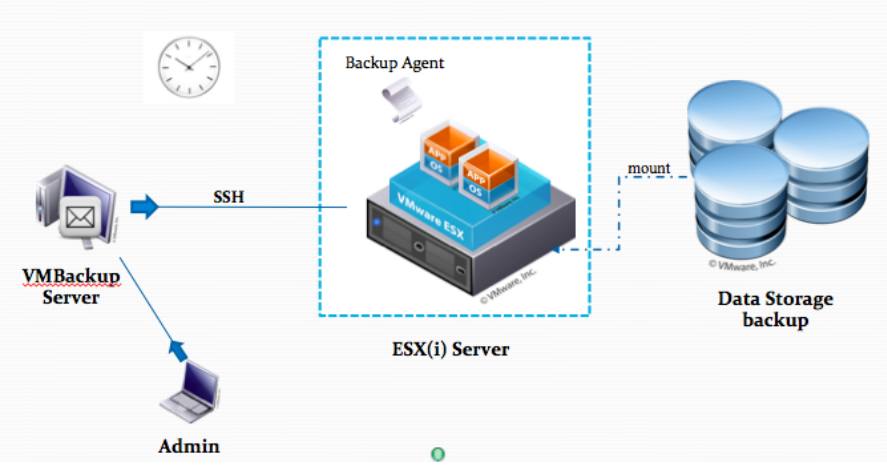

Figure 3. Work principle form backup system virtual machine.

From figure 3 can explain the working principle of the system in more detail as follows:

1. Users access the web server and provide the server command to perform a backup on a virtual machine.
2. Then, web server execute remote commands for VMware via SSH protocol and then run the backup agent.
3. Agent runs backup program to back up VMware host servers and put in backup storage that has been determined.

4. After processing user can get result in form either logs or emails.

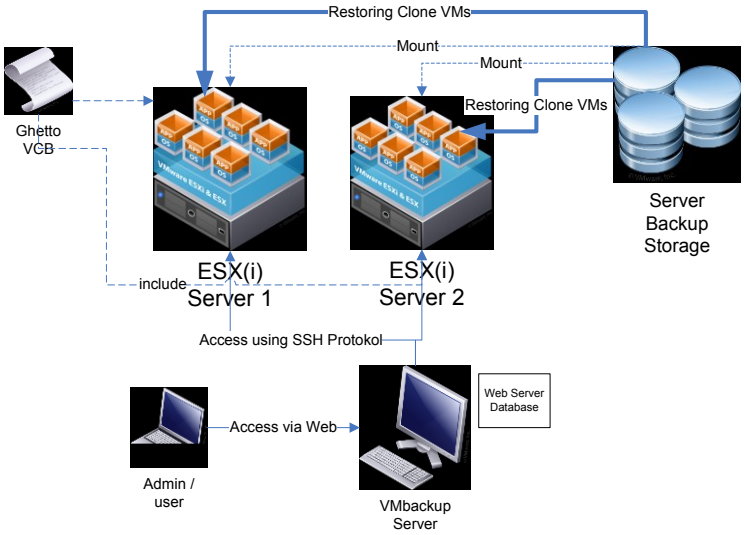

Figure 4. Work principle form restore system virtual machine.

From figure 4 can explain the working principle of the system in more detail as follows:

1. Users access the web server and provide the server command to restore broken virtual machine.
2. Then, web server execute remote commands for VMware via SSH protocol and then run a backup agent to restore virtual machine's clone which contained in the backup storage server.
3. Agent runs restore program to restore Vmware virtual machine and place in ESXi Server that has been determined.

5. EXPERIMENT AND ANALYSIS

We build the system using PHP code[4] and here are the result of application virtual machine. Login page to access the configuration system shown on figure 5.

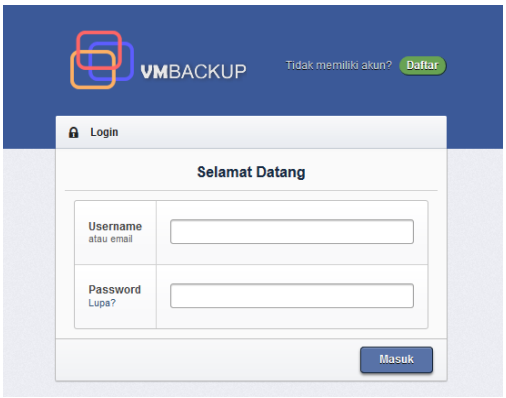

Figure 5. Login Form

Configuration Page on figure 6 would be shown to select to configure name of the virtual machine, backup format and rotation count.

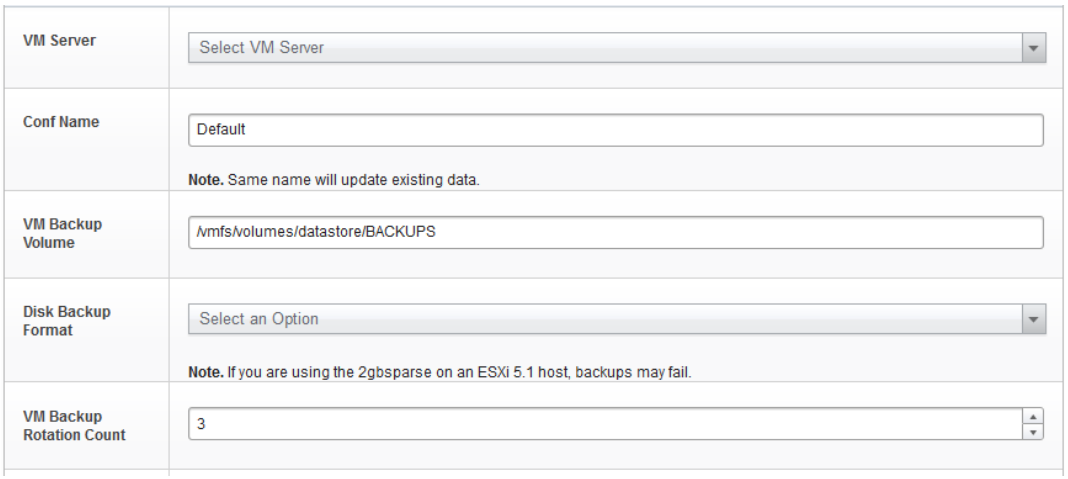

Figure 6. Configuration Page

One of the feature of the backup system is backup schedule that we can configure dynamicly shown on the figure 7. And the history of the scheduling backup show on the figure 8.

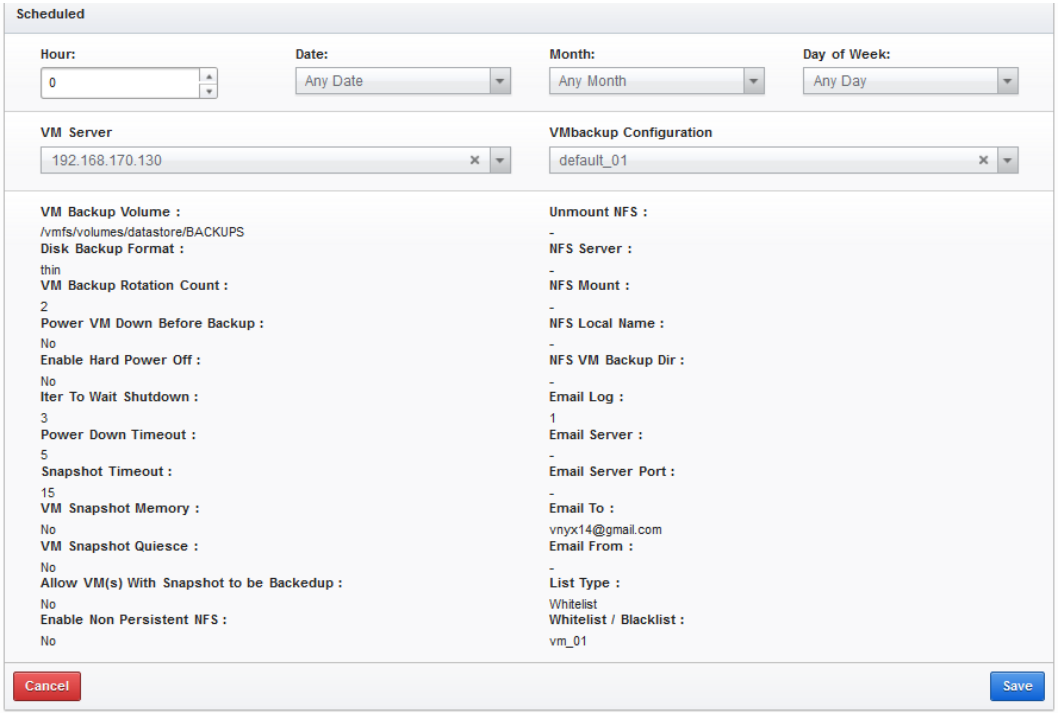

Figure 7. Scheduled Backup Page

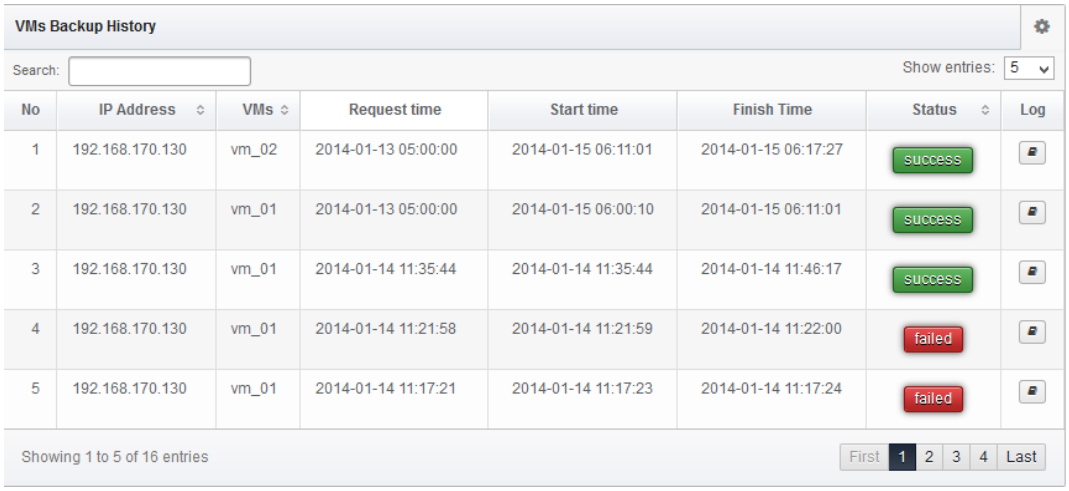

Figure 8. Backup's Result

Here are details of the testing that has been done, we try to compare the performance in different disk format of the virtualization (Table 1) and made some condition of the virtual machine to test the backup system (Table 2).

Table 1. Testing against different disk format of virtual machine

Format	Size VM	Backup Size	Provizioned Size	Duration Backup
Thin	4 GB	1.11 GB	4 GB	00:01:56
Zeroed Thick	4 GB	0.77 GB	4 GB	00:01:53
Eager Zeroed Thick	4 GB	4 GB	-	00:07:19

Eager Zeroed Thick[5]: An eager zeroed thick disk has all space allocated and wiped clean of any previous contents on the physical media at creation time. Such disks may take longer time during creation compared to other disk formats. The entire disk space is reserved and unavailable for use by other virtual machines.

Zeroed Thick[5]: A thick disk has all space allocated at creation time. This space may contain stale data on the physical media. Before writing to a new block a zero has to be written, increasing the IOPS on new blocks compare to Eager disks. The entire disk space is reserved and unavailable for use by other virtual machines.

Thin[4]: Space required for thin-provisioned virtual disk is allocated and zeroed on demand as the space is used. Unused space is available for use by other virtual machines.

Table 2. Testing against condition of the virtual machine.

Test	Start Condition		Process Condition		Finish Condition		Backup Status
	Power	Snapshot	Power	Snapshot	Power	Snapshot	
1	On	No	On	Yes	On	No	Succeed
2	On	Yes	On	On	On	No	Succeed
3	On	Yes	On	Yes	On	Yes	Fail

Test	Start Condition		Process Condition		Finish Condition		Backup Status
	Power	Snapshot	Power	Snapshot	Power	Snapshot	
4	On	No	Off	No	On	No	Succeed
5	Off	No	Off	No	Off	No	Fail

Note :

1. Test 1 used configuration “powering off No”, “hard powered off No”, “Allow VMs with snapshot backed up No”.
2. Test 2 used configuration powering off No”, “hard powered off No”, “Allow VMs with snapshot backed up Yes”.
3. Test 3 used configuration “powering off No”, “hard powered off No”, “Allow VMs with snapshot backed up No”.
4. Test 4 used configuration “powering off Yes”, “hard powered off Yes”, “Allow VMs with snapshot backed up No”.
5. Test 5 used configuration “powering off No”, “hard powered off No”, “Allow VMs with snapshot backed up No”.

Table 3. Testing against scheduled backup dan restore.

Process	Backup status
Scheduled Backup	Succeed
Restore	Succeed

Table 4. Testing against different storage type.

Storage	Start Time	Finish Time	Duration
NFS	01:07:37	02:54:52	01:47:15
NFS (FreeNAS)	04:56:45	05:01:30	00:04:45
iSCSI (FreeNAS)	12:32:56	12:37:59	00:05:03

From test table in Table 1 , Table 2 , Table 3 , Table 4 can be analyzed that system was working as it should according to design system has been made . Both in testing the backup system or restore system .

In Table 1 it can be seen that every disk format has a significant difference, for type zeroed thick and thin discs are not all sectors are in virtual machine backed up , but that only disk has data backed up so that it can speed up backup’s process . As for the type of eager zero thick all sectors are backed up so that backup’s capacity greater as original virtual machine. In Table 2 it can be seen that if the configuration enable parameter "Allow VMs with snapshots to be backups ", snapshot on the virtual machine will be deleted . In Table 3 it can be seen that the scheduling system and restore virtual machine works well . In Table 4 it can be seen that significant differences occurred in the backup process using the 3 models of storage . On the NFS server backup process longer than NFS (FreeNAS)[8][10] / iSCSI (FreeNAS) because disk backup is shared . While on NFS (FreeNAS) / iSCSI (FreeNAS) is dedicated.

6. CONCLUSION

From the test results and analysis we conclude:

1. Backing up a virtual machine use thin disk or zeroed thick type faster than using the type of the eager zeroed thick.
2. This backup system will not work if virtual machine has snapshots. However, the system will create a snapshot that can be used when a failure occurs during backup process.
3. Scheduled system has worked well. Either restore system.
4. Physical ability of storage can affect performance backup process.

For the future works, this system would be implement for dynamic storage system and implement an algorithm to find out the best performance of the virtual machine backup environment.

REFERENCES

Journal:

[1] Xiaoying Wang , Zhihui Dua, Yinong Chen, Sanli Li, "**Virtualization-based autonomic resource management for multi-tier Web applications in shared data center**", Journal of Systems and Software, Volume 81, Issue 9, Pages 1591–1608, September 2008.

[2] Xiangzhen Kong, Chuang Lin, Yixin Jiang, Wei Yan, Xiaowen Chu, "**Efficient dynamic task scheduling in virtualized data centers with fuzzy prediction**", Journal of Network and Computer Applications, Volume 34, Issue 4, Pages 1068–1077, July 2011.

[3] Hai Jin, Wei Gao, Song Wua, Xuanhua Shi, Xiaoxin Wub, Fan Zhou, "**Optimizing the live migration of virtual machine by CPU scheduling**", Journal of Network and Computer Applications, Volume 34, Issue 4, Pages 1088–1096, July 2011.

Texbooks:

[4] Lukmanul Hakim, **Membongkar Trik Rahasia Para Master Php**, Lokomedia, 2011.

Internet:

[5] **Thick vs Thin Disks and All Flash Arrays**.
http://blogs.vmware.com/vsphere/2014/05/thick-vs-thin-disks-flash-arrays.html
Accessed on 03-02-2014.

[6] **Vmware Communities**.
http://communities.vmware.com/docs/DOC-8760. Accessed on 06-01-2014.

[7] **Network File Sistem (NFS) + Samba**.
http://lecturer.eepis-its.edu/~idris/files/admin_jarkom/nfs_samba.pdf. Accessed on 27-01-2014.

[8] **Belajar membuat server NAS dengan FREENAS**.

http://iwing.wordpress.com/black-box/belajar-membuat-server-nas-dengan-freenas/. Accessed on 06-01-2014.

[9] **Configuring iSCSI for Vsphere esx(i)**. http://www.everything-virtual.com/2013/05/configuring-freenas-8-3-iscsi-and-nfs-storage-for-vmware-vsphere/. Accessed on 03-02-2014.

[10] **How to Setup Synologi NAS as VMware Server Datastore**. https://www.synology.com/en-uk/support/tutorials/508. Accessed on 03-02-2014.

EMITTER International Journal of Engineering Technology
Vol.2, No.1, December 2014
ISSN:2355-391X

AC-DC PFC Converter Using Combination of Flyback Converter and Full-bridge DC-DC Converter

Moh. Zaenal Efendi*, Abdul Rizal*, Aldi Erzanuari*, Suryono*, Novie Ayub Windarko*

*)Electro-industrial Engineering Study Program,
Department of Electrical Engineering, Politeknik Elektronika Negeri Surabaya
Kampus PENS, Keputih Sukolilo, Surabaya
E-mail: zenefendi@gmail.com

Abstract

This paper presents a combination of power factor correction converter using Flyback converter and Full-bridge dc-dc converter in series connection. Flyback converter is operated in discontinuous conduction mode so that it can serve as a power factor correction converter and meanwhile Full-bridge dc-dc converter is used for dc regulator. This converter system is designed to produce a 86 Volt of output voltage and 2 A of output current. Both simulation and experiment results show that the power factor of this converter achieves up to 0.99 and meets harmonic standard of IEC61000-3-2.

Keywords: Flyback Converter, Fullbridge DC-DC Converter, Power Factor Correction.

1. INTRODUCTION

Generally, electronic equipments need a dc power source. However, the power source provided by electric grid is an ac power source. Therefore, its needs a rectifier circuit which is used to transform the AC power source to the DC power source. The rectifier circuit requires a capacitor as filter to reduce the output voltage ripple. But, the usage of capacitor causes the current harmonics and the current distortion, so that the rectifier circuit has a low power factor.

To reduce the harmonics and to improve the power factor can be done by several methods. The first method is adding a large inductor filter [1]. But, this method is not commonly used because the rectifier circuit is heavier, because it works at low frequency of 50-60 Hz. A good method is adding pre-regulator of power factor correction converter known as two stages power factor correction converter. The most common two stages power factor correction converter used are boost converter [2], [3], buck converter [4], [5], buck-boost converter [6], [7] and other types of dc-dc converter [8], [9]. Two

Copyright © 2014 EMITTER International Journal of Engineering Technology - Published by EEPIS

stages power factor correction converter can produce sine input current, low harmonics and high power factor.

This paper presents and develops a new configuration of two stages power factor correction converter combining Flyback Converter and Full-bridge dc-dc converter in series connection. This configuration is designed to produce high power factor and low input current harmonics that meets the international harmonic standard of IEC6100-3-2 [10].

The block diagram of the two stages power factor correction converter proposed is shown in Fig. 1.

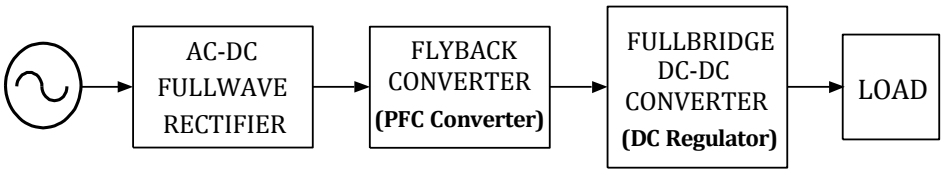

Figure 1. Block diagram of the proposed of two stages power factor correction converter

2. CONVERTER CONFIGURATION

Circuit configuration of the two stages power factor correction converter proposed in this paper is shown in Fig. 2. This configuration uses a Flyback converter as a pre-regulator of power factor corrector. The Flyback converter is series connected to a Full-bridge dc-dc converter in two stages.

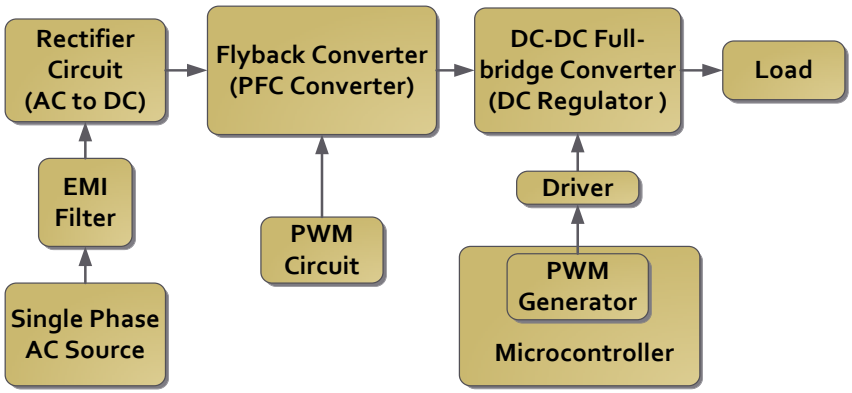

Figure 2. The block diagram of system

Based on the block diagram as seen in Fig. 2, the converter system uses two converters. They are Flyback converter and Full-bridge dc-dc converter in series connection. The complete circuit is shown in Fig. 3.

The Flyback converter operates in discontinuous conduction mode. Hence, if the converter operates in discontinuous conduction mode, the converter will have a high power factor [11], [12].

Basically, Flyback converter, which is shown in Fig. 4(a), is used as power factor corrector and operates in discontinuous conduction mode. It

has an magnetizing inductor (L_m) and other components. An input current and a magnetizing current waveforms of Flyback converter is shown in Fig. 4(b). This converter has an input resistance (R_i) that is calculated from the input voltage $V_{i(t)}$ and the input current $i_{i(t)}$ at one switching period.

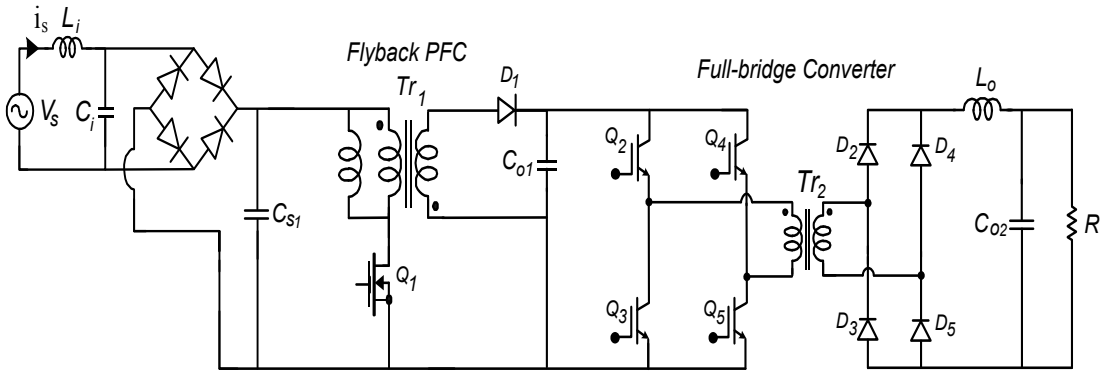

Figure 3. The circuit of AC-DC PFC Converter Using Combination of Flyback Converter and Full-bridge DC-DC Converter

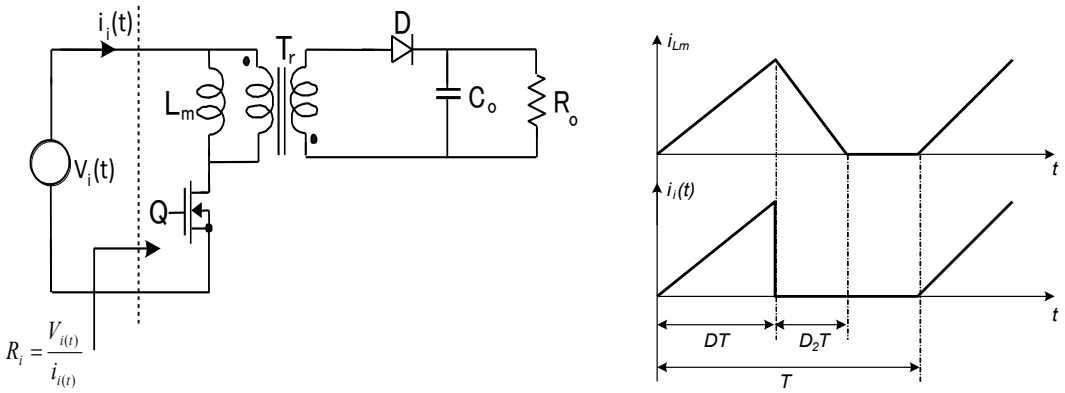

(a) (b)

Figure 4. (a) Flyback converters in discontinuous conduction mode; (b) waveform of inductor magnetizing and input current

The input resistance of the converter system can be calculated using equation 1:

$$R_i = \frac{V_{i(t)}}{i_{i(t)}} \tag{1}$$

According to Fig. 4(b), the input current is determined in equation 2:

$$i_{i(t)} = \frac{\frac{1}{2} i_{lm} DT}{T} \tag{2}$$

where i_{Lm} is magnetizing inductor current, D is the duty ratio and T is the switching periode. The magnetizing inductor current can be calculated by equation 3:

$$i_{lm} = \frac{V_{i(t)}|\sin \omega t|DT}{T} \tag{3}$$

where $V_{i(t)}|\sin \omega t|$ is the input voltage. If the equation 3 is substituted into equation 2, the input current become as equation 4:

$$i_{i(t)} = \frac{\frac{V_{i(t)}|\sin \omega t|DT}{2L_m}DT}{T} = \frac{V_{i(t)}|\sin \omega t|D^2T}{2L_m} \tag{4}$$

Finally, equation 4 is substituted into the equation 1, thus the input resistance is determined in equation 5:

$$R_i = \frac{V_{i(t)}}{i_{i(t)}} = \frac{2L_m}{D^2T} \tag{5}$$

The equation 5 shows the resistance (R_i) depends on the value of magnetizing inductance, switching period, and duty ratio. If the Flyback converter operates in discontinuous conduction mode and in constant duty ratio, the input resistance becomes constant. Therefore, the shape of the input current waveform $i_{i(t)}$ follows the shape of the input voltage waveform $V_{i(t)}$ and the Flyback converter becomes as power factor corrector.

After processing Flyback converter as PFC converter, to obtained output voltage regulation, the Full-bridge dc-dc converter is connected on the converter system. The circuit of the Full-bridge dc-dc converter is shown in Figure 5 and it is designed in continuos mode operation. The Full-bridge dc-dc converter is designed using equation 6 to equation 8.

Assume that d is duty cycle, then:

$$d = \frac{N_1 \times V_o}{2 \times N_2 \times V_{in}} \tag{6}$$

The filter inductor can be obtained from:

$$L_{cri} = \frac{(1-d)}{4} \times RT \tag{7}$$

And, the filter capacitor is:

$$C_o = (1-d) \times \frac{V_o}{32 L_o f^2 \Delta V_o} \tag{8}$$

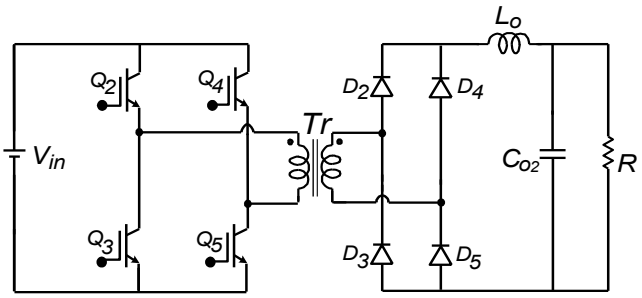

Figure 5. Circuit of Full-bridge dc-dc converter

3. SIMULATION AND EXPERIMENT

The prototype of AC-DC PFC Converter Using Combination of Flyback Converter and Full-bridge DC-DC Converter that has been discussed previously is designed with the parameters as seen in Table 1 and Table 2 to meets the requirement of converter operation. Actually, this converter can be implemented for power supply of all of electronic equipments. However, in this paper, converter can be applied as battery charger. The battery used for this experiment has a 72 Volt of voltage that consists of 6 pieces of 12 Volt of battery. So, to comply the requirement of charging voltage, the output voltage of converter system is setted at 86 Volt.

To ensure the converter operates in a good performances, it is simulated using SCAT K.460PRI software. The simulation circuit shown in Fig. 6 is built based on the circuit on Fig. 3 and the parameters that used in this circuit are declared in Table 1 and Table 2. The parameters observed are input voltage, input current, harmonic spectrum, output voltage, and output current.

Table 1. Parameters of Flyback PFC converter

Parameter	Value
AC input voltage (V_i)	220 Volt
Output voltage (V_{o1})	120 Volt
Switching frequency (f_s)	25 kHz
Switch Q_1 Diode D_1	IGBT 1MBH60-100 STTH60L06C
Transformer T_{r1}	N_1: N_2 = 6: 4
Capacitor C_{o1}	680 µF,450 Volt

Table 2. Parameters of Full-bridge dc-dc converter

Parameter	Value
Input voltage ($V_{i(fb)}$=V_{o1})	120 Volt

Output voltage (V_{o2})	86 Volt
Switching frequency (f_s)	25 kHz
Inductor L_o	866 µH
Switch Q_{2-5}	IGBT 1MBH60-100
Diode D_{2-5}	STTH60L06C
Transformer T_{r2}	N_3:N_4= 16:14
Capacitor C_{o2}	68 µF ,250Volt

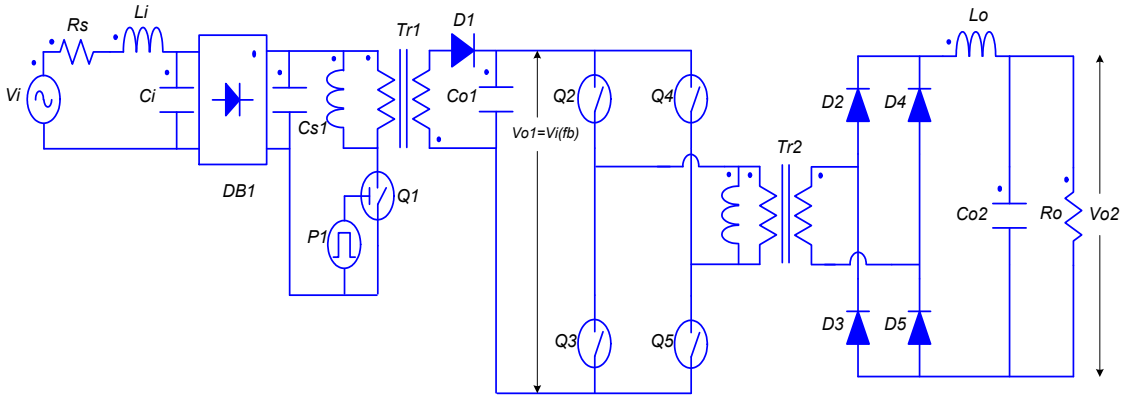

Figure 6. Simulation circuit of converter

The waveforms of the input voltage and the input current are shown in Fig. 7. Also, Fig 7 shows that the converter has high power factor of 0.9946, meets Harmonics standard IEC61000-3-2 class.

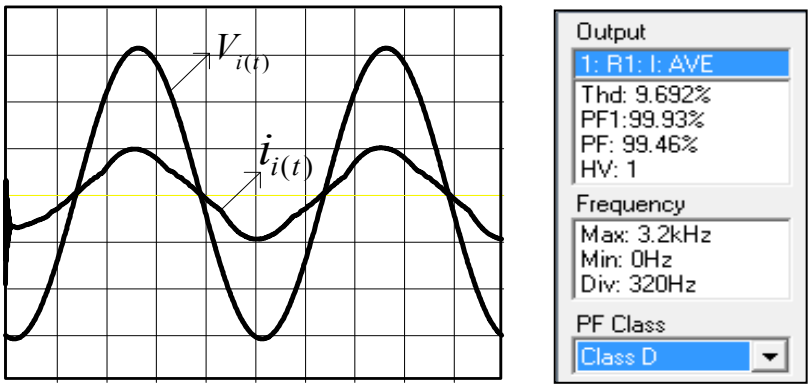

Figure 7. Wavefoms of input voltage and input current and power factor (pF) of converter

Futhermore, the converter is built using above parameters in real circuit. Experiment about the circuit is done using power harmonic analyzer Fluke 41B. The parameters that have been observed are the input current, the input voltage, power factor, and current harmonic spectrum. Fig. 8 shows

the values of the input parameters which are measured by Fluke 41B and Fig. 9 shows the input current waveform, the input voltage waveform and the current harmonic spectrum.

.

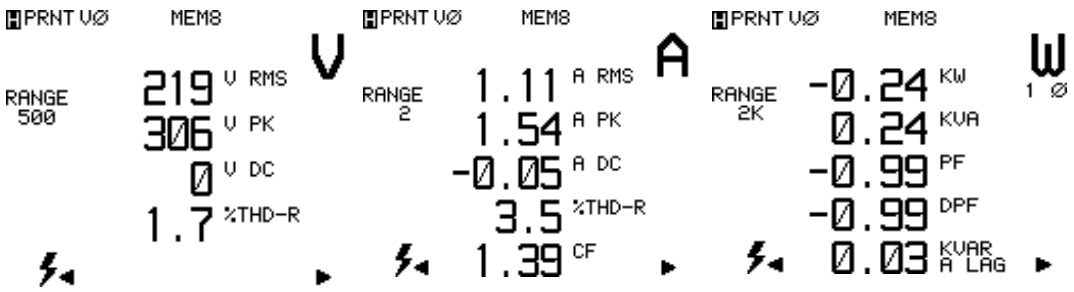

Figure 8. Experimental data of the converter system

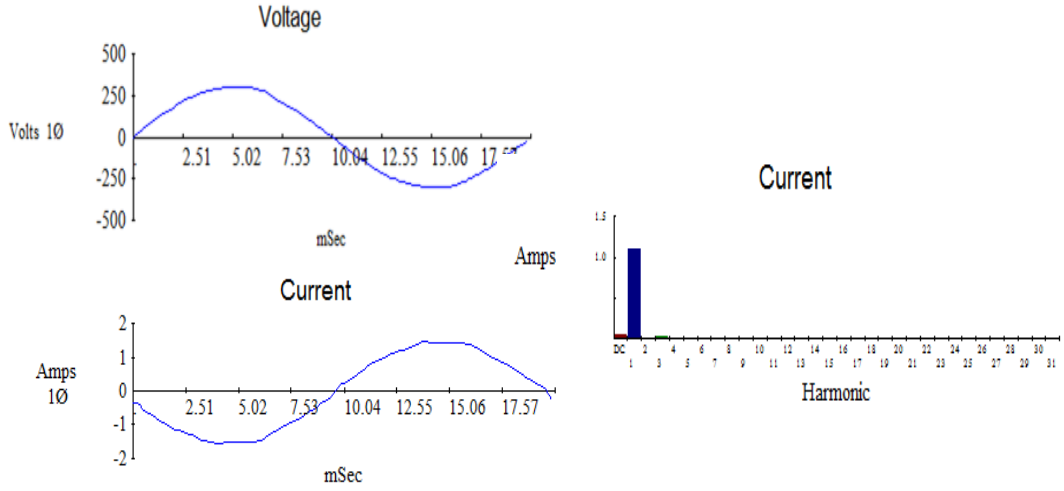

Figure 9. Waveforms of the input voltage and current and the current harmonic spectrum

According to Fig. 8, maximum power factor measured by power harmonic analyzer is 0.99 and the Total Harmonics Distotion of the input current (THD_i) is 3.5% to 8.2 %. The complete results of the experiment are also presented in Table 3. Based on the data in Table 3, on the nominal currect, it can be achived the highest power factor (near unity) and low harmonics.

To know the converter meets harmonics standards, it is made a comparison between the current harmonic spectrum of system testing and harmonic standard of class A and class D. Fig. 10(a) and 10(b) are shown this comparation. According to its, the proposed converter system and meets harmonics standards of IEC61000-3-2 class A so that it can be implemented for power supply of audio equipment and dimmer circuit of incandescent

lamps. And also it has low harmonics input current meets the standards of IEC61000-3-2 class D so that it can be implemented for power supply of computers and monitors.

Table 3. Experiment result of the converter

V_i (V)	I_i (A)	V_o (V)	I_o (A)	pF	THDi (%)
220	1.12	86	2	0.99	3.5
220	0.9	86	1.8	0.99	4.8
220	0.81	86	1.6	0.98	5.2
220	0.7	86	1.3	0.97	5.2
220	0.57	86	1	0.97	5.9
220	0.46	86	0.8	0.95	8.2

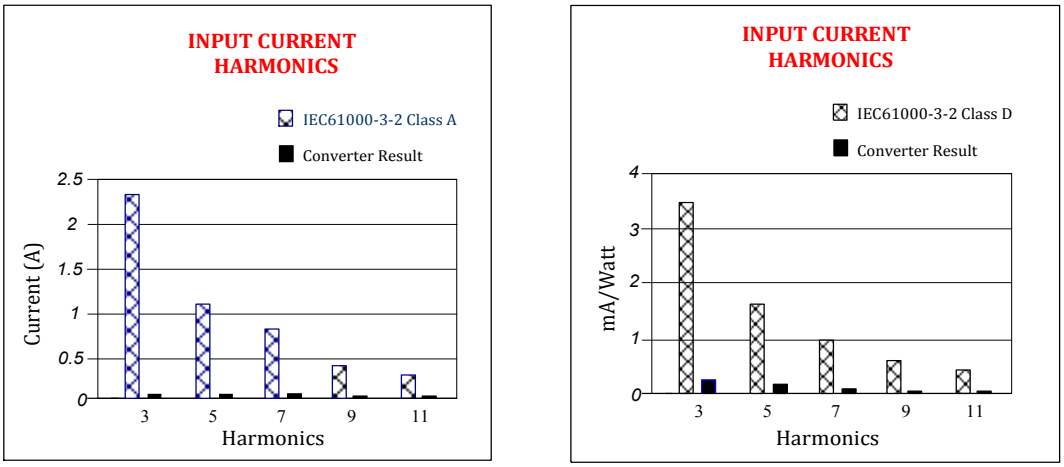

(a) (b)

Figure 10. Comparison of input current harmonics of class A and class D

4. CONCLUSION

This paper presented about the combination of AC-DC Flyback converter with full bridge dc-dc converter that has power factor correctorn. According to both simulation and experimetal results, this converter system has a high power factor up to 0.99 and low harmonics input current and meets harmonics standard of IEC61000-3-2 class A and class D.

Acknowledgements

This paper is published based on the research supported by Research Unit of Politeknik Elektronika Negeri Surabaya (PENS) to Energy and Transportation Research Centre, budgeting year of 2014. We would thank chairman and staff of Research Unit of PENS.

REFERENCES

[1] Arthur W. Kelly, **Rectifier Design for Minimum Line-Current Harmonics and Maximum Power Factor**, *IEEE Transaction on Power Electronics*, Vol. 7, No. 2, April, 1992.

[2] Dragan Maksimovic, Robert W. Erickson, **Universal input, High Power Factor Boost Doubler Rectifiers**, *IEEE Applied Power Electronics Conference*, 1995.

[3] Seleme Isaac Jr. Seleme, Lenin Martins Ferreira Morais, Arthur Hermano Rezende Rosa, Leonardo Antônio Borges Torres, **Stability in passivity-based boost converter controller for power factor correction**, *European Journal of Control*, Volume 19, Issue 1, January 2013.

[4] Hisahito Endo, Takashi Yamashita, Toshiyuki Sugiura, **A High Power Factor Buck Converter**, *IEEE Applied Power Electronics Conference*, 1992.

[5] J.M. Alonso, M.A. Dalla Costa, C. Ordiz, **Integrated buck-flyback converter as a high-power-factor off-line power supply,** *Industrial Electronics IEEE Trans,* 55 (3), 2008.

[6] M.C. Ghanem, K. Al-Haddad, G. Roy, **A New Single Phase Buck-Boost Converter With Unity Power Factor**, *In Conference Record of The 1993 IEEE Industry Applications Society Annual Meeting*, IAS 1993.

[7] Huai Wei, **Power Factor Correction Circuits**, *Power Electronics Handbook (Third Edition)*, 2011.

[8] Bor-ren Lin, Tsang-sum Huang, **Zero current switching cuk converter for power factor correction**, *Electric Power Systems Research*, Volume 41, Issue 2, May 1997.

[9] Mohd Rodhi Sahid, Abdul Halim Mohd Yatim, **Modeling and simulation of a new Bridgeless SEPIC power factor correction circuit**, *Simulation Modelling Practice and Theory*, Volume 19, Issue 2, February 2011.

[10] Schaffner EMC,**IEC61000-3-2 Harmonics Standard Overview**, May 2006.

[11] Robert W Erickson, M. Madigan, S. Singer, **Design of a simple High Power Factor Rectifier Based on Flyback Converter**, *IEEE Applied Power Electronics Conference*, 1990.

[12] Zhang Jun, D.D.-C. Lu, Sun Ting, **Flyback-based single-stage power-factor-correction scheme with time-multiplexing control**, *Industrial Electronics IEEE Trans*, 57 (3), 2010.